Universität Stuttgart

Institut für Wasser- und Umweltsystemmodellierung

Mitteilungen

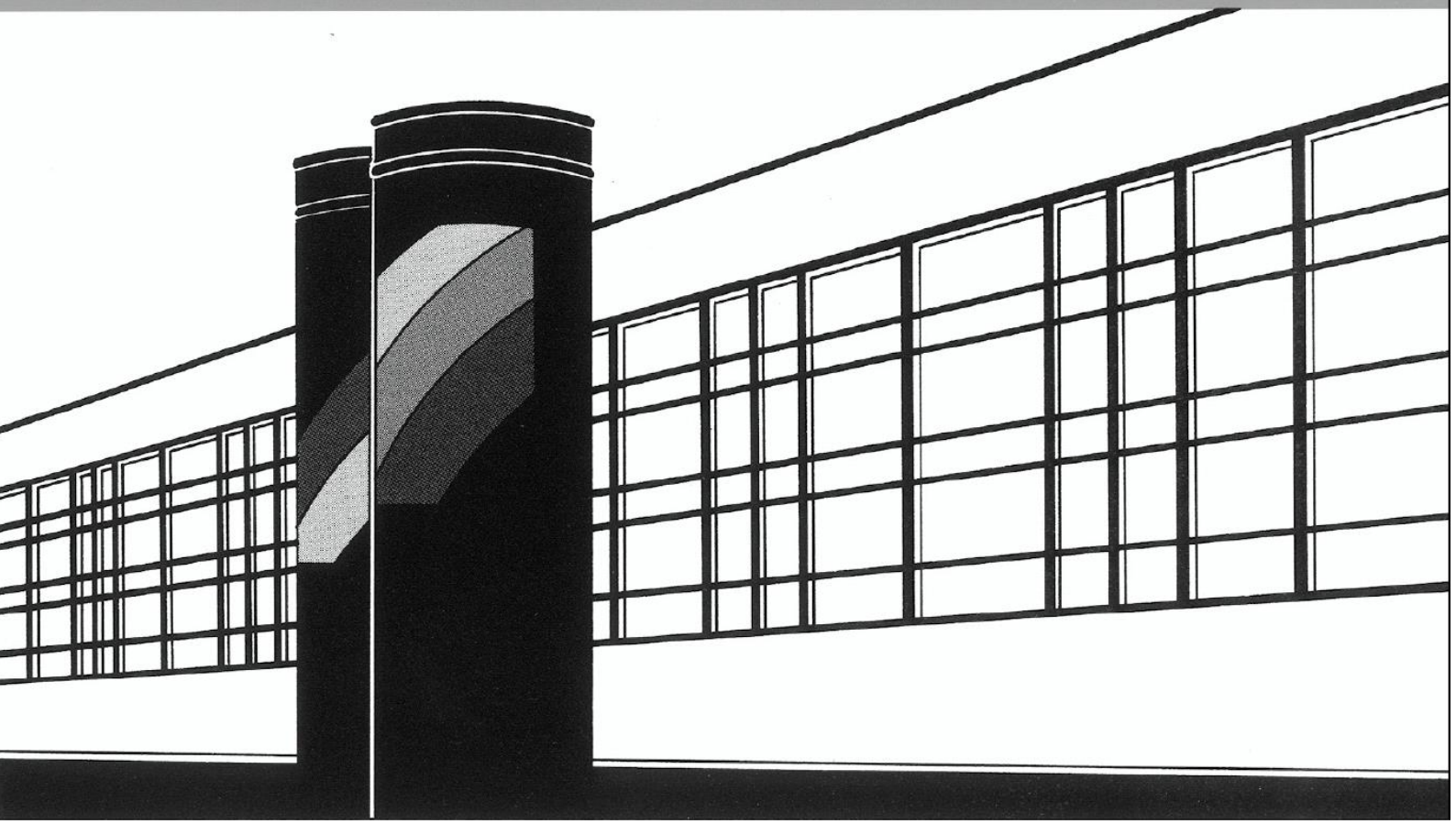

Heft 248 Yingchun Huang

Study on the Spatial and Temporal Transferability of Conceptual Hydrological Models

Study on the Spatial and Temporal Transferability of Conceptual Hydrological Models

von der Fakultät Bau- und Umweltingenieurwissenschaften der Universität Stuttgart zur Erlangung der Würde einer Doktor-Ingenieurin (Dr.-Ing.) genehmigte Abhandlung

vorgelegt von

Yingchun Huang

aus Longyan, China

Hauptberichter:	Prof. Dr. rer.nat. Dr.-Ing. András Bárdossy
Mitberichter:	Prof. Dr. Thorsten Wagener

Tag der mündlichen Prüfung: 07. 10. 2016

Institut für Wasser- und Umweltsystemmodellierung
der Universität Stuttgart
2016

Heft 248 Study on the Spatial and Temporal Transferability of Conceptual Hydrological Models

von
Dr.-Ing.
Yingchun Huang

Eigenverlag des Instituts für Wasser- und Umweltsystemmodellierung
der Universität Stuttgart

D93 Study on the Spatial and Temporal Transferability of Conceptual Hydrological Models

Bibliografische Information der Deutschen Nationalbibliothek
Die Deutsche Nationalbibliothek verzeichnet diese Publikation in der Deutschen Nationalbibliografie; detaillierte bibliografische Daten sind im Internet über http://www.d-nb.de abrufbar

Huang, Yingchun:
Study on the Spatial and Temporal Transferability of Conceptual Hydrological Models, Universität Stuttgart. - Stuttgart: Institut für Wasser- und Umweltsystemmodellierung, 2016

(Mitteilungen Institut für Wasser- und Umweltsystemmodellierung, Universität Stuttgart: H. 248)
Zugl.: Stuttgart, Univ., Diss., 2016
ISBN 978-3-942036-52-8

NE: Institut für Wasser- und Umweltsystemmodellierung <Stuttgart>: Mitteilungen

Herausgegeben 2016 vom Eigenverlag des Instituts für Wasser- und Umweltsystem-modellierung

Druck: Document Center S. Kästl, Ostfildern

Acknowledgment

Firstly, I would like to express my sincere gratitude to my supervisor Prof. Dr. rer.nat. Dr.-Ing. András Bárdossy. I gratefully thank him for the immeasurable amount of guidance, encouragement and support he provided in every stage of my study. I am truly indebted and thankful to Prof. Dr. Thorsten Wagener for accepting to co-supervise this work. Thank you for the valuable suggestions during my research visit to Penn State University and throughout this work.

It is a great pleasure to thank the ENWAT International Doctoral Program for providing the academic framework for my study. I owe sincere and earnest thankfulness to Dr. -Ing. Gabriele Hartmann for the time she dedicated to proofreading and suggesting improvements in writing my work.

My sincere appreciation also goes to all my colleagues at the Department of Hydrology and Geohydrology for their sharing, discussions and friendship. The help of Micha Eisele and Tobias Mosthaf with the German summary is gratefully acknowledged. In particularly, I would like to thank Mrs. Astrid Lemp for her assistance and patience.

I would like to extend my acknowledgment further to the China Scholarship Council for the financial support.

Last but not least, I would like to show my gratitude to my family, my parents and my sister for their love and encouragements.

Contents

List of Figures

List of Tables

List of Abbreviations

API	Antecedent Precipitation Index
CDF	Cumulative Distribution Function
ECD	Empirical Copula Density
GLUE	Generalized Likelihood Uncertainty Estimation
HBV	Hydrologiska Byråns Vattenbalansavdelning model
HYMOD	Hydrological Model
IWS	Institute for Modeling Hydraulic and Environmental Systems
GK	Kling-Gupta efficiency
MOPEX	Model Parameter Estimation Experiment
NCDC	National Climate Data Center
NOAA	National Oceanic and Atmospheric Administration
NS	Nash-Sutcliffe efficiency
NSB	Combination of Nash-Sutcliffe efficiency and bias constraint
PUB	Prediction in Ungauged Basins
ROPE	Robust Parameter Estimation
LNS	Logarithm transformed flow Nash-Sutcliffe
USGS	United States Geological Survey
WMO	World Meteorological Organization
XAJ	Xinanjiang model

Abstract

Hydrological modeling through conceptual, empirical or even physical models has arisen to be a fundamental element to solve water related issues. Rainfall-runoff models are widely used to describe catchment behavior, and for subsequent use for flood forecasting, integrated basin management, the prediction of the impacts of climate change and other purposes. In general, the model applications require calibration procedure to identify the model parameters and strongly depend on the how well the models are calibrated. The applications are often limited by the quality or quantity of input data, the model structure, the uncertainty of model parameters and the change of climate conditions for both gauged and ungauged regions. Improving the transferability of hydrological model parameters and providing more reliable predictions of runoff characteristics is nowadays the primary goal of modern hydrology.

This research is an attempt to investigate the spatial and temporal transferability of conceptual hydrological models in making better usage of the available knowledge and technology on rainfall-runoff processes of catchments. Different conceptual models, like HBV, HYMOD, and Xinanjiang (XAJ) models, are tested using Robust Parameter Estimation (ROPE) algorithm in various catchments like American, German and Chinese catchments.

Conceptual rainfall-runoff models are usually calibrated for selected catchments individually using specific performance criteria. The calibration procedure assumes that the catchments show the individual hydrological response. Therefore, the transfer of model parameters to ungauged basins is problematic. In this thesis, the spatial transferability of model parameters is investigated. This study explores to what extent do different catchments share a similar dynamical rainfall-runoff behavior and can be modeled using the same model parameters with the exception of the newly introduced individualized water balance parameter η. The models are restructured by introducing a new parameter η which exclusively controls water balances. This parameter is considered as individual to each catchment, all other parameters, which mainly control the dynamics of the discharge (dynamical parameters), are considered for spatial transfer. Three hydrological models combined with three different performance measures are used in four different numerical experiments to investigate the transferability of dynamical parameters. The first numerical experiment, involving individual calibration of the models for 15 selected Model Parameter Estimation Experiment (MOPEX) catchments shows that it is difficult to identify which catchments share common dynamical parameters. Parameters of one catchment might be good for another catchment but not the opposite. In the second numerical experiment, a common spatial calibration strategy is applied. It is explicitly assumed that the similar catchments share common dynamical parameters. This strategy leads to parameters which perform well on all catchments. A leave-one-out simultaneous calibration shows that in this case a good

parameter transfer to ungauged catchments can be achieved. In the third numerical experiment, the common calibration methodology is used for 96 MOPEX catchments. Another set of 96 MOPEX catchments is used to test the transferability of common dynamical parameters. The results show that even a large number of catchments share similar dynamical parameters. The performance is worse than those obtained by individual calibration, but the transfer to ungauged catchments remains possible. The performance of the common parameters in the second experiment is better than in the third one, indicating that the selection of the catchments for common calibration is important. In the fourth numerical experiment, the common parameters obtained from the 96 MOPEX catchments are used to model two selected German and a Chinese catchment. The results indicate that the dynamical model parameters have skill even under very different conditions.

Hydrological models highly relies on the observational data for parameter identification. Studies show that the model parameters might be significantly different for different calibration time period. This questions the transferability of model parameters in time. The temporal transferability of model parameters under changing climatic conditions is investigated in this thesis. HBV and HYMOD are used to test model performance in different periods for 50 selected MOPEX catchments. The effects of incorporating bias constraints into calibration routines when model parameters are used for predicting runoff in various weather conditions are tested by comparison of two different performance measures. Calibration result shows that model parameters are strongly influenced by the climatic conditions during calibration time period. The sub-period calibration and cross-validation approaches indicate that the variability of climate conditions often leads to different parameters for the same catchment. The incorporation of bias constraint with Nash-Sutcliffe efficiency strategy always achieves better water balance than the unconstrained one when model parameters are subsequently used for greatly different climate conditions. The transferability of model parameters strongly depends on the data set that used for model calibration which is detected by the dissimilarity of catchment characteristics using empirical copula density. To cope with the instability of model parameters under non-stationary conditions, two model calibration strategies, the common calibration for multi sub-periods and the weather adjustment with weight function are tested on HBV model. These approaches tend to slightly improve model performance for most of the simulations as compared to traditional calibration, although the benefit is small.

The reliability of hydrological models highly influenced by the quality and quantity of data set used for parameter identification. However, the knowledge of how much data and which period of data set should be selected to effectively calibrate the model is still lacking. How to adequately use information for model calibration in data-limited regions also needs to be explored. In this study, the impacts of input data quality and quantity on hydrological model parameter identification are investigated. HBV model is calibrated using the different length of data period for 15 MOPEX catchments. The transferability of the calibrated model parameters is then validated in two different time periods. The result indicates that the transferability of model parameters increases with the increasing of data length used for calibration for most of the study catchments. The sensitivity of data length for parameter estimation varies for the catchments. In general, a length of data ranging from five years to ten years is sufficient to calibrate a particular rainfall-runoff process. The result also shows

that the flood events have significant influence in model parameter estimation, especially for the surface runoff correlated parameters. For catchments with limited data and ungauged watersheds, the common calibration approach is presented by using information from spatial proximity catchments. The result shows that for more than half of the simulations, the model performance and transfer quantity can be slightly improved by using information from similar catchments. However, for one-third of the simulations, the model parameters calibrated by simultaneous calibration leads to worse model performances than the one by individual calibration.

Zusammenfassung

Hydrologisches Modellieren mit konzeptionellen, empirischen und physikalischen Modellen ist ein wesentliches Element bei der Bearbeitung wasserbezogener Fragestellungen. Niederschlags-Abfluss-Modelle werden dabei im Wesentlichen dazu verwendet das Verhalten von Einzugsgebieten zu beschreiben, Hochwasservorhersagen zu treffen, integrierte Bewirtschaftungspläne von Flusseinzugsgebieten zu erstellen und Vorhersagen über den Einfluss des Klimawandels zu formulieren. Die Verwendung hydrologischer Modelle setzt in der Regel einen Kalibrierungsprozess voraus, in welchem die Werte der Modellparameter bestimmt werden. Die Güte hydrologischer Modelle und somit deren Anwendbarkeit wird durch diese Modellparameter, sowie durch die Qualität und Quantität der Eingangsdaten, die Modellstruktur und die klimatischen Verhältnisse im betrachteten Einzugsgebiet bestimmt. Ein Primärziel der modernen Hydrologie ist dabei, die Verbesserung der Übertragbarkeit hydrologischer Modellparameter von beobachteten auf unbeobachtete Regionen bzw. Zeiträume und somit die Bereitstellung zuverlässigere Prognosen über die Abflusscharakteristik für unbeobachtete Regionen oder Zeiträume.

In der vorliegenden Arbeit soll untersucht werden, in wie fern die zeitliche und räumliche Übertragbarkeit von konzeptionellen hydrologischen Modellen mithilfe des derzeitigen Kenntnisstandes über Niederschlags-Abfluss-Prozesse verbessert werden kann. Dazu werden unterschiedliche konzeptionelle Niederschlags-Abfluss-Modelle, wie das HBV-Modell, HYMOD und Xinanjiang (XAJ) unter der Verwendung eines robusten Algorithmus zur Parameterschätzung (ROPE) in verschiedenen Einzugsgebieten in den USA, Deutschland und China getestet.

Konzeptionelle Niederschlags-Abfluss-Modelle werden in der Regel individuell für jedes Einzugsgebiet kalibriert, wobei angenommen wird, dass jedes Einzugsgebiet eine individuelle hydrologische Reaktion zeigt. Aus diesem Grund stellt sich die einfache Übertragung der Modellparameter von einem beobachteteten in ein unbeobachtetes Einzugsgebiet als problematisch dar. Um diese Übertragbarkeit von Modellparametern zu bewerten, wird untersucht bis zu welchem Ausmaß verschiedene Einzugsgebiete ein ähnliches dynamisches Niederschlags-Abfluss-Verhalten zeigen und ob diese mit den gleichen Werten der Modellparameter modelliert werden können. Die drei verwendeten Modelle werden dafür so umstrukturiert, dass ein zusätzlicher neu eingeführte Parameter η die Wasserbilanz steuern kann. Dieser Wasserbilanzparameter η wird dabei individuell für jedes Einzugsgebiet bestimmt, während die weiteren Modellparameter, die die Abflussdynamik steuern, für die Übertragung verwendet werden. Zur Untersuchung der Übertragbarkeit werden die drei hydrologischen Modelle jeweils mit drei verschiedenen Modellgüteparametern kombiniert und in vier verschiedenen numerischen Experimenten analysiert. Im ersten numerischen Experiment werden die Modelle für 15 ausgewählte Einzugsgebiete des Modellparame-

terschätzung Experiments MOPEX jeweils individuell kalibriert. Dabei zeigt sich, dass es schwierig ist, herauszufinden, welche Einzugsgebiete gleiche Abflussparameter besitzen. Überträgt man die Parameter von einem Einzugsgebiet A in ein anderes Einzugsgebiet B, erhält man eine gute Modellgüte für beide Einzugsgebiete. Beim umgekehrten Übertragen der Parameter vom Einzugsgebiet B ins Einzugsgebiet A jedoch nicht. Im zweiten numerischen Experiment wird die gleichzeitige räumliche Kalibrierungsweise angewandt, wobei explizit angenommen wird, dass ähnliche Einzugsgebiete die gleichen dynamischen Modellparameter besitzen. Mit dieser Vorgehensweise erhält man Modellparameter, die mit allen Einzugsgebieten gute Ergebnisse zeigen. Eine Kreuzvalidierung zeigt, dass in diesem Fall eine gute Parameterübertragung in unbeobachtete Einzugsgebiete erreicht werden kann. Im dritten numerischen Experiment werden 96 MOPEX Einzugsgebiete mit derselben Methode wie im zweiten numerischen Experiment kalibriert. Anschließend werden die dynamischen Modellparameter auf 96 andere MOPEX Einzugsgebiete übertragen. Die Ergebnisse zeigen, dass eine große Anzahl an Einzugsgebieten ähnliche dynamische Modellparameter besitzen. Die Modellergebnisse sind dabei schlechter als bei einer individuellen Kalibrierung, jedoch führt diese Übertragung der Modellparameter in unbeobachtete Einzugsgebiete dennoch zu vernünftigen Ergebnissen. Die Modellgte im zweiten Experiment ist besser als im dritten Experiment. Dies lässt schlussfolgern, dass die richtige Auswahl an Einzugsgebieten für die gemeinsame Kalibrierung wichtig ist. Im vierten numerischen Experiment werden die Modellparameter aus den 96 MOPEX Einzugsgebieten auf zwei ausgewählte Einzugsgebiete in Deutschland und China angewandt. Die Ergebnisse zeigen dabei, dass die dynamischen Modellparameter auch auf Einzugsgebiete mit anderen Bedingungen angewandt werden können.

Hydrologische Modelle sind für die Parameterbestimmung zu einen hohem Anteil auf Beobachtungsdaten angewiesen. Untersuchungen zeigen, dass Modellparameter signifikante Unterschiede bei der Kalibrierung mit Daten aus unterschiedlichen Zeiträumen aufweisen können. In dieser Arbeit wird der Fragestellung nachgegangen, in wie weit sich Modellparameter unter wechselnden Klimabedingungen auf andere Einzugsgebiete übertragen lassen. Dabei werden mithilfe des HBV-Modells und HYMOD 50 ausgewählte MOPEX Einzugsgebiete in unterschiedlichen Zeiträumen untersucht. Den Einfluss zusätzlicher Randbedingungen in der Kalibrierung wird durch den Vergleich zweier Modellgüteparameter bestimmt. Die Ergebnisse aus der Kalibrierung zeigen, dass die Modellparamater stark durch die klimatischen Verhältnisse im Kalibrierungszeitraum beeinflusst werden. Die Kalibrierung und Kreuzvalidierungsansätze des in kleine Zeitschritte unterteilten Kalibrierungszeitraums zeigen, dass die Variabilität der klimatischen Verhältnisse oftmals zu verschiedenen Modellparametern für das gleiche Einzugsgebiet führen. Werden die Modellparameter nach der Kalibrierung auf Einzugsgebiete mit stark unterschiedlichen Klimabedingungen angewandt, können durch die Kombination des Nash-Sutcliffe-Gütemaß mit zusätzlichen Randbedingungen für die Wasserbilanz immer bessere Ergebnisse erzielt werden, also ohne diese Randbedingungen. Die Übertragbarkeit der Modellparameter hängt dabei stark vom verwendeten Datensatz für die Kalibrierung ab. Dieser wird über die Ungleichheit der Einzugsgebietscharakteristik unter Verwendung der empirischen Copula-Dichte ermittelt. Um den wechselnden Größen der Modellparameter unter nicht-stationären Bedingungen zu begegnen, werden zwei Kalibrierungsstrategien anhand des HBV-Modells getestet. Die erste

Strategie beinhaltet eine gewöhnliche Kalibrierung mit vielen Teilzeiträumen. Die zweite Strategie beinhaltet eine Wetterkorrektur mithilfe einer Gewichtsfunktion. Diese Ansätze führen dabei für die meisten Simulationen zu leichten Verbesserungen der Modellgüte im Vergleich zur ursprünglichen Kalibrierung. Die Zuverlässigkeit von hydrologischen Modellen hängt stark von der Qualität und Quantität des Datensatzes ab, der für die Parameterbestimmung verwendet wird. Dabei fehlt jedoch immer noch das Wissen darüber, welchen Umfang und welche Zeitperiode der Kalibrierungsdatensatz für eine effiziente Kalibrierung des Modells umfassen soll. Zudem muss untersucht werden, wie die begrenzte Datenmenge in bestimmten Regionen für eine Modellkalibrierung sinnvoll genutzt werden kann. In dieser Arbeit werden die Einflüsse von Quantität und Qualität der Eingangsdaten auf die Bestimmung von Modellparametern untersucht. Das HBV-Modell wird dazu unter der Verwendung von Datensätzen verschiedener Quantität an 15 MOPEX Einzugsgebieten kalibriert. Die Übertragbarkeit der kalibrierten Modellparameter wird anschließend anhand zweier verschiedener Zeitperioden validiert. Die Ergebnisse zeigen, dass sich mit ansteigendem zeitlichen Umfang der Datensätze für die Kalibrierung bei der Übertragung der Modellparameter für die meisten Einzugsgebiete bessere Ergebnisse erzielen lassen. Der genaue zeitliche Umfang des Datensatzes für die Parameterbestimmung variiert dabei von Einzugsgebiet zu Einzugsgebiet. Im Allgemeinen ist jedoch ein Datenumfang von fünf bis zehn Jahren ausreichend für die Kalibrierung eines Niederschlag-Abfluss-Prozesses. Das Ergebnis zeigt auch, dass Hochwasserereignisse einen maßgeblichen Einfluss auf die Bestimmung der Parameter für den Oberflächenabfluss haben. Für Einzugsgebiete mit begrenztem Datensatz und für unbeobachtete Einzugsgebiete wird der gemeinsame Kalibrierungsansatz mithilfe von Informationen aus räumlich nahen Einzugsgebieten gewählt. Das Ergebnis zeigt, dass für mehr als die Hälfte der Simulationen, die Modellgüte durch die Verwendung von Informationen ähnlicher Einzugsgebiete leicht verbessert werden kann. Bei einem Drittel der Simulationen führt jedoch eine gemeinsame Kalibrierung zu schlechteren Modellergebnissen als bei einer individuellen Kalibrierung.

1 Introduction

1.1 Background

Hydrological models are the simplified representations of the hydrological process [Kaczmarek et al., 1996]. They are widely used around the world for multiple purposes such as water management, flood forecasting, climate change impact analysis and so forth. There are many different ways of classifying hydrological models [Clarke, 1973; Wheater et al., 1993; Beven, 2005]. The most fundamental distinction of models is usually made based on various spatial resolutions: lumped models and distributed models [Gharari, 2016]. The lumped models often deal with the entire study region as a single unit while the distributed models attempt to take account of the spatial patterns of the rainfall-runoff response within a catchment area. Along with the rapid growth of computer science and technology, the past several decades have seen a prompt development of rainfall-runoff models of various types and complexities of physical processes and spatial representations [Singh et al., 1995]. They range from simple empirical models, conceptual bucket models, to physically-based models.

No matter what type or scale a rainfall-runoff model belongs to, it was usually designed to be implemented in a particular watershed to fulfill a specific set of objectives, and its assumptions and approaches may not be valid under all conditions across different kinds of watersheds [Shamseldin, 1997; Abrahart et al., 2002]. Nearly, most of the model applications require calibration procedure to identify the model parameters and strongly depend on the how well the models are calibrated. The applications are often limited by the quality or quantity of input data, the model structure, the uncertainty of model parameters and the change of climate conditions for both gauged and ungauged regions [Beven and Freer, 2001; Beven, 2005]. Improving the transferability of hydrological model parameters and providing more reliable predictions of runoff characteristics is nowadays the primary goal of modern hydrology.

Hydrological modeling is always done for a specific catchment with observed precipitation, temperature and discharge data [Bárdossy et al., 2016]. The unknown and partly not measurable model parameters of a conceptual or to some extent physical-based model are typically adjusted in a calibration procedure to reproduce the measured runoff from the observed meteorological data and catchment characteristics. Due to the high variability of catchment properties and hydrological behavior [Beven, 2000], this modeling procedure is usually performed individually for each catchment. Different catchments are normally modeled using different models. This great variety of models and catchments makes a generalization of the description of the hydrological processes very challenging [Sivapalan,

2003]. Additionally, even for a selected model applied for a specific catchment, the parameter identification is still not unique. A great number of parameter sets might lead to a very similar performance for the model calibration [Beven and Freer, 2001].

Moreover, due to over-reliance on measured discharge for model calibration and validation, estimation of model parameters for ungauged basins is a tremendous challenge. Instead of model calibration, parameters should rather be estimated on the basis of other information [Sivapalan, 2003]. A decade of worldwide research efforts have been carried out for the runoff Prediction in Ungauged Basins (PUB) [Hrachowitz et al., 2013]. The PUB synthesis book [Blöschl, 2013] takes a comparative approach to learning from similarities between catchments and summarizes a great number of interesting methods that are being used for predicting runoff regimes in ungauged basins.

A commonly used way to obtain variables in ungauged catchments is to transfer information from gauged catchments. Central to this approach is the selection of supposedly similar catchments. In general, catchment similarity can be defined as apparent similarity as well as functional similarity [Oudin et al., 2008, 2010]. The apparent similarity is defined on the basis of observable catchment properties (e.g. drainage area, shape factor or land use), while the functional similarity, which reflects the transformation of precipitation to discharge, could be formulated using dependence measures relating discharge series or tested through the utilizing of hydrological models. For understanding target catchment processes based on previously studied catchments, information needs to be transferred from a similar catchment based on the similarity between donor and receiver catchments. The drawback of using only catchment characteristics as attributes for classification is that similarity in catchment properties does not necessarily result in similarity in catchment hydrological response [Oudin et al., 2010]. The point is how to increase our knowledge about the overlap between the apparent similarity and the functional similarity, how can we best represent catchment characteristics of form. Many attempts have been made to develop catchment classification schemes to identify groups of catchments which behave similarly [Grigg, 1965; Sawicz et al., 2011; Ali et al., 2012; Sivakumar and Singh, 2012; Toth, 2013]. However, the task is of great importance. McDonnell and Woods [2004] discussed the need for a widely accepted classification system and Wagener et al. [2007] pointed out that a good classification would help to model the rainfall–runoff process for ungauged catchments.

Razavi and Coulibaly [2012] give a comprehensive review of catchment regionalization methods for predicting streamflow in data-limited and ungauged basins. Catchment similarity can be determined by comparing their corresponding discharge series. Correlations [Archfield and Vogel, 2010] or copulas [Samaniego et al., 2010] can be used for this purpose. Much of the variability in discharge time series is controlled by the climate patterns. Therefore, it is likely that similarity in discharge is higher for catchments with well correlated weather, which often requires geographical closeness [Archfield and Vogel, 2010]. However, discharge series generated by similar catchments can be significantly different under different meteorological conditions. Even the same catchment behaves differently in a dry and a wet period. Due to the different weather forcing, the above methods would consider that the same catchment in one time period as dissimilar to itself in another period.

The functional similarity can be defined using hydrological models [McIntyre et al., 2005;

Oudin et al., 2010; Razavi and Coulibaly, 2012]. Catchments are similar if they can be modeled reasonably well by the same model using the same model parameters [Bárdossy, 2007]. Due to observational errors and specific features in the calibration period, the adjustment of the model can be very specific to the observation period leading to an overcalibration [Andréassian et al., 2012]. To overcome such limitations, a regional calibration [Fernandez et al., 2000] approach is suggested to identify single parameter sets that perform well for all catchments within the modeled domain. Parajka et al. [2007] indicate that the iterative regional calibration indeed reduced the uncertainty of most parameters. Regional calibration can result in a better temporal robustness than normal individual calibration [Gaborit et al., 2015]. It provides an effective approach in large-scale hydrological assessments [Ricard et al., 2012] and prediction in ungauged catchments [Bárdossy et al., 2016].

Since climate change becomes a major issue in both science and society, the impacts of climate change on hydrology have been extensively investigated over the past two decades [Vaze and Teng, 2011; Vaze et al., 2011; Coron et al., 2012]. Previous studies have shown that climate change caused by increasing atmospheric concentration of greenhouse gases may have significant influence on the water availability and hydrological circulations [Rind et al., 1992]. Floods and droughts are the greatest potential natural disasters that "stimulates" other factors such as economics, industry, agriculture and others to adapt to the changes in climate behavior [Barnett and Adger, 2007]. It is really important for hydrologists to be able to predict the potential impact of climate change on catchment behaviors and therefore develop sustainable water management strategies. Under the changing climate conditions and land use types, the hydrological process may be considered as non-stationary. The statement "hydrological non-stationarity" has been widely used to describe climate and runoff variability evident in different time periods within a long hydro-climate time series to changes in hydrological responses and catchment characteristics [Chiew et al., 2014; Vaze et al., 2015]. Milly et al. [2007] initiated significant discussions and considerable investigations on the researches of hydrological non-stationarity.

The non-stationarity conditions also cause several inconveniences for the application of hydrological models. An applicable rainfall-runoff model should be able to capture the essential features of the target catchment and therefore be transferable to different conditions. As many model applications are based on the stationary assumptions, this questions the sufficiency for predicting further changes or time variability. A considerable amount of researches have shown that parameter estimations for different calibration time period might be significantly different. This limits the application of hydrological models under non-stationary conditions [Bastola et al., 2011; Li et al., 2012].

In addition, the reliability of hydrological models is highly influenced by the quality and quantity of data sets used for model parameter identification [Yapo et al., 1996; Beven, 2011]. Previous studies [Duan et al., 1994; Yapo et al., 1996] have indicated that the data selected for model calibration should be "representative" of the various phenomena experienced by the catchments. Some people have attempted to satisfy this requirement by using as large as data sets possible. However, observation records of continuous hydro-meteorological data that used for model calibration and validation are available only for a small number of sites. Thus, the application of hydrological models is often limited due to the lack of observation

data.

This thesis is an attempt to investigate the spatial and temporal transferability of conceptual hydrological models in making better usage of the available knowledge and technology on rainfall-runoff processes of catchments. The simultaneous calibration of hydrological models in geographical space was introduced and applied in different regions. The transferability of model parameters in time within different climate conditions was tested. The strategies of simultaneous calibration for multi sub-periods and weight functions were applied to reduce the uncertainty of hydrological model parameters under non-stationarity conditions. Moreover, the influences of data quality and quantity over the calibration period on model parameters parameterization were evaluated.

1.2 Outline of the thesis

This thesis is an attempt to pave a way toward a framework which can: lead to a better understanding of conceptual hydrological models, a better understanding of the interaction of model performance and catchment characteristics, robust estimation of model parameters and prediction in ungauged basins.

In the next chapter (chapter 2), this work starts with a description of the three selected regions used in this study.

The theoretical background of hydrological models and performance criteria is briefly viewed in Chapter 3.

Chapter 4 elaborates the parameter optimization strategy used for model calibration. The basic idea and an example of the Robust Parameter Estimation(ROPE) algorithm [Bárdossy and Singh, 2008] is explained.

In Chapter 5, the development of a new technique for simultaneous calibration of hydrological models in a geographical space is described. The models are restructured by introducing a new parameter η which exclusively controls water balances. Three hydrological models combined with three different performance measures are used in four different numerical experiments to investigate the transferability of dynamical parameters.

In Chapter 6, the temporal transferability of model parameters under changing climatic conditions is investigated. The effects of incorporating bias constraints into calibration routines when model parameters are used for predicting runoff in different weather conditions are tested by a comparison of two different performance measures. The common calibration for multi sub-periods and the weather adjustment with weight function strategies are introduced to cope with the instability of hydrological model parameters under the non-stationary circumstance.

Chapter 7 deals with the impacts of quality and quantities of data series on model calibration. This chapter also provides the use of the method for data limited area and ungauged basins.

At the end of this thesis (Chapter 8), a summary of this study and a short outlook of the future work are outlined.

2 Study Area

The studies were held in three different regions. The research experiments were mainly carried out on the 279 MOPEX catchments located in the eastern United States. The Upper Neckar catchment, located in the southern part of Germany and the Chengcun catchment, located in eastern of China were selected for testing the spatial transferability of hydrological models. The overview of the study areas is presented in this chapter.

2.1 The MOPEX catchments

The first study area consists of 279 catchments distributed in the eastern half of the United States. Figure 2.1 shows the location of the streamgauges for these catchments. The catchments are a subset of the catchments used for the international Model Parameter Estimation Experiment (MOPEX) project [Duan et al., 2006; Brooks et al., 2011]. MOPEX is an international project aimed at developing enhanced techniques for the a priori estimation of parameters in hydrologic models and in land surface parameterization schemes of atmospheric models [Duan et al., 2006]. The MOPEX hydrological dataset has been widely used for hydrological model comparison studies and catchment classification research in recent decades [Sawicz et al., 2011; Kollat et al., 2012; Arsenault et al., 2013; Sawicz et al., 2014].

The MOPEX data set includes hydro-meteorological data for more than 400 U.S. catchments. Data available at each catchment contains daily precipitation, maximum and minimum air temperature, potential evapotranspiration and streamflow. Streamflow information within this dataset was originally provided by the United States Geological Survey (USGS) gauges, while precipitation and temperature were supplied by the National Climate Data Center (NCDC).The daily potential evapotranspiration was calculated based on the National Oceanic and Atmospheric Administration (NOAA) Evaporation Atlas [Farnsworth and Thompson, 1983]. A total of 279 catchments which are minimally impacted by human influences were considered in this study (Figure 2.1). Data for most of the selected catchments is available from the first day of 1948 to the end of 2003.

These study catchments range in size from 67 km^2 to 10 096 km^2 and range in elevation between 21 m and 1 212 m above sea level. The climates in this region vary considerably due to a great variety of topographic and geographical conditions. The environment situation changes from marine to dry to moist from the west to the east coast while ranging from cold to hot climate from northern to southern part of the United States, The study area lies in the moist environment with three different climate conditions based on Koeppen-Geiger climate classification, which is still the most frequent classification system used today [Kottek et al., 2006]. The runoff coefficients which relate observed discharge volumes to precipitation are

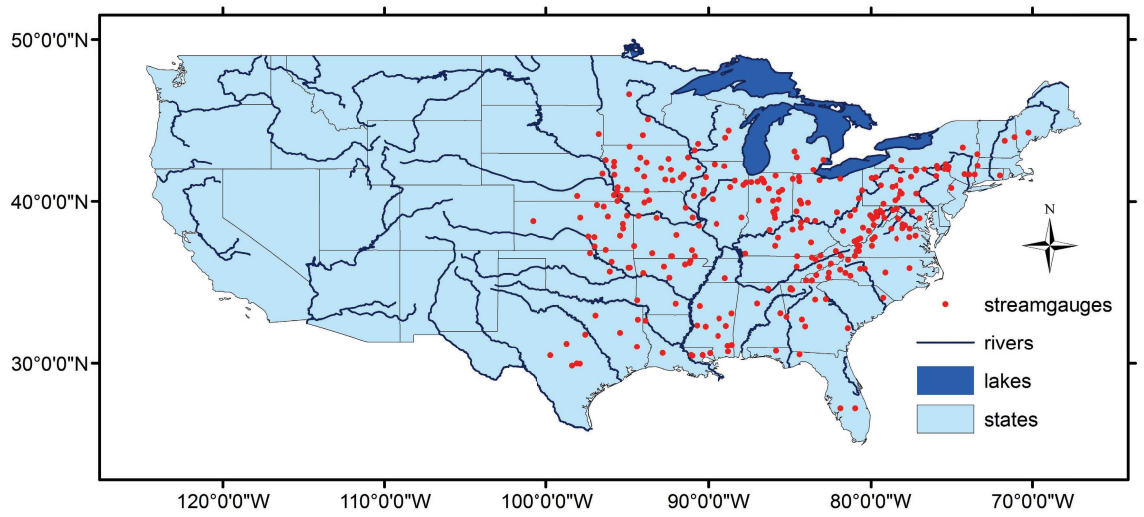

Figure 2.1: Study area: 279 MOPEX catchments in the eastern United States.

between 0.046 and 0.754 for these catchments. Figure 2.3 plots the value of runoff coefficients for the selected MOPEX catchments. From this color map, we can see clearly that the runoff coefficients show a quite smooth spatial behavior and the climate situation changes from dry to moist from the west to the east coast.

The study was mainly tested on 15 selected catchments with reliable data and slightly varying catchment properties. The locations of the streamgauges for these 15 selected catchments are shown in Figure 2.4. These 15 catchments are all influenced by humid continental climate with relatively cool summers and heavy snow in winters. Table 2.1 lists the core catchment properties [Falcone et al., 2010] and Table 2.2 summarizes the meteorological conditions for the selected 15 catchments, respectively. The tables indicate that despite their geographical proximity, these catchments have quite different climate and hydro-graphic properties.

2.2 The Upper Neckar Catchments

The Upper Neckar catchment, with a drainage area of about 4 000 km^2, is situated in South-West Germany in the state of Barden-Württemberg. A great number of hydrologically related researches have been done in this region [Samaniego, 2003; Hartmann, 2007; Götzinger, 2007; Singh, 2010] with elevations ranging from 238 m above sea level at the watershed outlet to about 1 000 m in the upstream site that is covered by vegetation and forest. The study region is influenced by Atlantic climate and is that semi-humid and temperate. The high variability in altitude is responsible for variations in climatic conditions on the local scale. Summers are relatively warm and the winters tend to be cold, the annual average temperature across the Upper Neckar catchment is about 8.7 ^{0}C. The precipitations are distributed along the whole year and show a weak seasonality. The wettest period is around

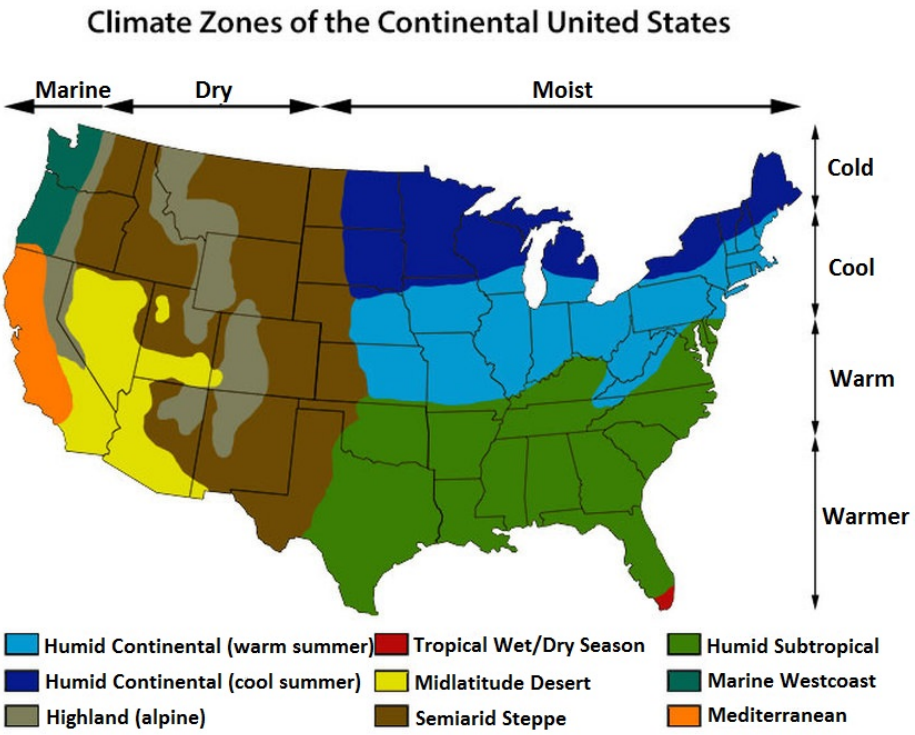

Figure 2.2: Distribution of climate zones of the continental United States. [Source: https://www.imagepermanenceinstitute.org/webfm_send/635]

the month of June, and the driest one is around the month of October. The minimum annual precipitation is around 650 mm/year in the region of Stuttgart and increases to 1 800 mm/year in the western part of the catchment.

The whole Upper Neckar catchment was divided into 13 subcatchments representing different land use and elevation types [Hartmann, 2007]. Two upstream subcatchments where the runoff characteristics are not affected by larger hydropower plants or other human activities were considered in this study. Figure 2.5 shows the locations of the selected subcatchments and Table 2.3 lists the physical and hydrological characteristics.

The historical data from 1971 to 1980 that used in this study was provided by the State Institute for Environmental Protection Baden-Württemberg. The daily precipitation from 151 rain gauges and average air temperature from 74 climatic stations were used in this research. The hydro-meteorological input required for the rainfall-runoff model was interpolated from the observations with External Drift Kriging [Ahmed and De Marsily, 1987] using topographical elevation as external drift [Das et al., 2008]. The discharge data from Rottweil and Suessen streamgauges was collected for modeling.

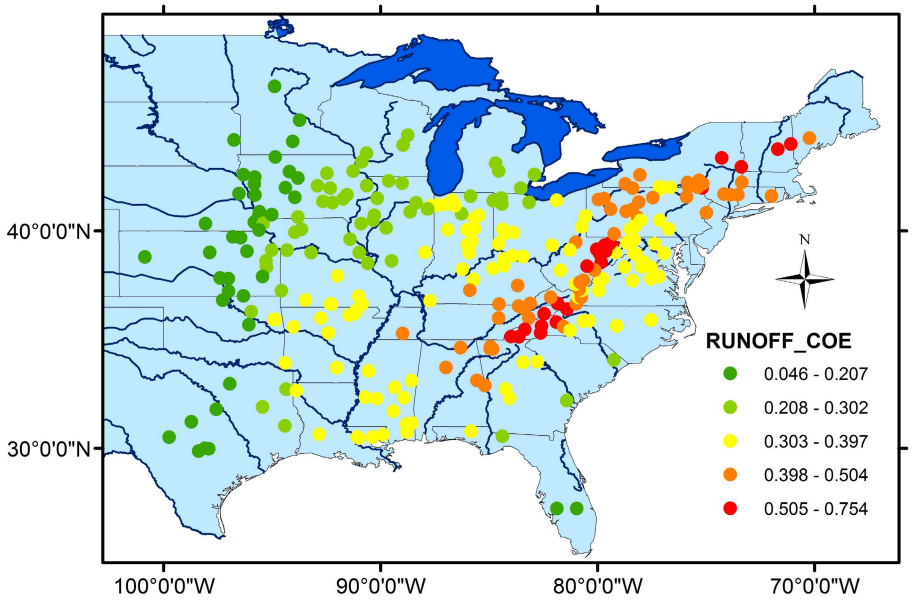

Figure 2.3: Spatial distribution of runoff coefficients for the 279 selected MOPEX catchments in the eastern United States.

2.3 The Chengcun Catchment

The chengcun catchment is located in the southern mountainous area of Anhui Province, China (Figure 2.6). The size of this catchment is 290 km^2 and the longest stream length is around 3.6 km. The long-term annual average precipitation is nearly 1 600 mm/year. Due to the dominance of monsoon climate [Yao et al., 2012], more than 60% of annual rainfall occurs during the flood season (mainly from May to August). The annual potential evapotranspiration is approximately 670 mm/year. The average maximum and minimum air temperature are about 24 ^{0}C and 0 ^{0}C, respectively.

For the Chengcun catchment, daily precipitation, potential evapotranspiration and observed streamflow were provided by Anhui Hydrological Bureau, China. The available data from 1986 to 1995 was selected for model simulation in this study.

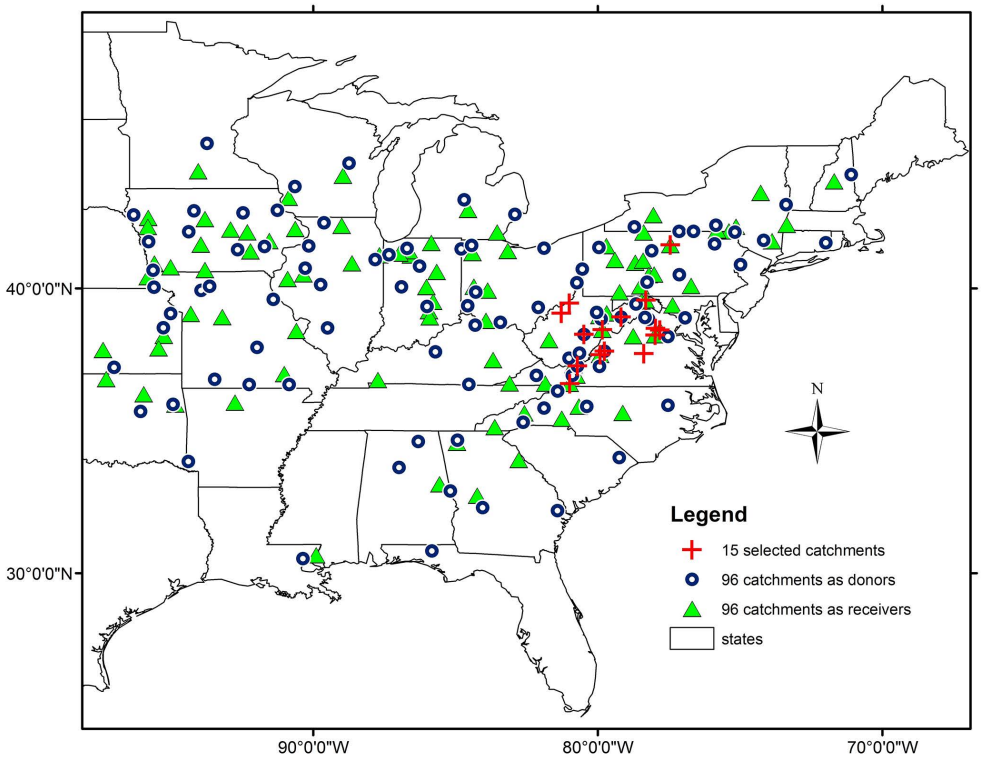

Figure 2.4: Location of the MOPEX catchments selected for the experiments. The red plus symbols show the location of 15 selected catchments in a close geometrical setting; the blue circles show 96 randomly selected catchments and the green triangles show another set of 96 catchments.

Table 2.1: Catchment characteristics for the 15 selected MOPEX catchments.

Streamgauge ID	Streamgauge name	Drainage area (km^2)	Shape factor	Field capacity	Average porosity	Base flow index	Snow proportion (%)
01548500	Pine Creek at Cedar Run, PA	1564	0.14	0.32	0.42	0.44	26.6
01606500	So. Branch Potomac River near Petersburg, WA	1663	0.15	0.31	0.28	0.45	19.5
01611500	Cacapon River near Great Cacapon, WV	1753	0.17	0.269	0.27	0.41	15.6
01663500	Hazel River at Rixeyville at Rixeyville, VA	743	0.16	0.30	0.39	0.51	12.1
01664000	Rappahannock River at Remington, VA	1606	0.11	0.294	0.40	0.50	11.8
01667500	Rapidan River near Culpeper, VA	1222	0.13	0.32	0.40	0.51	10.6
02016000	Cowpasture River near Clifton Forge, VA	1194	0.18	0.28	0.27	0.43	16.0
02018000	Craig Creek at Parr, VA	852	0.24	0.27	0.30	0.44	11.3
02030500	Slate River near Arvonia, VA	585	0.20	0.30	0.46	0.48	8.5
03114500	Middle Island Creek at Little, WV	1186	0.14	0.36	0.27	0.21	15.6
03155500	Hughes River at Cisco, WV	1171	0.14	0.36	0.27	0.22	14.9
03164000	New River near Galax, VA	2929	0.09	0.29	0.43	0.64	13.3
03173000	Walker Creek at Bane, VA	790	0.24	0.32	0.37	0.46	13.5
03180500	Greenbrier River at Durbin, WV	344	0.26	0.36	0.27	0.37	25.3
03186500	Williams River at Dyer, WV	332	0.33	0.36	0.28	0.36	24.3

Table 2.2: Climate variables for the 15 selected MOPEX catchments.

No	Streamgauge ID	Annual precipitation (mm)	Average temperature (^{o}C)	Annual potential evapotranspiration (mm)	Annual runoff (mm)
1	01548500	951.7	7.2	727.0	495.1
2	01606500	948.6	10.3	716.3	378.3
3	01611500	905.6	10.8	800.0	310.5
4	01663500	1049.9	11.7	897.2	402.6
5	01664000	1027.7	12.0	906.1	367.5
6	01667500	1087.4	12.3	915.2	380.4
7	02016000	1029.5	11.0	746.0	402.9
8	02018000	1010.6	11.4	764.6	406.3
9	02030500	1075.9	13.5	918.2	350.3
10	03114500	1089.7	11.4	737.4	483.9
11	03155500	1057.8	11.6	740.0	443.7
12	03164000	1247.9	10.6	807.4	593.3
13	03173000	958.6	11.1	762.7	371.9
14	03180500	1224.2	8.3	710.9	543.2
15	03186500	1401.5	9.1	710.9	945.0

Table 2.3: Catchment characteristics for the two selected subcatchments in the Upper Neckar catchment.

Subcatchments	Drainage area (km^2)	Mean elevation (m)	Annual precipitation (mm)	Average temperature (^{o}C)	Annual runoff (mm)
Rottweil, Neckar	454.7	700.0	929.0	7.5	363.2
Süssen, Fils	345.7	625.2	1003.5	8.5	543.3

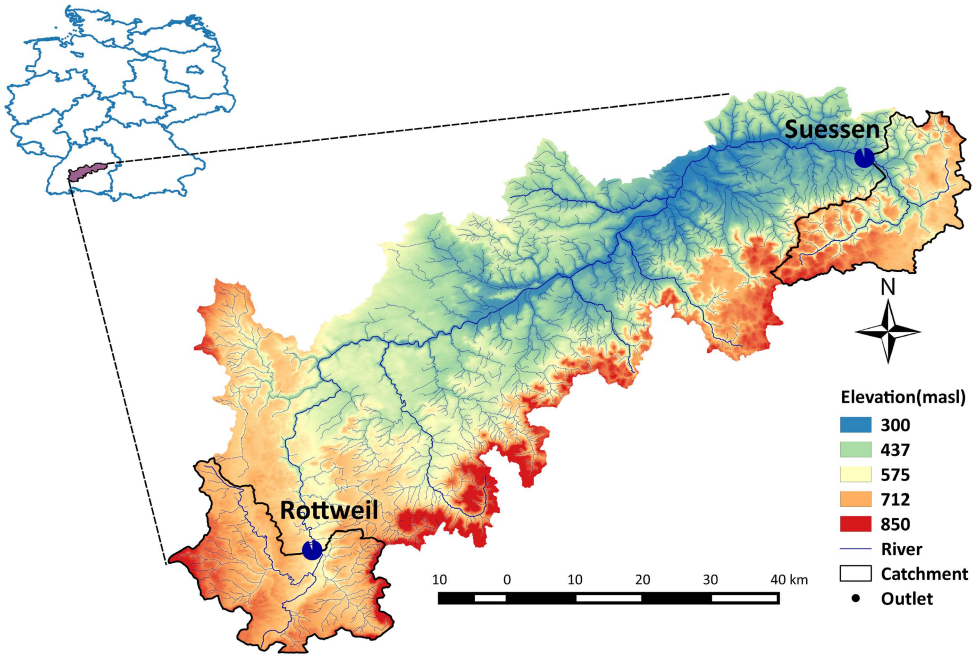

Figure 2.5: Study area: two selected subcatchments in the Upper Neckar catchment, Germany.

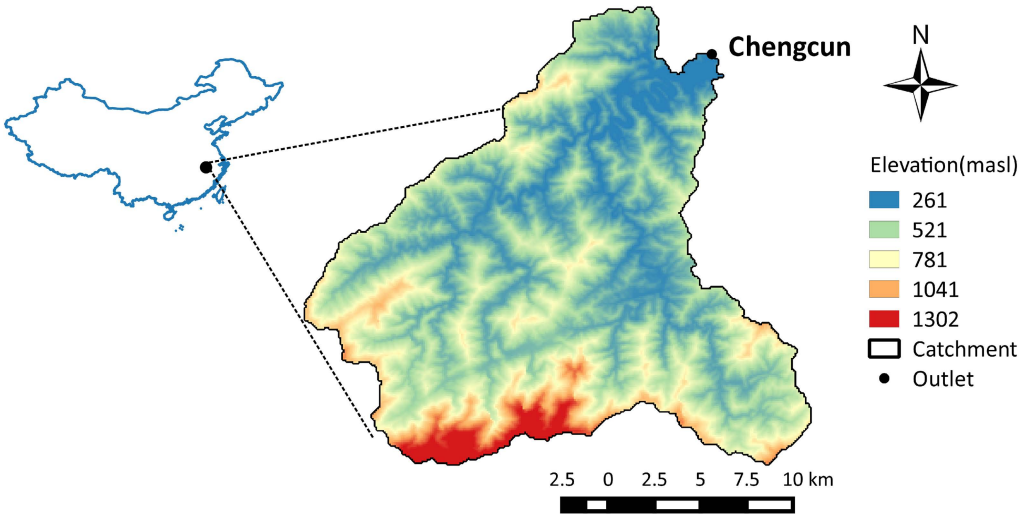

Figure 2.6: Study area: Chengcun catchment in the southeast of China.

3 Hydrological Models and Performance Criteria

Hydrological models are widely used to describe the rainfall-runoff behaviors for catchments. Different models always have different levels of complexity in conceptualization and parameterization. Therefore, it is critical to see if the simulation results are similar to different models and performance measures. In this study, three conceptual models with five different performance measures were considered and compared. The overview of the models and performance criteria used in this research are presented in this chapter.

3.1 Hydrological Models

In this research, we used three simple conceptual rainfall-runoff models: HBV, HYMOD and Xinanjiang model. The reason for this is that the vast number of calibration and validation experiments could only be easily performed with relatively simple model structures.

3.1.1 HBV Model

The conceptual HBV model was developed by the Swedish Meteorological and Hydrological Institute (SMHI) in early 1972 [Bergström and Forsman, 1973]. It has been widely used in rainfall-runoff simulation for the reason of few free calibration parameters and simple to use and calibrate. The model version used in this research has been modified at the Institute for Modeling Hydraulic and Environmental Systems (IWS), University of Stuttgart. Figure 3.1 shows the schematic representation of HBV-IWS model [Singh, 2010]. The model consists of conceptual routines for snow accumulation and snowmelt, soil moisture and runoff generation, runoff concentration within the subcatchments, and flood routing of the flow in the river network [Hartmann, 2007; Singh, 2010].

In HBV model, the amount of snow accumulation and snowmelt is calculated by a degree-day method [Rango and Martinec, 1995] as shown in Equation 3.1, including two parameters of degree-day factor (DD) and threshold temperature for snowmelt (TT). In this approach, it is assumed that if the air temperature (T) is above the threshold temperature, the observed precipitation is considered to occur as rainfall, otherwise, as snowfall.

$$Snowmelt = DD \cdot (T - TT), \quad \text{if} \quad T > TT \tag{3.1}$$

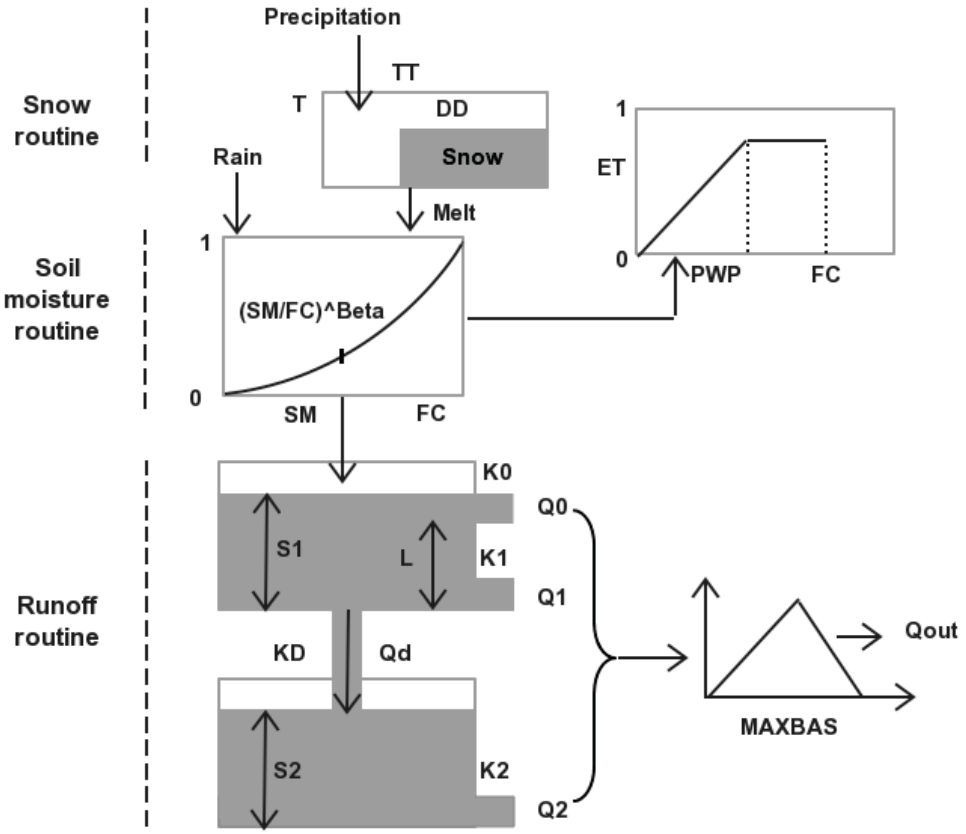

Figure 3.1: Schematic representation of lumped HBV model [Singh, 2010].

In general, soil moisture is calculated by balancing precipitation and evapotranspiration using field capacity (*FC*) and permanent wilting point (*PWP*) as parameters. The index of wetness ($\frac{\Delta Q}{\Delta P}$) can be calculated as follow:

$$\frac{\Delta Q}{\Delta P} = (\frac{SM}{FC})^{Beta} \tag{3.2}$$

Here *SM* represents the actual soil moisture and $Beta$ is a shape factor. The potential evapotranspiration for a given day (E_{tp}) is calculated by long-term monthly average potential evapotranspiration (PE_M) and long-term monthly average temperature (T_M) that based on the Penman formula [Penman, 1948]:

$$E_{tp} = (1 + C(T - T_M))PE_M \tag{3.3}$$

Here C is the coefficient of evapotranspiration. The actual evapotranspiration (E_{ta}) is calcu-

lated as below:

$$E_{ta} = \begin{cases} E_{tp} & \text{if} \quad SM > PWP \\ \frac{SM}{PWP} \cdot E_{tp} & \text{else} \end{cases} \tag{3.4}$$

Runoff generation is calculated by a non-linear function of actual soil moisture and effective precipitation as shown in Equation 3.2. Afterwards, runoff routing on the hill slopes is modeled by two parallel non-linear reservoirs representing the direct surface flow and the groundwater response:

$$Q_0 = K_0(S_1 - HL) \tag{3.5}$$

$$Q_1 = K_1 S_1 \tag{3.6}$$

$$Q_d = K_d S_1 \tag{3.7}$$

$$Q_2 = K_2 S_2 \tag{3.8}$$

Where Q_0 is the surface runoff, Q_1 is the interflow, Q_d is the percolation from the upper reservoir to the lower reservoir and Q_2 is the baseflow. K_0, K_1, K_d and K_2 represent the surface flow storage constant, interflow storage constant, percolation storage constant and baseflow storage constant respectively. S_1 is the upper reservoir water level while S_2 is the lower reservoir water level. *HL* is the threshold water level for surface discharge.

The sum of the outflows from upper and lower reservoirs ($Q_0 + Q_1 + Q_2$) represents the total runoff. The total outflow is then smoothed using a transformation function, consisting of a triangular weighting function with parameter *MAXBAS*.

Inputs for lumped HBV model are daily precipitation, average air temperature, long-term mean monthly potential evapotranspiration and temperature. There are in total 15 parameters to describe the model, out of which nine parameters are selected for calibration in this study. Table 3.1 shows the general range of the parameters which need to be calibrated by the model.

Table 3.1: Description of the HBV model parameters and parameter ranges for model calibration.

Parameter	Description	Max	Min
TT	Threshold temperature for snowmelt (^{0}C)	2	-2
DD	Degree-day factor	3	1.5
FC	Field capacity (mm)	600	50
Beta	Shape coefficient	8	0.2
K_0	Near surface flow storage constant	0.8	0.2
K_1	Interflow storage constant	0.25	0.1
K_2	Baseflow storage constant	0.1	0.01
K_d	Percolation storage constant	0.2	0.05
HL	Threshold water level for near surface flow (mm)	100	1

3.1.2 HYMOD Model

The HYMOD [Boyle et al., 2001] is a conceptual rainfall-runoff model based on the probability-distributed principle of Moore [1985]. Figure 3.2 shows the schematic representation of HYMOD model. The model assumes that the soil moisture storage capacity varies across each catchment and the proportion of the catchment with saturated soils varies with time. The soil moisture accounting module of HYMOD utilizes a Pareto distribution function of storage elements of varying sizes. The storage elements of the catchment are distributed according to a probability density function defined by the maximum soil moisture storage *CMAX* and the distribution of soil moisture store β [Wagener et al., 2001]. Evaporation from the soil moisture store occurs at the rate of the potential evaporation estimates using the Hamon approach [Hamon, 1963]. After evapotranspiration, the remaining rainfall and snowmelt are used to fill the soil moisture stores. A routing module divides the excess rainfall using a split parameter α which separates fluxes amongst two parallel conceptual linear reservoirs meant to simulate the quick (R_q) and slow flow response (R_s) of the system (defined by residence times k_q and k_s). More detailed description of the model can be found in Moore [1985]; Boyle et al. [2001] and Wagener et al. [2001].

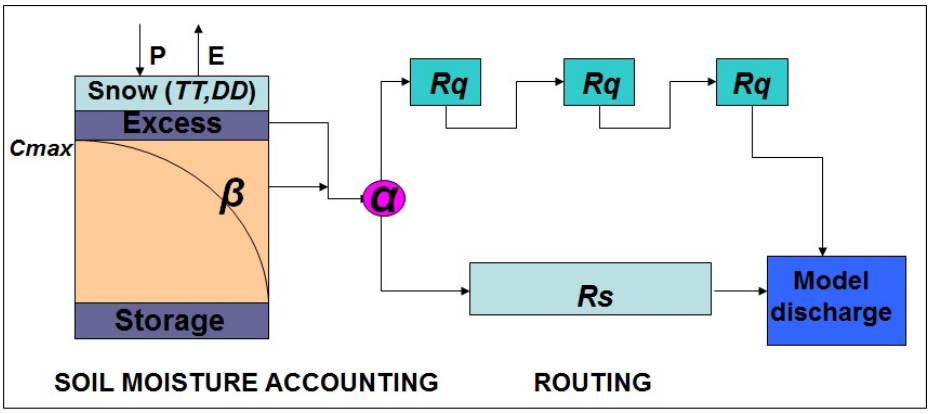

Figure 3.2: Schematic representation of lumped HYMOD model.

In this study, the model is configured as a lumped version that using the entire catchment as the computing unit. Table 3.2 shows the general range of the seven parameters that need to be calibrated by model with historical data.

3.1.3 Xinanjiang Model

The Xinanjiang model (XAJ) was established by Hohai University, China in the early 1970s [Zhao and Liu, 1995]. Similar to the HBV and HYMOD model, the XAJ model is a general purpose model for rainfall-runoff simulation, flood forecasting and water resources planning and management. The main feature of XAJ model is the concept of runoff formation on the repletion of storage, which means the flow is not produced until the soil moisture concern of the aeration zone reaches field capacity, and thereafter runoff equals the rainfall

Table 3.2: Description of HYMOD model parameters and parameter ranges for model calibration.

Parameter	Description	Max	Min
TT	Threshold temperature for snowmelt (^{0}C)	2	-2
DD	Degree-day factor	3	1.5
CMAX	Maximum soil moisture storage (mm)	600	50
β	Degree of spatial variability of the soil moisture capacity	8	0.2
α	Flow distributing factor	0.8	0.2
k_s	Residence times of the slow reservoir	0.2	0.01
k_q	Residence times of the quick reservoirs	0.8	0.2

excess without further loss [Yao et al., 2012]. This conceptual rainfall-runoff model has been applied to a large number of catchments in the humid and semi-humid regions in China. The lumped version of XAJ model consisted of four main components [Zhao and Liu, 1995]. The evapotranspiration is represented by a three-layer soil moisture module which differentiates upper, lower and deeper soil layers. Runoff generation is calculated based on rainfall and soil storage deficit; tension water capacity curve is introduced to provide a non-uniform distribution of tension water capacity throughout the whole catchment. The runoff separation module separates the determined runoff into three parts, namely surface runoff, interflow and groundwater. Finally, the flow routing module transfers the local runoff to the outlet of the catchment. The flow chart of the XAJ model is shown in Figure 3.3.

In XAJ model, the actual evapotranspiration depends on the soil moisture conditions and the potential evaporation. The areal mean soil moisture capacity (*WM*) is normally divided into three components: the upper part (*WUM*), the lower part (*WLM*) and the deeper part (*WDM*). Here, *WU*, *WL* and *WD* represent the storage state corresponding to these three-layers, while *EU*, *EL* and *ED* stands for the evapotranspiration from corresponding layers [Zhao and Liu, 1995]. Firstly, the evapotranspiration occurs at the potential rate until the storage on the upper layer is exhausted. Afterwards, according to the water storage in the lower layer, any remaining potential evapotranspiration is applied to it with certain reduction by parameter *C*. Finally, the evapotranspiration is applied to the deeper layer when the lower storage *WL* is reduced to a specified proportion. The actual evapotranspiration can be calculated by the following formulas:

if $P + WU \geqslant E_{tp}$, then

$$EU = E_{tp}, EL = 0, ED = 0 \tag{3.9}$$

if $P + WU < E_{tp}$, then

$$EU = P + WU \tag{3.10}$$

if $WL \geqslant C \times WLM$, then

$$EL = (E_{tp} - EU) \times \frac{WL}{WM}, ED = 0 \tag{3.11}$$

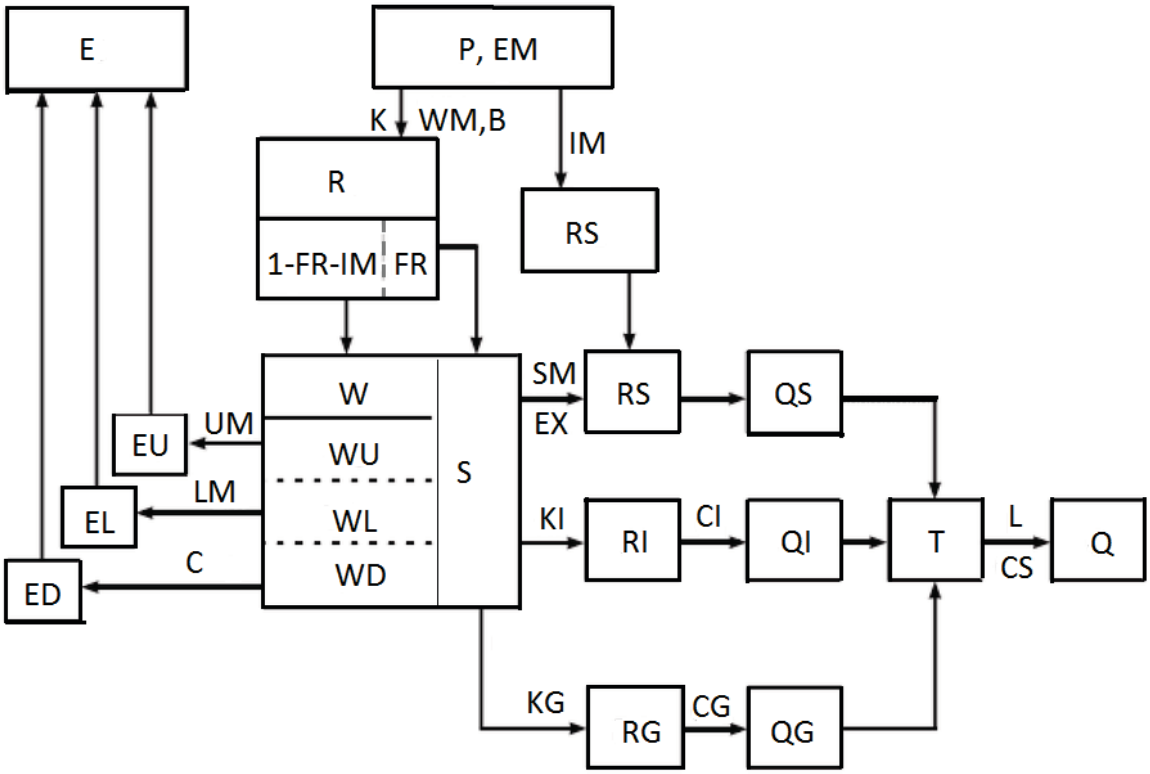

Figure 3.3: Flow chart of the XAJ model [Zhao and Liu, 1995].

else if $WL < C \times WLM$ and $WL \geqslant C \times (E_{tp} - EU)$, then

$$EL = C \times (E_{tp} - EU), ED = 0 \tag{3.12}$$

else if $WL < C \times WLM$ and $WL < C \times (E_{tp} - EU)$, then

$$EL = WL, ED = C \times (E_{tp} - EU) - WL \tag{3.13}$$

Where P is the effective rainfall amount. E_{tp} represents the potential evapotranspiration and C is the coefficient of tension water capacity.

In XAJ model, a distribution of tension water capacity is suggested by Zhao and Liu [1995] to deal with the non-uniform distribution of soil moisture deficit. Figure 3.4(a) represents the proportion of the previous area of the study catchment whose tension water capacity is less than or equal to the value of the ordinate $W'M$. WMM is the maximum tension water capacity and the tension water capacity at a given point can be estimated by the following relationship:

$$(1 - f/F) = (1 - W'M/WM)^B \cdot (1 - IM) \tag{3.14}$$

Here B is the index of tension water capacity and IM represents the ratio of impervious area to the whole catchment.

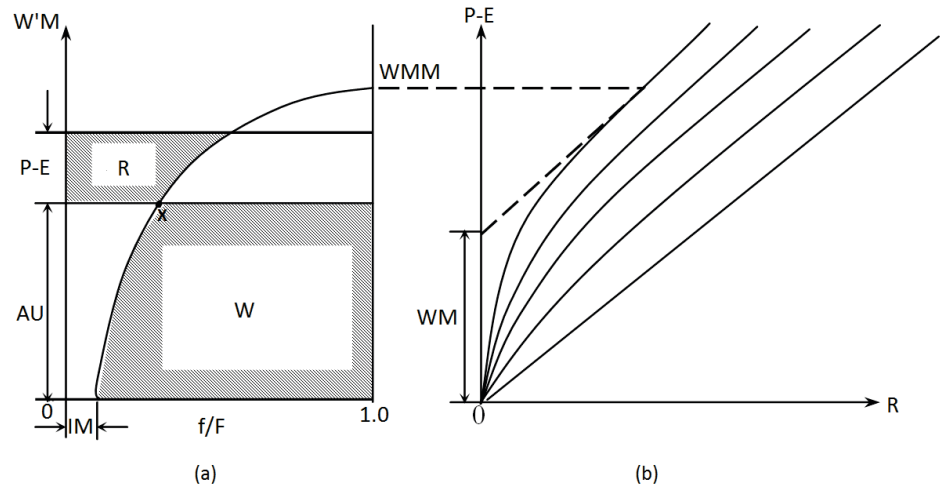

Figure 3.4: The distribution of tension water capacity (a) and rainfall-runoff relationship (b) of XAJ model.

The area mean tension water capacity *WM* constitutes an alternative parameter to *WMM* Zhao and Liu [1995]. These are connected by the shape factor parameter B, which can be shown by the integration of Equation 3.14:

$$WMM = WM \cdot (1 + B)/(1 - IM) \tag{3.15}$$

As shown in Figure 3.4(a), the soil state of the catchment is assumed to be represented by a point x on the curved line. The area to the right and below this point is proportional to the areal mean tension water storage W. By doing this, we assumed that each point in the catchment is either at capacity tension (points to the left of x) or at a constant tension (points to the right of x) [Zhao and Liu, 1995].

If the effective rainfall amount exceeds the actual evapotranspiration, the ordinate of Figure 3.4(a) is increased by the excess, then point x moves upwards along the curve and runoff is generated proportional to the gray area as shown in Figure 3.4(a). The generated runoff can be calculated as below:

If $P - E_{tp} + AU$ is less than *MM*, the generated runoff R is:

$$R = P - E_{tp} - WM + W + WM \cdot (1 - (P - E_{tp} + AU)/WMM)^{(1+B)} \tag{3.16}$$

otherwise,

$$R = P - E_{tp} - WM + W \tag{3.17}$$

Similar to HBV model, the runoff produced of XAJ model during relatively wet time period is further separated into three parts: surface runoff (*RS*), interflow (*RI*) and groundwater (*RG*) (Figure 3.5). These three different components normally take different ways from the location where they were produced to the local streams. Afterwards, they will flow together towards the catchment outlets, forming the outflow of the catchment. The surface runoff

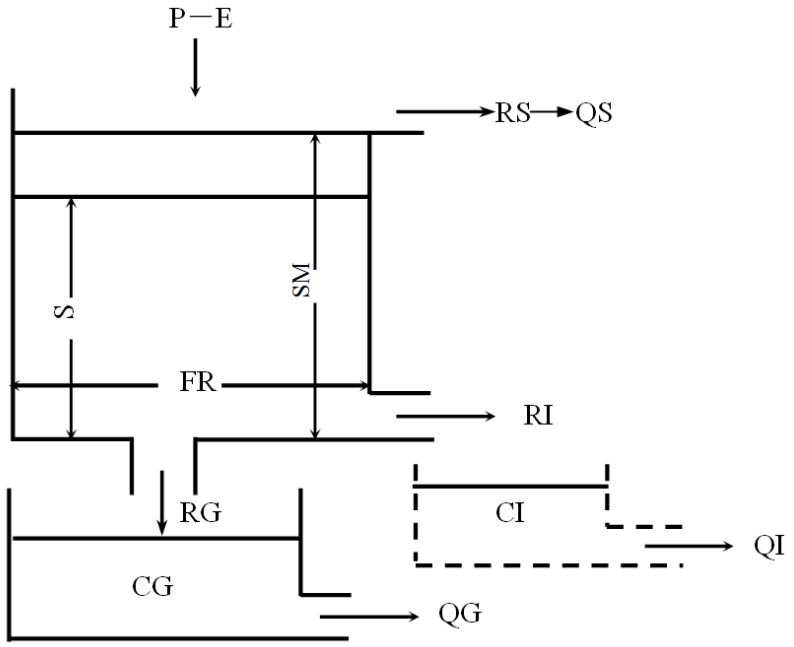

Figure 3.5: Structure of free-water reservoir [Zhao and Liu, 1995].

is treated to be unmodified passing over the hillslope while the interflow and groundwater are routed through linear reservoirs by parameter *KI* and *KG* [He, 2008].

XAJ model was originally applied for the southeast region of China and the snowmelt routine was not considered in the model. In this study, to account for the precipitation that is contributed from snowmelt, the degree-day snowmelt approach is added in the model. A total of 16 parameters were selected to be adjusted using calibration. Table 3.3 lists the general range of the parameters needed to be calibrated by the model.

3.2 Model Performance Criteria

Hydrological models are often used for different purposes and usually different objective functions are used for model calibration. Previous studies have shown that model calibration depends strongly on the performance criteria used [Yapo et al., 1998; Madsen, 2000]. In this study, in order to obtain reasonable general results and investigate the effect for the selection of objective functions, five different criteria including Nash-Sutcliffe efficiency, Kling-Gupta, the logarithm transformed flow Nash-Sutcliffe efficiency, the combination of Nash-Sutcliffe and logarithm transformed flow Nash-Sutcliffe and the combination of Nash-Sutcliffe and Bias constraint were applied to evaluate the model performance.

Table 3.3: Description of XAJ model parameters and parameter ranges for model calibration.

Parameter	Description	Max	Min
TT	Threshold temperature for snowmelt (^{0}C)	2	-2
DD	Degree-day factor	3	1.5
K	Evapotranspiration coefficient	1.2	0.3
B	Exponent of tension water capacity	0.9	0.3
C	Coefficient of tension water capacity	0.4	0.02
WM	Areal mean tension water capacity (mm)	250	100
WUM	Upper layer areal mean tension water capacity (mm)	50	5
WLM	Lower layer areal mean tension water capacity (mm)	100	30
IM	Area of impervious/total area	0.03	0.01
SM	Areal mean of water capacity (mm)	200	10
EX	Exponent of freewater capacity curve	1.8	1
KG	Outflow coefficient of freewater storage to groundwater	0.5	0.1
KI	Outflow coefficient of freewater storage to interflow	0.5	0.1
CG	Recession constant of groundwater storage	1	0.95
CI	Recession constant of lower interflow storage	0.9	0.6
CS	Recession constant of near surface flow	0.7	0.01

3.2.1 Nash-Sutcliffe Efficiency

The Nash-Sutcliffe Efficiency [Nash and Sutcliffe, 1970] between the observed and modeled runoff is the most frequently taken as the first evaluation criterion.

$$O^{(1)} = 1 - \frac{\sum_{t=1}^{T} \left(Q_o(t) - Q_m(t)\right)^2}{\sum_{t=1}^{T} \left(Q_o(t) - \bar{Q_o}\right)^2} \tag{3.18}$$

Here $Q_o(t)$ is the observed discharge and $Q_m(t)$ is the simulated discharge on a given day t. The abbreviation NS is used subsequently for this performance measure.

3.2.2 Kling-Gupta Efficiency

This model performance criterion was often criticized [Schaefli and Gupta, 2007] and several modifications and other criteria were suggested. One interesting suggestion was published in Gupta et al. [2009], the authors suggest using a performance measure which accounts for the water balances and the correlation of the observed and modeled time series separately. Their approach was slightly modified, and the following performance criterion was introduced:

$$O^{(2)} = 1 - \alpha \left(\frac{\sum_{t=1}^{T} \left(Q_o(t) - Q_m(t)\right)}{\sum_{t=1}^{T} Q_o(t)} \right)^2 - (1 - r(Q_o, Q_m))^2 \tag{3.19}$$

Here $r(Q_o, Q_m)$ is the correlation coefficient between the observed and modeled time series of discharge. α is a weight to express the importance of the water balance - in our case $\alpha = 5$ was chosen. The reason for selecting this version of the coefficient is that a model should produce good water balances and appropriate discharge dynamics simultaneously. The quadratic form in Equation (3.19) assures that both aspects are considered, and the worst of them is dominating. The abbreviation GK is used subsequently for this performance measure.

3.2.3 Logarithm Transformed Flow NS

The Nash-Sutcliffe coefficient of the logarithm of the discharges is focusing on the low flow conditions more than the traditional NS efficiency.

$$O^{(3)} = L_{NS} = 1 - \frac{\sum_{t=1}^{T} \left(\log(Q_o(t)) - \log(Q_m(t))\right)^2}{\sum_{t=1}^{T} \left(\log(Q_o(t)) - \log(\bar{Q}_o)\right)^2} \tag{3.20}$$

The abbreviation LNS is used subsequently for this performance measure.

3.2.4 Combination of NS and Logarithm Transformed Flow NS

To equally concentrate on high and low flows, a combination of the original and the logarithmic NS is used as a fourth measure:

$$O^{(4)} = \frac{O^{(1)} + O^{(3)}}{2} \tag{3.21}$$

The abbreviation (NS+LNS) is used subsequently for this performance measure.

3.2.5 Combination of NS and Bias Constraint

There are many methods of incorporating a bias constraint in model objective function [Madsen et al., 2002; Chiew et al., 2009]. One useful suggestion was offered by Viney et al. [2009], the authors propose to incorporate bias constraints into calibration routines by using the following performance criterion:

$$O^{(5)} = NS - 5\,|ln(1 + B)|^{2.5} \tag{3.22}$$

Here B is the the bias value, representing the difference between the modeled and observed discharges over the whole calibration time period with respect to the total observed discharges:

$$B = \frac{\sum_{t=1}^{T} Q_m(t) - \sum_{t=1}^{T} Q_o(t)}{\sum_{t=1}^{T} Q_o(t)} \tag{3.23}$$

The constants in Equation (3.22) are the balancing factors to control the severity and shape of the resulting constraint penalty. Figure 3.6 shows the form of the log-bias constraint. The coefficients of Equation (3.22) control the severity and shape of the resulting constraint penalty. This kind of coefficient could help a model simulation to produce appropriate discharge dynamics and achieve good water balances simultaneously [Viney et al., 2009]. The abbreviation NSB is used subsequently for this performance measure.

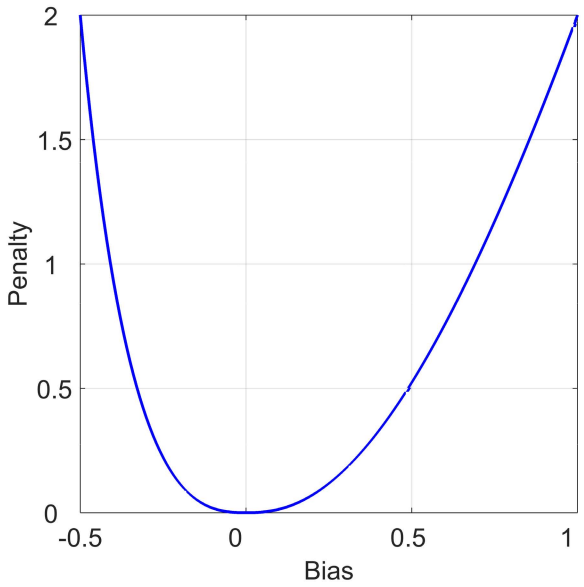

Figure 3.6: Graphical representation of the penalty for the log-bias constraint.

In the model application, all these five performance criteria have been modified as the higher their value, the better the model performs. The best possible value for all of them is 1.

4 Robust Estimation of Model Parameters

As the performance of a hydrological model strongly depends on the model parameters that calibrated using historical data, obtaining model parameters is a very important task to be done. The value of those parameters should be estimated in such a good way in order to reproduce runoff series using the historical data as closely as possible to the observed discharge. This approach leads to minimizing the errors in order to achieve a good model performance. Gupta et al. [2003] defined this simulation process as a model calibration. Generally, model calibration can be carried out in two ways. A prior type called manual calibration is a method which relies on the determination of model parameters chosen by the experts and hydrologists [Gupta et al., 1998]. However, this approach still has some shortcomings as it is a very subjective case and time-consuming [Gupta et al., 2003]. The second method for model calibration is the automatic calibration which takes the algorithm to optimize the parameters based on the predetermined objective functions. Boyle et al. [2001] pointed out that the automatic calibration beats the manual calibration in terms of relatively fast and easiness of its implementation. In this research, model parameters were estimated by automatic calibration after firstly setting the initial values of parameters within certain ranges. The automatic Robust Parameter Estimation (ROPE) algorithm [Bárdossy and Singh, 2008], which was developed by Bardossy and Singh at University of Stuttgart, was taken for model calibration and parameter optimization in this research.

The non-uniqueness of the model parameters makes the model calibration complicated [Bárdossy, 2007]. With the help of the ROPE algorithm, it is possible to find multiple sets of proper parameters and to identify the deep parameter vectors, which could efficiently minimize the uncertainty of model parameters [Bárdossy and Singh, 2008; Krauße et al., 2013a]. This chapter gives a brief introduction about the concept and the general idea of the ROPE algorithm.

4.1 Data Depth

The ROPE algorithm was developed based on the concept of data depth. A great number of mathematicians have focused on the studies of computational geometry and multi-variate statistics, and they have found that points being geometrically deep within a data set are more robust to represent the whole data set [Krauße et al., 2013a]. Researches also indicate that these robust points can be estimated by the concept of data depth [Liu et al., 2006; Serfling, 2006].

4.1.1 Definition

Data depth, as a key concept of non parametric approach for the analysis of multivariate data[Vencálek, 2011], was first introduced by Tukey [1975] in the 1970S. Data depth is a function of measuring how deep (central) a given point is relative to the whole dataset [Liu et al., 1999].It is a useful tool for defining order or ranks of multivariate data. According to the definition of depth function, a point that is located at the boundary has a lower depth value, and a position close to the center always has a higher depth. Data depth increase monotonically from the boundary that has a low depth to a higher depth at the center.

In a multivariate data set, in order to have a consistent and well-founded center-outward ordering of data points, a depth function normally should fulfill the following four properties [Zuo and Serfling, 2000]:

- Affine invariance: The depth of a given point should not depend on the underlying coordinate system. In other words, the depth values will not be changed by the choice of axes and it is useful to remove the scale effect when treating several variables.
- Maximality at Center: For a multivariate data set, the depth function should always reach maximum value at the center.
- Monotonicity Relative to Deepest Point: The data depth should decrease monotonically as moving away from the deepest point.
- Vanishing at Infinity: When moving away from the deepest position to infinity, the depth of a given point should reach the minimum value.

4.1.2 Half-space Depth

There are several types of data depth functions that have been widely used in different fields of scientific research. Among them, Mahalanobis depth [Mahalanobis, 1936], convex hull peeling depth [Liu et al., 1999] and half-space depth [Tukey, 1975] are the well-known measures in non-parametric statistics and computational geometry. Liu et al. [2006] provided a detailed overview of different kinds of depth functions and the corresponding applications for multivariate data analysis.

The data depth measure used in this study is the half-space depth. The reasons for the selection of half-space depth is that it has proved to be a very robust measure to identify the center of a multivariate data set. In the following, a brief introduction of half-space depth is described.

For a given set X in the d dimensional space R^d, the half-space depth for a specific point p is defined as the minimum value of points of the whole data set that lying on one side of a hyperplane through p [Bárdossy and Singh, 2008]. It should be noted that the minimum number is estimated over all possible hyperplanes. Therefore, the half-space depth of the given point p with respect to the data set X in the d dimensional space R^d is:

$$D_X(p) = \min_{n_h}(min(|\{x \in X(n_h, x-p) > 0\}|), (|\{x \in X(n_h, x-p) < 0\}|)) \tag{4.1}$$

Here n_h is an arbitrary unit vector that denoting the standard vector of a selected hyperplane. Points on the center have high depth value while points near the boundary have relatively low depth. In this section, as shown in Figure 4.1, we took a two dimension data set to illustrate the systematic estimation of data depth for half-space depth. The x-axis represents the first parameter and the y-axis represents the second parameter, respectively. Ten black circulars were distributed in these two dimensional space and the data depth of the rectangular point was assumed to be calculated using half-space depth. Firstly, as shown in Figure 4.1(a), a random hyperplane was drawn passing through the rectangular point. The total number of circulars at each side of this hyperplane was measured and the minimum value of these two sides was recorded. Afterwards the hyperplane was turned around continuously in clockwise direction for all 360-degree (Figure 4.1(b∼d)) For each rotation, the number of circulars lying on both sides was counted and the minimum number of them was recorded. Finally, the minimum value of all these minimum numbers was considered as the data depth for the rectangular point. In this example, the minimum value of the minimums is 4, so the depth of the rectangular point is 4 in the bivariate data set. The half-space depth function fulfilled all the properties of depth function [Zuo and Serfling, 2000] and it is invariant to affine transformations of the space [Liu et al., 1990; Singh, 2010].

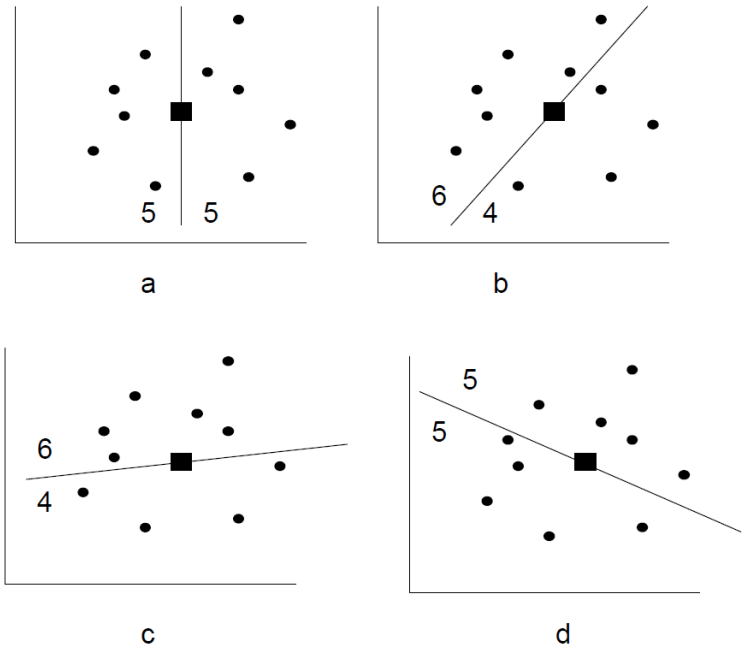

Figure 4.1: Schematic example of the half-space depth function [Singh, 2010].

4.2 Robust Parameter Estimation algorithm

Based on the concept of half-space depth function, Bárdossy and Singh [2008] introduced the ROPE algorithm to identify robust model parameter vectors. The benefits of the ROPE algorithm is that it could ensure the calibrated model parameter sets are representative and insensitive. The following describes the general procedure of the ROPE algorithm [Bárdossy and Singh, 2008]:

(1) Determination of the possible range of the d selected model parameters;

(2) Generation of a predetermined number (n) of random parameter vectors forming the set X_N in the d dimensional rectangle boundary by the ranges defined in step 1;

(3) Operation of the hydrological model for each parameter vector in X_N and assessment of the corresponding model performances;

(4) Identification of the subset X_N^* of the good performing parameters;

(5) Generation of new random parameter sets Y_M according to the "good" subset X_N^* based on the half-space depth function;

(6) Replacement of the set X_N with Y_M and repetition of step 3∼6 until the model performances corresponding to X_N and Y_M do not differ more than the expected observation errors [Singh, 2010].

Figure 4.2 shows a pictorial explanation of the ROPE algorithm. As a first step, based on the possible range of model parameters, a large pre-determined number of parameter sets (X_N) is generated randomly as shown in Figure 4.2(a). Afterward, the hydrological model is run for all parameter sets and the best subset ($X_N^{'}$) of the parameters is selected as shown in Figure 4.2(b). After removing the parameters outside the boundary of the subset $X_N^{'}$, another set of the same number of parameters is generated such that it has higher depth and the parameters are within the boundary space (Figure 4.2(c)). The model is run again and the new "best" subset of parameters is selected according to the simulated model performance. The cycle of iteration is continued until the pre-determined number of iterations is over or the variation in model performance is within a selected range. By doing this, calculation goes deeper and deeper into a data set which gives a more structured combination of model parameters.

The ROPE algorithm is a powerful tool for the model parameter optimization as the study shows that the parameter vectors with high depth are more insensitive and transferable to other time period. More details about the ROPE algorithm can be found in Singh [2010] and Krauße et al. [2013b].

Figure 4.3 and Figure 4.4 present an example for the distribution of calibrated HBV model parameters and model performance, respectively. For a MOPEX catchment (catchment ID: 01548500), HBV model was selected to simulate the rainfall-runoff behavior for the period 1971-1980 using NS as objective function. And the observed data from 1991 to 2000 was used to validate the model performance. A total of 9 parameters were adjusted in the model and

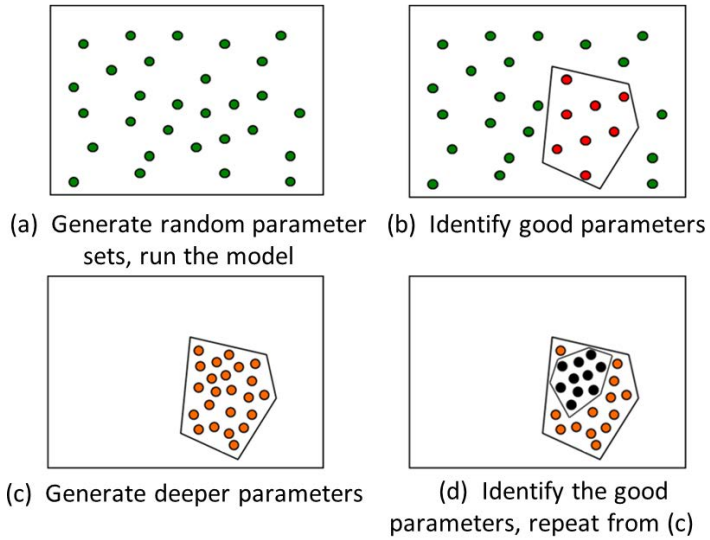

Figure 4.2: Systematic representation of the ROPE algorithm.

a pre-determined number (10 000 in this example) of parameter sets was identified using the ROPE algorithm. We can see clearly from Figure 4.3 that the calibrated parameters are very heterogeneous. However, the model performances are similar for the calibration period and the transfer to a different time period works quite well. The example denotes that the data depth based parameter sampling can be beneficial for the identification of robust hydrological model parameters.

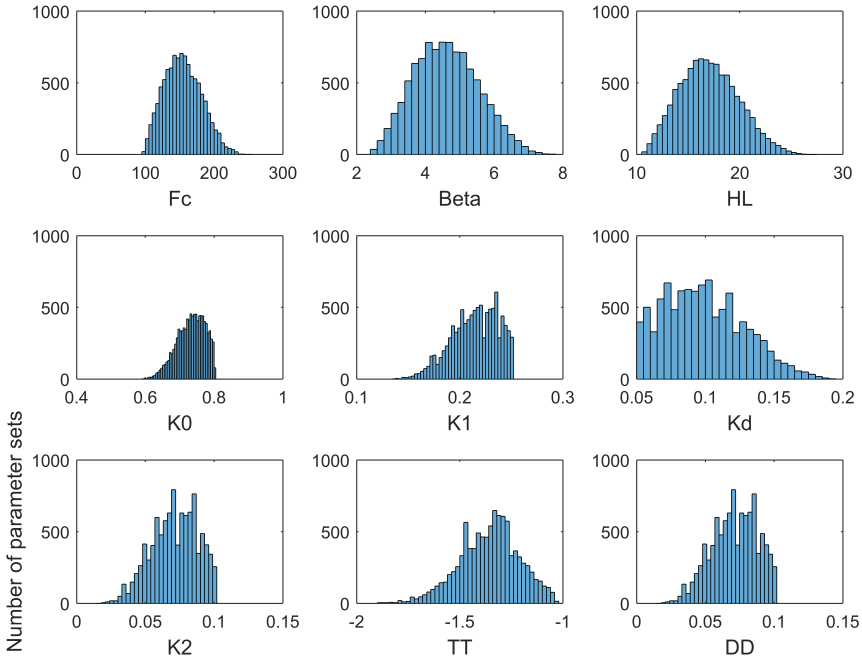

Figure 4.3: An example of model parameters calibrated using the ROPE algorithm. A total of 9 HBV model parameters were calibrated for a MOPEX catchment (streamgauge ID: 01548500) using the data set from 1971 to 1980. NS was taken as the performance measure.

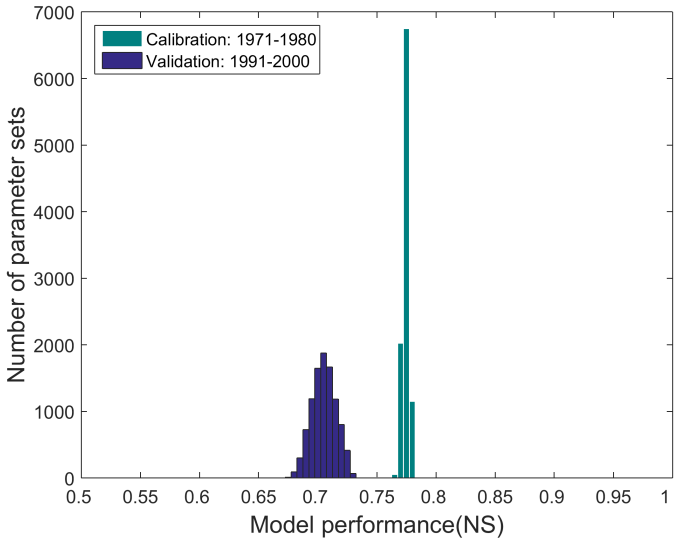

Figure 4.4: An example of the NS model performance that parameters were calibrated using the ROPE algorithm. HBV model was calibrated for a MOPEX catchment (streamgauge ID: 01548500) for the period 1971-1980 and validated for 1991-2000.

5 Simultaneous Calibration of Hydrological Models

This chapter presents the approach of simultaneous calibration of hydrological model parameters in geographical space and its application in ungauged basins.

5.1 Introduction

Hydrological models are widely used to describe catchment behavior, and for subsequent use for water management, flood forecasting, and other purposes. Hydrological modeling is usually done for catchments with observed precipitation and discharge data. The unknown (and partly not measurable) parameters of a conceptual or to some extent physics-based model are adjusted in a calibration procedure to reproduce the measured discharge from the observed weather and catchment properties. Due to the high variability of catchment properties and hydrological behavior [Beven, 2000], this modeling procedure is usually performed individually for each catchment. Different catchments are often modeled using different models. This great variety of models and catchments makes a generalization of the description of the hydrological processes very challenging [Sivapalan, 2003]. Additionally, even for a selected model applied for a specific catchment, the parameter identification is not unique. A great number of parameter vectors might lead to a very similar performance [Beven and Freer, 2001].

Moreover, due to over-reliance on measured discharge for model calibration, estimation of model parameters for ungauged basins is a big challenge. Instead of model calibration, parameters should rather be estimated on the basis of other information [Sivapalan, 2003]. A decade of worldwide research efforts have been carried out for the runoff prediction in ungauged basins (PUB) [Hrachowitz et al., 2013]. The PUB synthesis book [Blöschl, 2013] takes a comparative approach to learning from similarities between catchments and summarizes a great number of interesting methods that are being used for predicting runoff regimes in ungauged basins. Many attempts have been made to develop catchment classification schemes to identify groups of catchments which behave similarly [Grigg, 1965; Sawicz et al., 2011; Ali et al., 2012; Sivakumar and Singh, 2012; Toth, 2013]. However, the task is of great importance. McDonnell and Woods [2004] discussed the need for a widely accepted classification system and Wagener et al. [2007] pointed out that a good classification would help to model the rainfall–runoff process for ungauged catchments.

Razavi and Coulibaly [2012] give a comprehensive review of regionalization methods for predicting streamflow in ungauged basins. Catchment similarity can be determined by comparing their corresponding discharge series using correlation [Archfield and Vogel, 2010] or

copulas [Samaniego et al., 2010]. Much of the variability in discharge time series is controlled by the weather patterns. Therefore, it is likely that similarity in discharge is higher for catchments with well correlated weather, which often requires geographical closeness [Archfield and Vogel, 2010]. However, discharge series produced by similar catchments can be very different under different meteorological conditions. Even the same catchment behaves differently in a dry and in a wet year. Due to the different weather forcing, the above methods would consider the same catchment in one time period as dissimilar to itself in another time period.

One can also define catchment similarity using hydrological models [McIntyre et al., 2005; Oudin et al., 2010; Razavi and Coulibaly, 2012]. Catchments are similar if they can be modeled reasonably well by the same model using the same model parameters [Bárdossy, 2007]. Due to observational errors and specific features in the calibration period, the adjustment of the model can be very specific to the observation period leading to an overcalibration [Andréassian et al., 2012]. To overcome such limitations, a regional calibration [Fernandez et al., 2000] approach is suggested to identify single parameter sets that perform well for all catchments within the modeled domain. Parajka et al. [2007] indicate that the iterative regional calibration indeed reduced the uncertainty of most parameters. Regional calibration can result in a better temporal robustness than normal individual calibration [Gaborit et al., 2015] and it provides an effective approach in large-scale hydrological assessments [Ricard et al., 2012].

The focus of this chapter is to investigate if the transformation of precipitation to discharge can possibly be independent of the weather. For this purpose, the hydrological model parameters are separated into two groups:

1. Parameters describing the water balances which are strongly related to climate; and
2. Parameters describing the dynamics of the runoff triggered by weather.

The second group of parameters is supposed to be climate independent and represent the focus of this study. To simplify the problem, a single new parameter η was introduced to describe water balance. This parameter is conditional on the other model parameters and adjusts the long-term water balances.

The purpose of this study is to investigate to what extent do different catchments share a similar dynamical rainfall-runoff behavior and can be modeled using the same model parameters with exception of the newly introduced individualized water balance parameter η.

Hydrological models are usually judged according to the degree of reproducing discharge dynamics and water balances, while water balances are mainly driven by weather in terms of precipitation, temperature, radiation and wind. Dynamics are controlled by catchment properties in terms of size, terrain, slopes, soils, etc. Formation of Landscapes as a result of long-time climate is a quasi-equilibrium process. The hypothesis of this study is that this equilibrium is mirrored in a similar dynamic behavior. Thus a large number of catchments can be modeled by using the same dynamic parameters.

5.2 Methodology

5.2.1 Water Balance Parameter η

Climatic conditions are of central importance for water balances. The relationship of potential to actual evapotranspiration can differ strongly due to water or energy limitations. This suggests that catchments might have similar dynamical behavior but with different water balances. In order to account for this, the model parameters could be separated to form two groups, one group with parameters controlling the water balances and another controlling the discharge dynamics. This separation of existing model parameters is difficult, as they often influence simultaneously both components. Instead of an artificial model specific separation, a new parameter η was introduced to all three models. This parameter controls the ratio between daily potential and actual evapotranspiration depending on the available water and depends on the long-term water balance only. This parameter η gives:

$$E_{ta} = \begin{cases} E_{tp} & \text{if} \frac{SM}{CMAX} > \eta \\ \min\left(\frac{SM}{\eta \cdot CMAX} E_{tp}, SM\right) & \text{else} \end{cases} \tag{5.1}$$

Here *SM* is the actual soil water available for evapotranspiration. *CMAX* is the maximum possible soil moisture. E_{tp} stands for the potential and E_{ta} for the actual evapotranspiration, respectively.

The parameter η regulates the water balances in accordance with the dynamical parameters. It can be calculated directly for each parameter vector θ. This is necessary as it is thought to establish correct water balances. Thus it is a catchment and parameter vector dependent parameter. Let V_{iO} denote the total observed discharge volume and V_{iM} denote the total modeled discharge volume, respectively. $f(\eta) = V_{iM}(\eta, \theta)$ is a monotonically decreasing function of η. If the model can provide correct long-term water balances then:

$$V_{iM}(1, \theta) < V_{iO} < V_{iM}(0, \theta) \tag{5.2}$$

As $f(\eta) = V_{iM}(\eta, \theta)$ is continuous, there is a unique $\eta(\theta)$ for which:

$$V_{iM}(\eta(\theta), \theta) = V_{iO} \tag{5.3}$$

If Equation (5.2) is not fulfilled, then the parameter vector θ is not appropriate for the model.

The parameter η is fitted individually for each θ - this way a correct water balance is assured for the calibration period.

5.2.2 Design of Numerical Experiments

All three conceptual hydrological models, HBV, HYMOD and XAJ models were considered, the descriptions of these models have been presented in Chapter 3. The models were restructured by the new parameter η which exclusively controls water balances. This parameter was considered as individual to each catchment. All other parameters, which mainly control the dynamics of the discharge (dynamical parameters), were considered for spatial transfer. The NS, GK and NS+LNS performance criteria were selected for evaluating the model performance. The ROPE algorithm was applied for model parameter optimization, each calibration yielded 10 000 convex sets of good parameter vectors.

Four different numerical experiments, including calibration and validation procedures, are carried out for different sets of selected catchments:

1. The usual catchment-by-catchment calibration is carried out. In order to test if dynamical model parameters are shared, the parameters are directly transferred to all of other catchments.
2. Instead of the traditional catchment by catchment calibration, it is assumed that the model parameters are similar for a set of catchments in a close geometrical setting. Thus a simultaneous calibration of the models is carried out and tested both in a gauged and an ungauged version.
3. The geographical extent of the catchments used for simultaneous calibration is expanded. A great number of assumed ungauged catchments are used for testing the hypothesis.
4. Finally, the transferability of the model parameters to catchments under very different climatic and geographical conditions is tested.

The hypothesis is that the rainfall-runoff process can be described using the same dynamical hydrological model parameters for a number of catchments. The very different climatic conditions and water balances of the catchments are considered by the newly introduced specific parameter η controlling the long-term water balance of each catchment individually. The other model parameters control the discharge dynamics on both short and long time scales. These dynamical parameters are supposed to be shared despite the great heterogeneity of the catchments. This procedure simplifies the hydrological model parameter estimation for ungauged catchments, namely the procedure is reduced to the estimation of a single parameter η, which can be related to long-term water balances.

For a clear explanation and understanding of the methods, the procedure and results of these four experiments are presented in the following four sections.

5.3 Experiment 1: Normal Individual Calibration

As a first step, 15 MOPEX catchments with reliable data and slightly varying catchment properties in the eastern United States were selected. The details of these 15 catchments have been described in Section 2.1.

For the 15 selected catchments, an individual calibration was performed using the ROPE algorithm using all three models and three performance measures and the time period between 1971-1980. This leads to 9 calibrations for each catchment. Each calibration yielded convex sets $\mathcal{G}_i$ of good parameters for each catchment i. A total of 10 000 parameter vectors from each of these sets were generated. (Note that the corresponding parameter η was estimated for each element of the parameter set separately.) Let $O_i^{(j)}(\theta)$ denote the value of the objective function j for a parameter vector θ in catchment i. The best objective function value for each individual catchment is denoted with $O_i^{(j)*}$.

Table 5.1 lists the average calibration model performance for all 15 catchments using three hydrological models and three performance measures for the calibration time period 1971-1980. As expected, the models perform differently in different catchments. The reasons for this are observation errors both in input and output and a possible inability of the model to reasonably well represent the main hydrological processes. The observed data between 1991 and 2000 were used to validate the model performance. Table 5.2 shows the average model performance for the validation period using the model parameters calibrated on 1971-1980.

Table 5.1: The mean model performances for the calibration period 1971-1980 that using three models (HBV, HYMOD and XAJ) and three modeling objectives (NS, GK and NS+LNS).

Measure	NS			GK			NS+LNS		
Catchment	HBV	HYMOD	XAJ	HBV	HYMOD	XAJ	HBV	HYMOD	XAJ
01548500	0.77	0.69	0.66	0.99	0.96	0.97	0.74	0.66	0.60
01606500	0.71	0.63	0.64	0.98	0.96	0.96	0.73	0.68	0.69
01611500	0.71	0.60	0.59	0.98	0.95	0.95	0.73	0.65	0.63
01663500	0.66	0.60	0.56	0.96	0.94	0.93	0.69	0.65	0.63
01664000	0.82	0.69	0.64	0.99	0.97	0.96	0.80	0.71	0.69
01667500	0.77	0.63	0.57	0.99	0.96	0.94	0.80	0.72	0.69
02016000	0.81	0.68	0.65	0.99	0.97	0.97	0.78	0.70	0.69
02018000	0.74	0.63	0.63	0.98	0.96	0.96	0.71	0.66	0.67
02030500	0.71	0.56	0.53	0.98	0.94	0.93	0.75	0.64	0.64
03114500	0.71	0.60	0.52	0.98	0.95	0.95	0.67	0.62	0.51
03155500	0.70	0.59	0.53	0.98	0.95	0.95	0.65	0.61	0.53
03164000	0.87	0.72	0.69	1.00	0.98	0.97	0.85	0.74	0.73
03173000	0.77	0.67	0.66	0.98	0.97	0.97	0.73	0.67	0.68
03180500	0.71	0.67	0.66	0.98	0.97	0.96	0.71	0.69	0.68
03186500	0.61	0.59	0.54	0.94	0.93	0.93	0.59	0.58	0.49

The ranges of the model parameters are relatively large. As a first step, we checked if the catchments have common parameter vectors. For each pair of catchments (i, j), for the same performance measure and time period, the intersection of the convex hull of the good pa-

Table 5.2: The mean model performances for the validation period 1991-2000 that using three models (HBV, HYMOD and XAJ) and three modeling objectives (NS, GK and NS+LNS).

Measure	NS			GK			NS+LNS		
Model	HBV	HYMOD	XAJ	HBV	HYMOD	XAJ	HBV	HYMOD	XAJ
01548500	0.71	0.68	0.68	0.97	0.96	0.97	0.73	0.69	0.65
01606500	0.58	0.55	0.59	0.94	0.91	0.95	0.67	0.64	0.65
01611500	0.57	0.54	0.60	0.97	0.95	0.95	0.66	0.65	0.65
01663500	0.54	0.50	0.51	0.82	0.91	0.92	0.59	0.56	0.61
01664000	0.64	0.57	0.55	0.96	0.95	0.94	0.70	0.66	0.64
01667500	0.63	0.54	0.49	0.94	0.93	0.92	0.70	0.63	0.62
02016000	0.70	0.61	0.63	0.95	0.95	0.96	0.71	0.63	0.68
02018000	0.64	0.57	0.61	0.95	0.94	0.96	0.69	0.64	0.66
02030500	0.72	0.69	0.63	0.95	0.97	0.95	0.72	0.67	0.67
03114500	0.65	0.57	0.54	0.96	0.95	0.95	0.65	0.62	0.56
03155500	0.70	0.57	0.54	0.97	0.96	0.95	0.69	0.62	0.58
03164000	0.81	0.70	0.71	0.99	0.97	0.98	0.82	0.76	0.77
03173000	0.69	0.60	0.62	0.95	0.95	0.96	0.72	0.66	0.69
03180500	0.66	0.65	0.66	0.96	0.97	0.97	0.70	0.69	0.69
03186500	0.58	0.60	0.57	0.93	0.94	0.94	0.58	0.58	0.53

rameter sets $\mathcal{G}_i \cap \mathcal{G}_j$ is empty showing that there are no common best parameters. Seemingly none of the catchments are similar.

As a next step, the 10 000 generated best dynamical parameter vectors for a given time period and hydrological model obtained for catchment i were applied to model all other catchments using the same hydrological model and time period. Note that the value of η is not transferred but adjusted to the true long-term water balance. Figure 5.1 shows the color-coded matrices for the mean performance of the three hydrological models using transferred parameters for all 15 catchments for a calibration period (1971-1980) for the NS, GK, and NS+LNS performance measures.

The performance of the transferred parameter vectors shows a strongly varying picture. While in some cases the catchments seem to share parameter vectors with reasonably good performance, in other cases the transfer lead to weak performances. A further surprising fact is that none of the matrices is symmetrical. One can see that some catchments are good donors - their parameters are good for nearly all catchments, while others have parameters which are hardly transferable.

The asymmetry of the parameter transition matrices cannot be explained by catchment properties. Two different catchments seem to share well performing parameters if calibrated on one catchment and no common good parameters if calibrated on the other one. Examples for the NS performance are catchments 1 and 12. Parameters for catchment 1 are not good for catchment 12 for any of the hydrological models, but parameters of catchment 12 perform reasonably well for catchment 1. The matrices for NS show different performances

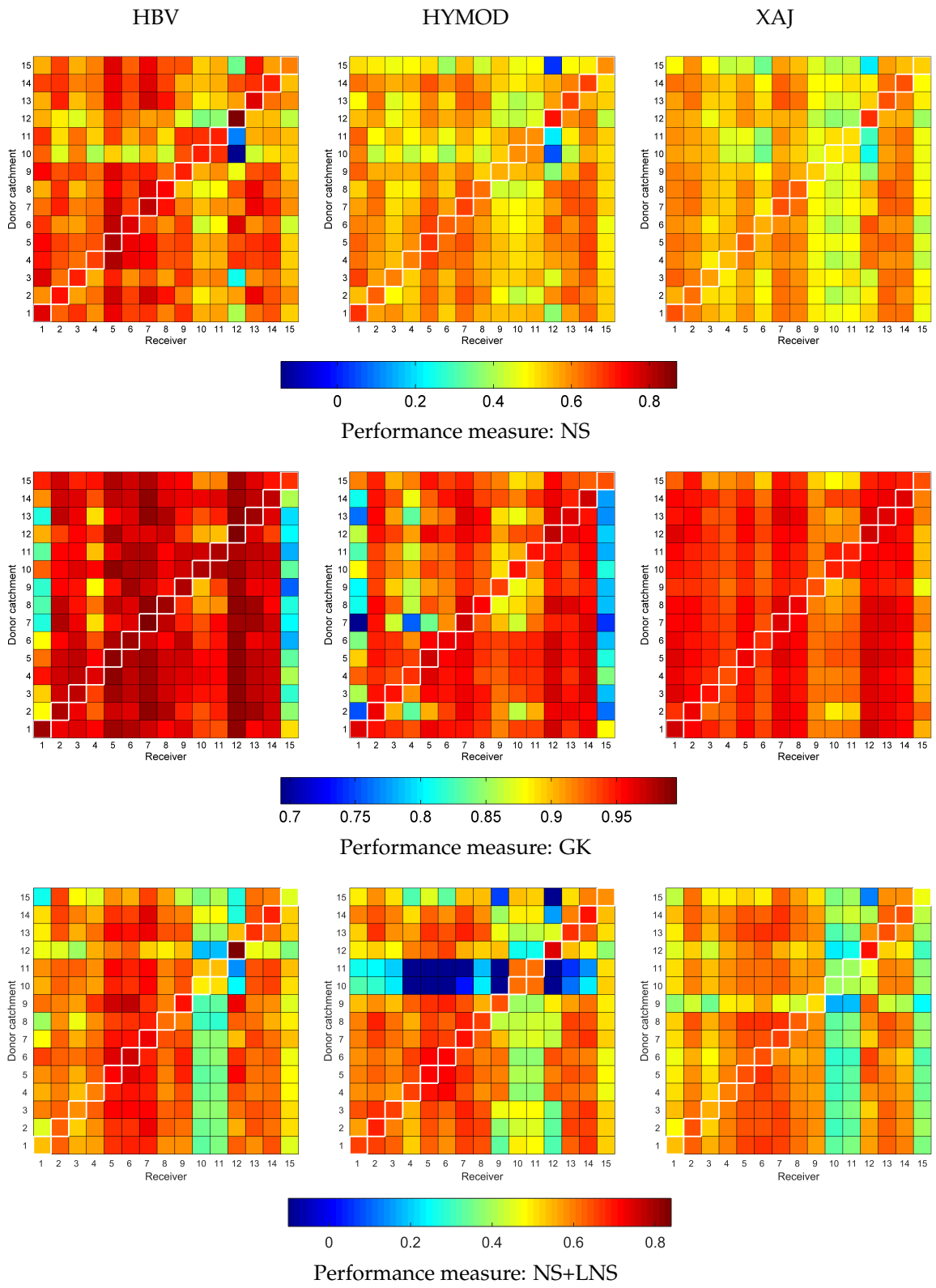

Figure 5.1: Color-coded matrices for the mean NS, GK and NS+LNS performances for the selected 15 catchments for the calibration period 1971-1980. The values of y-axis represent the catchment taken as donor catchment for parameters estimation, and the values of x-axis represent the catchment used for parameter transfer.

- HBV being the best. From the viewpoint of parameter transferability, these three models perform similarly, if a parameter transfer is reasonable from catchment i to j for one model then it is also reasonable for another model. The results for the GK performance differ from those of the NS. Here the XAJ model seems to give the generally best transferable parameters. Model parameters from other catchments are almost useless for catchment 15 for all three models.

The difference of the transferability for these three performance measures could be explained by different focuses - while NS is mainly focusing on the squared difference between the observed and modeled discharge, GK focuses on water balances and good timing and log NS is strongly influenced by low flow events. It is interesting to observe that catchment 12 is a very bad receiver for model parameters for NS, while it is an excellent receiver for GK. This means that different events have different influences on the performance. A possible explanation for the asymmetry is the fact that the catchments have different weather forcing in the calibration period. It could be that runoff events which are most important for a performance measure occur in the calibration period frequently in one catchment leading to good transferability and seldom in the other causing weak transferability of the parameters from one catchment to another.

The transferability of the model parameters was also tested for an independent validation period. Figure 5.2 shows the corresponding color-coded results for NS as the performance measure. The matrices are similar to those obtained for calibration. Catchment 12 remained a bad receiver but a good donor indicating that the bad performance is unlikely to be caused by observation errors. Further for some columns, the off-diagonal elements are larger than the diagonal ones which are a sign of a possible overcalibration.

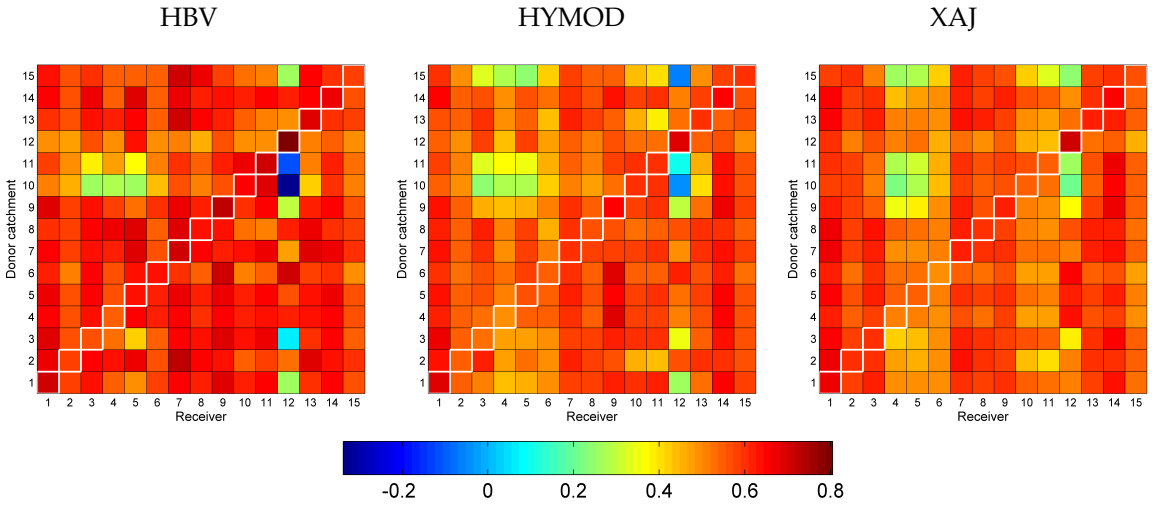

Figure 5.2: Color-coded matrix for the mean NS performances for the selected 15 catchments for the validation period 1991-2000. The values of y-axis represent the catchment taken as donor catchment for parameters estimation, and the values of x-axis represent the catchment used for parameter transfer.

To investigate the influence of climate on calibration, the hydrological models calibrated for

different time periods using the same model and the performance measure were compared. As the different time periods represent different weather conditions, the calibrations lead to different parameter sets. As a comparison, the differences in calibrated model parameters using the same model and performance measure for different catchments were compared. As an example, Figure 5.3 shows two parameters of the model from the good parameter set obtained from the calibration for catchment 13 on three different ten-year time periods. Figure 5.4 shows the same parameters obtained by calibration for three different catchments (7, 8 and 13) that all calibrated on the time period 1951-1960. The structural similarity of the two figures suggests that the difference between the different catchments is comparable to the difference between the different time periods. In hydrological modeling, it is usually assumed that model parameters are constant over time assuming no significant change in climate or other characteristics. These results, however, show that the assumption that parameters are the same over space is not completely unrealistic. The figure even suggests that there might be parameter vectors which perform reasonably well for all 15 catchments. Thus as a next step, an experiment to test this assumption was devised.

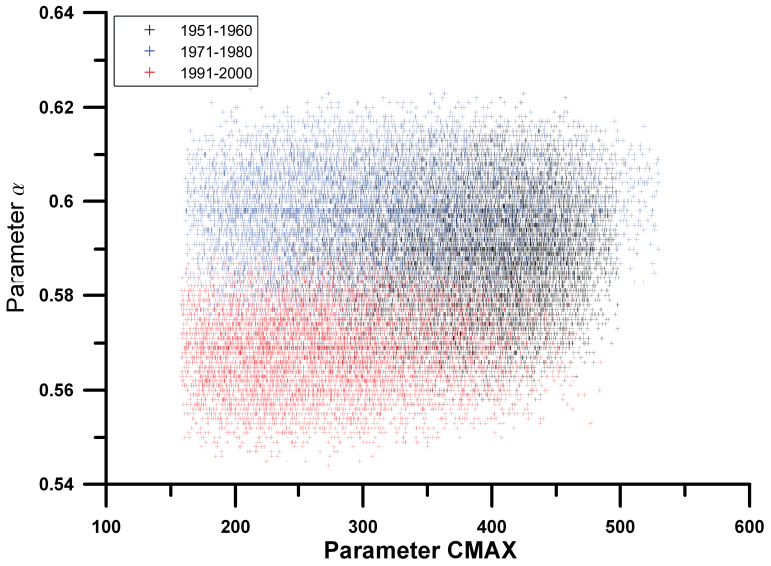

Figure 5.3: An example of scatterplots for two selected HYMOD parameters CMAX (maximum soil moisture storage) and α (flow distributing factor) for different calibration periods. HYMOD was calibrated using NS as the performance measure for catchment 13 for the period 1951-1960 (black), 1971-1980 (blue) and 1991-2000 (red).

5.4 Experiment 2: Simultaneous Calibration

The result of experiment 1 (Chapter 5.3) shows for many pairs of catchments, that the parameter transfer worked reasonably well. As a next step, it was investigated if there are parameters which perform reasonably well for all catchments. As seen in the previous sec-

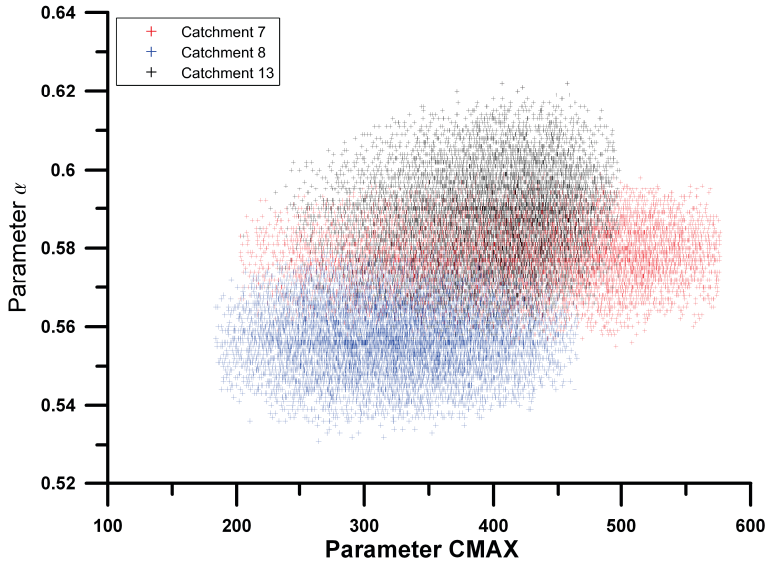

Figure 5.4: An example of scatterplots for two selected HYMOD parameters CMAX (maximum soil moisture storage) and α (flow distributing factor) for different catchments. HYMOD was calibrated using NS as the performance measure for catchment 7 (red), 8 (blue) and 13 (black) for the period 1951-1960.

tion, none of the catchments share optimal parameters. Therefore, common sub-optimal parameters have to be found.

To identify parameter vectors which perform simultaneously well for each catchment, the hydrological models were calibrated for all 15 catchments simultaneously. The simultaneous calibration of the model for all catchments is a multi-objective optimization problem. The goal is to find parameter vectors which are almost equally good for all catchments with no exception. As the models perform differently for the different catchments due to data quality and catchment particularities, the performance was measured by the loss in performance compared to the usual individual calibration. Thus the objective function is formulated using the formulation of the compromise programming method [Zeleny, 1981]:

$$R^{(j)}(\theta) = \sum_{i=1}^{n} (O_i^{(j)*} - O_i^{(j)}(\theta))^p \tag{5.4}$$

Here index j indicates the type of the individual performance measures. The goal in this objective function is to minimize $R^{(j)}$. Here p is the so called balancing factor. The larger p is the more the biggest loss in performance contributes to the common performance. In order to obtain parameters which are good for all catchments, a relatively high $p = 4$ was selected for all three performance measures.

The same way as individual calibration, the ROPE algorithm was used for the simultaneous calibration. The optimized parameter sets $\mathcal{H}^{(j)}$ performed simultaneously well for each model and time period. Figure 5.5 compares the performance of the individually calibrated and the common calibration for the 15 selected catchments for all three models using NS

as the performance criterion. As expected, the results show that the individual calibrations lead to better performances for all models, but the joint parameter vectors perform reasonably well for all catchments. The loss of the performance for HBV is larger than HYMOD and XAJ.

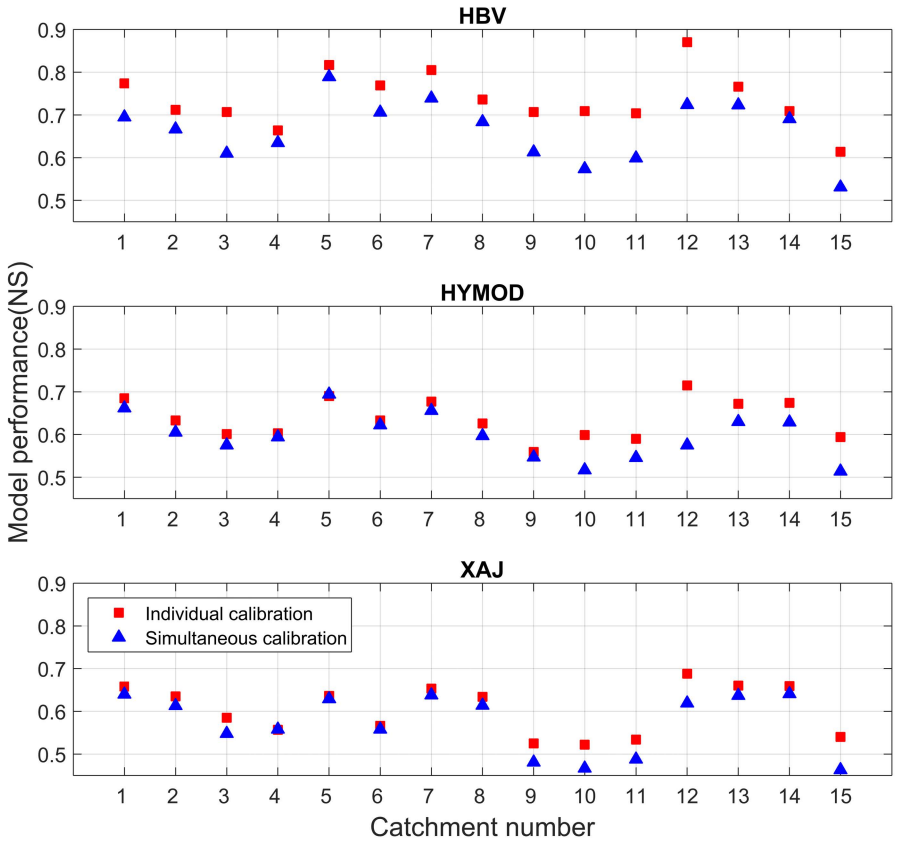

Figure 5.5: Mean model performances of the individually calibrated (red rectangles) and the common calibrated (blue triangles) models using NS as performance criterion for the calibration period 1971-1980.

As the goal of this modeling is not the reconstruction of already observed data, the performances on a different validation period (1991-2000) were also compared. Figure 5.6 shows the mean model performances for the 15 individually calibrated and the commonly calibrated datasets. The result shows the use of the parameters obtained from the common calibration for each catchment is sometimes even better than those obtained by using the individually calibrated parameters. The observation that parameter vectors obtained through common calibration may outperform individual on-site calibration may also indicate the weakness of the calibration process for an individual catchment, which should ideally be able to identify the best parameters.

These results indicate that instead of transferring model parameters from a single catchment, a parameter transfer might perform better if the parameters obtained through com-

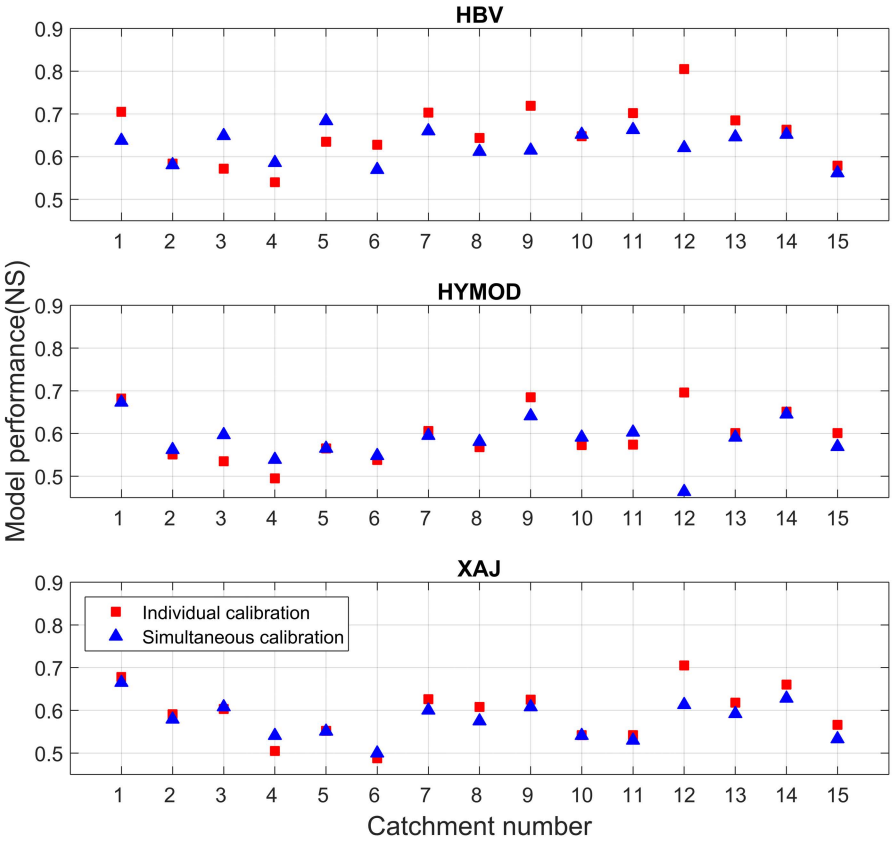

Figure 5.6: Mean model performances of the individually calibrated (red rectangles) and the common calibrated (blue triangles) models using NS as the performance criterion for the validation period 1991-2000.

mon calibration on all other catchments are used. In order to test this kind of parameter transfer, a set of simple "leave-one-out" calibrations were performed. This means that for a catchment i, the hydrological models were simultaneously calibrated for the remaining 14 catchments. Each time another catchment i was not considered for calibration, leading to 15 simultaneous calibrations. These common model parameters were then applied for the catchment which was left out. The performance of the models on these catchments in the calibration period is reasonably good for all catchments. Figure 5.7 shows the result of HBV, HYMOD and XAJ using the NS performance measure. It compares the performance of the parameters obtained via individual calibrations (red x-mark), parameter transfers from other catchments individually (blue plus) and the transfer of the common parameters obtained by leave-one-out procedure (green diamond). The performance of common parameters is obviously weaker than that of the individual calibration but better than many parameter transfers obtained using individual parameter transfer. To test the effective potential of the transferability of the common parameters, a validation period was used. Figure 5.8 shows the results for the validation time period 1991-2000. In this case, the common cal-

ibration performs very well. For HYMOD, it outperforms the model obtained by individual calibration for 6 out of the 15 catchments. For the other catchments, the loss in performance is relatively small. Note that this good performance of the common models was obtained without using any information of the target catchment. The transfer of parameters obtained from individual calibrations on other catchments shows a highly inhomogeneous picture as described in the previous experiment. The transferred common calibration is better than most of these performances. Further note that the results of individual transfer show that there is no explanation why certain transfer work well and others do not. Thus for the transfer of model parameters to ungauged catchments, common calibration seems to be a reasonable method.

In order to illustrate how model parameters of the leave-one-out common calibration perform in validation, two hydrographs are presented. Figure 5.9 and 5.10 show a part of the observed, the modeled and the common calibration transferred hydrographs for a randomly selected parameter set obtained by individual calibration and leave-one-out common calibration of HBV for catchments 5 and 14. While for catchment 5, the common calibration leads to a hydrograph which is slightly better than that obtained by individual calibration, in the second case for catchment 14 the performance is reversed. However, in both cases, the common parameters, which were obtained without using any observations of the catchment perform surprisingly well.

5.5 Experiment 3: Simultaneous Calibration on Great Number of Catchments

The results of the previous experiment suggest that even more catchments might share parameters which perform well on all. The 15 catchments used in experiments 1 and 2 are all influenced by humid continental climate. They are however to some extent similar and can thus not necessarily be considered as representative of a great number of other catchments. Thus, for the third experiment, 192 catchments of the MOPEX dataset were considered. 96 of them were randomly selected for common calibration (marked as blue circles in Figure 2.4) , the other 96 catchments were used as receivers to test the performance of the common parameters (marked as green triangles in Figure 2.4). The HBV model using three selected performance measures was considered in this experiment.

For each of the 192 catchments, an individual model calibration was carried out using 1971-1980 as calibration period. Common calibration was performed for the selected 96 catchments the same way as in the previous numerical experiment, for HBV and HYMOD using all performance measures.

As a first step, the model performances for the individual and common calibration were compared. As expected and already seen in previous results, the performance for the common calibration is lower than for the individual one. For example, the mean NS performance over all 96 catchments drops from 0.69 to 0.50. When one applies the models for the validation period 1991-2000, the individually calibrated model mean performance is 0.65, while for the common calibration, the mean value increases to 0.51.

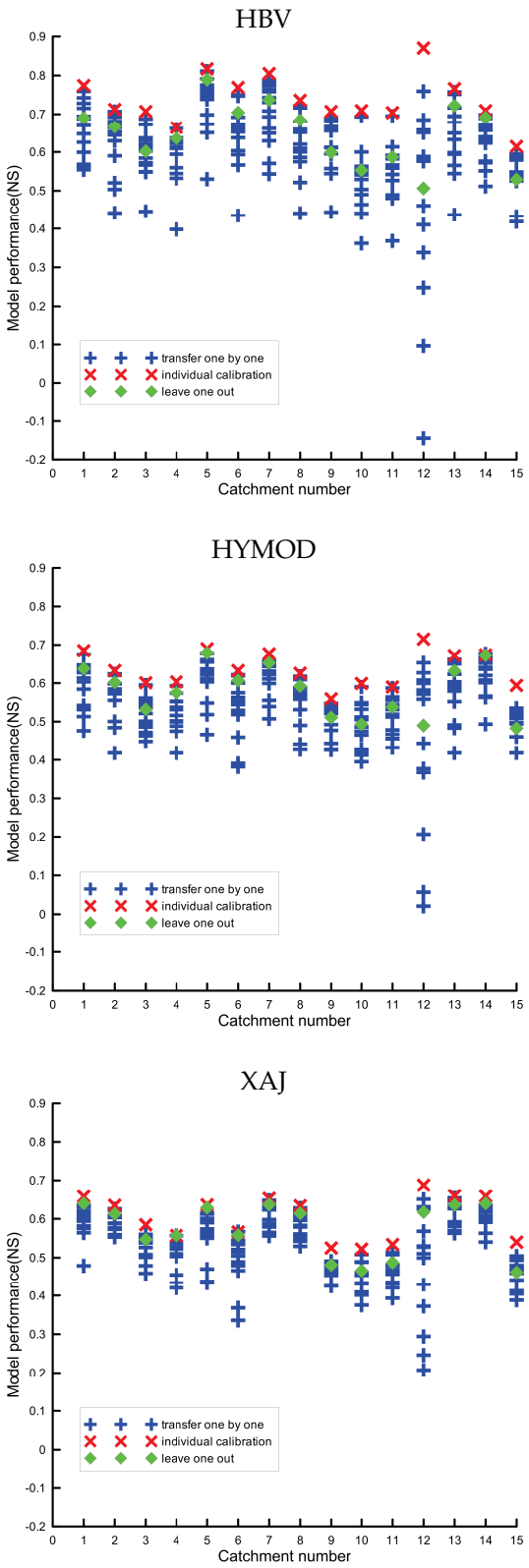

Figure 5.7: Mean NS model performance of the individual calibration (red x mark), Individual parameter transfer (blue plus) and for the leave-one-out transfer (green diamond) for the selected 15 catchments for the calibration period 1971-1980.

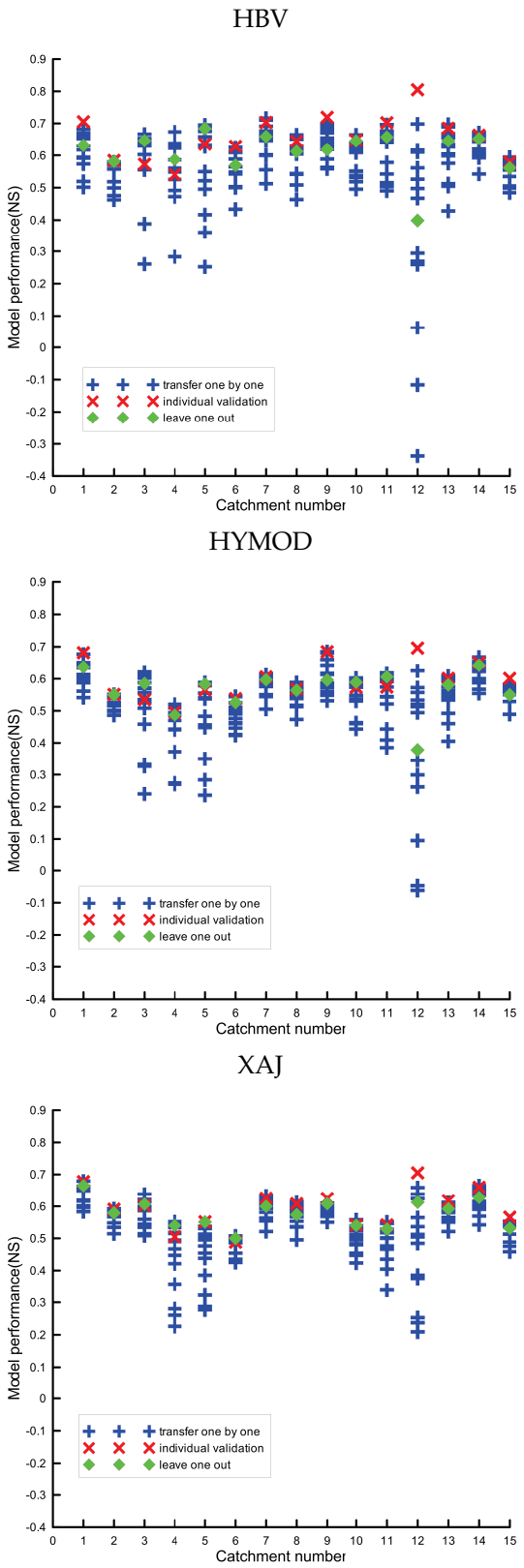

Figure 5.8: Mean NS model performance of the individual calibration (red x mark), Individual parameter transfer (blue plus) and for the leave-one-out transfer (green diamond) for the 15 selected catchments for the validation period 1991-2000.

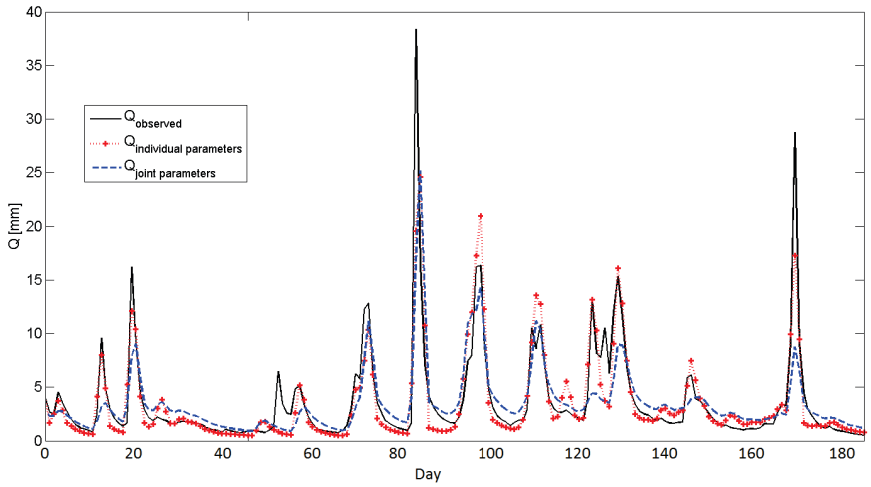

Figure 5.9: An example of runoff hydrographs for catchment 14 obtained using individual (red dot) and leave-one-out common (blue dash) calibrations. HBV model was calibrated using GK as the performance measure for the period 1971-1980. The black line indicates the observed discharge.

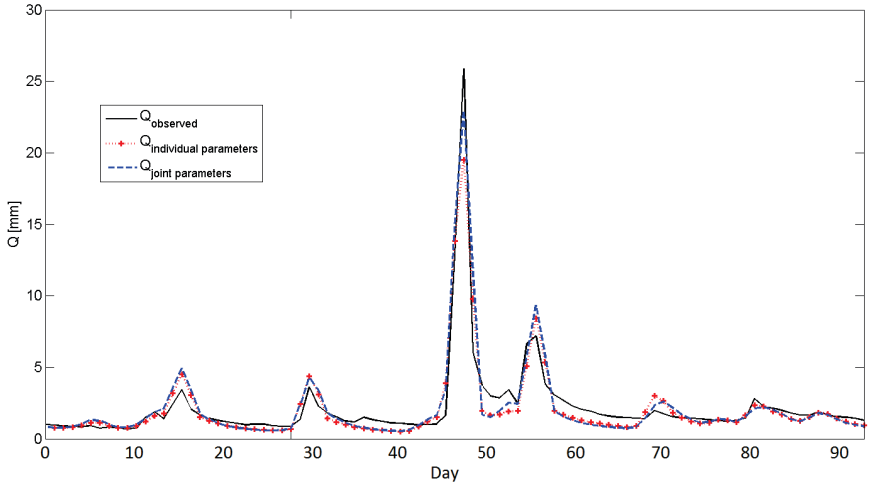

Figure 5.10: An example of runoff hydrographs for catchment 5 obtained using individual (red dot) and leave-one-out common (blue dash) calibrations. HBV model was calibrated using NS as the performance measure for the period 1971-1980. The black line indicates the observed discharge.

Figure 5.11 shows the histogram of the performance NS for both gauged and assumed ungauged catchments for the individual and the common calibrations for the calibration time period for the HBV model. Figure 5.12 shows the results for HYMOD. The transfer to the 96 assumed ungauged catchments shows very similar performance for the common parameters as for the catchments selected for common calibration. Figure 5.13 and 5.14 show the histograms of the performance NS for the validation time period. For both HBV and HYMOD, there is very little difference between the performance for the gauged and the ungauged catchments. In 90% of catchments, the common calibration works reasonably well even for the ungauged cases. The common parameters describing runoff dynamics of all 192 catchments indicate that there is a high degree of similarity of these catchments.

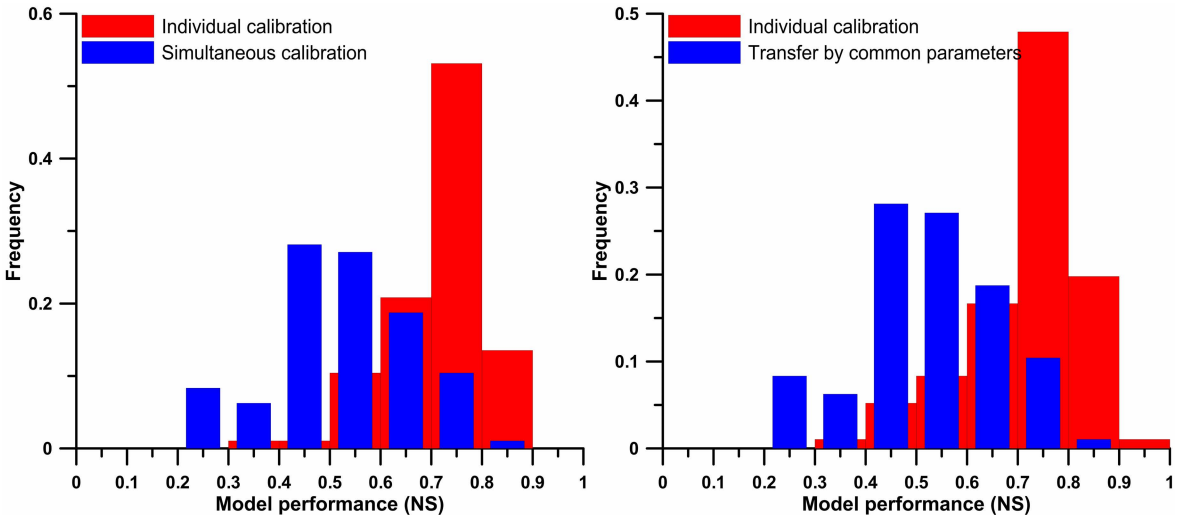

(a) Donor catchments

(b) Assumed ungauged catchments

Figure 5.11: Histograms of the mean NS model performances of HBV model for the calibration period 1971-1980. The blue bars show the model performances for the common calibrated parameter sets and the red bars show the individually calibrated model performance for reference.

Comparing the results of the common calibration using the 96 catchments to that obtained using the 15 catchments, one can observe that the increase of catchments considered for the common calibration lead to a decrease in the performance. This is as expected, as there is a less common behavior of a large set of catchments as for a few. Thus the parameters obtained through common calibration can be regarded to describe the common dynamical behavior of many very different catchments over a large geographical area. If one is interested to find model parameters for a specific ungauged catchment, the common calibration using a more careful selection of the donor set of catchments is likely to lead to good parameter transfers.

The water balances of the 192 catchments are different leading to different η parameters. Figure 5.15 shows the distribution of η values for three randomly selected common good parameter sets for HBV model using NS as the performance measure for the calibration time period. It can be seen clearly from the curve that for the same catchment, η is specific for different dynamical parameter sets. And due to the differences in water balance, dif-

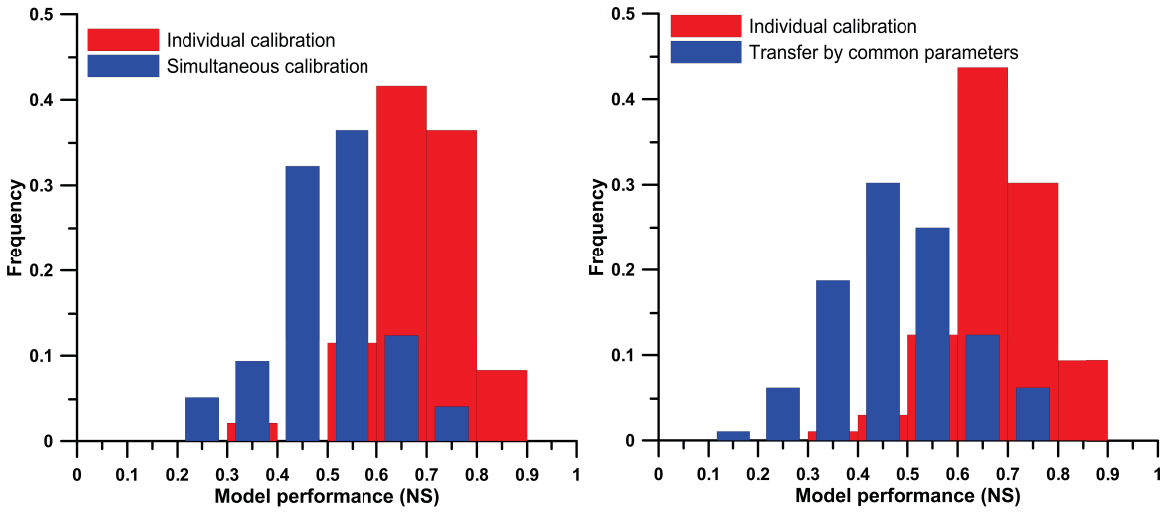

(a) Donor catchments (b) Assumed ungauged catchments

Figure 5.12: Histograms of the mean NS model performances of HYMOD model for the calibration period 1971-1980. The blue bars show the model performances for the common calibrated parameter sets and the red bars show the individually calibrated mode performance for reference.

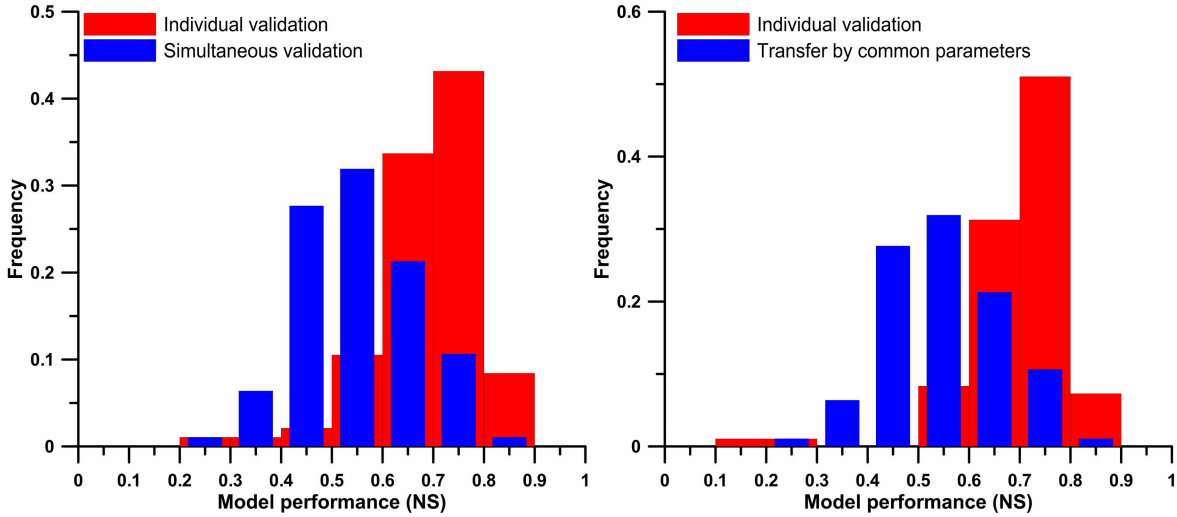

(a) Donor catchments (b) Assumed ungauged catchments

Figure 5.13: Histograms of the mean NS model performances of HBV model for the validation period 1991-2000. The blue bars show the model performances for the common calibrated parameter sets and the red bars show the individually validated mode performance for reference.

ferent catchments requires different η-s to control actual evapotranspiration. Furthermore, for all 192 catchments, parameter η present very similar tendency for different dynamical

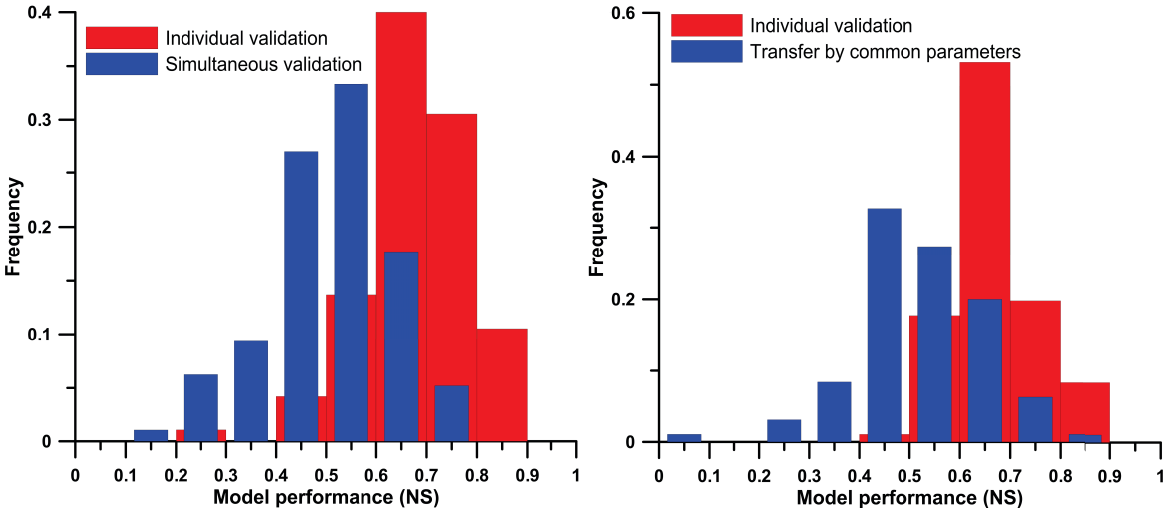

(a) Donor catchments (b) Assumed ungauged catchments

Figure 5.14: Histograms of the mean NS model performances of HYMOD model for the validation period 1991-2000. The blue bars show the model performances for the common calibrated parameter sets and the red bars show the individually validated mode performance for reference.

parameter sets. Figure 5.16 plots the mean η value against the ratio of the long-term actual evapotranspiration to potential evapotranspiration (E_{ta}/E_{tp}) for each catchment. It shows strong negative correlation (-0.72) between η and E_{ta}/E_{tp}. The relationship between potential and actual evapotranspiration differs strongly for different catchments. The water balances can be achieved by using parameter η.

5.6 Experiment 4: Application to Catchments in Other Geographical Regions

The 96 catchments used for the previous numerical experiment represent a large variety of hydrological and meteorological conditions. Their use for other catchments showed a quite good performance for all performance criteria. Therefore, the question arises whether theses parameters describe a general hydrological behavior independently of the location. In this section, the common parameters obtained by common calibration for 96 MOPEX catchments (see experiment 3) were used to model two German catchments and a Chinese catchment that have been described in Chapter 2.

The hydrometeorological daily data for Rottweil catchment and Fils catchment at Süssen from 1971 to 1980 and for Chengcun catchment from 1986 to 1995 were used to test the transferability of common parameter sets calibrated for the 96 MOPEX catchments. The simulation performances for these three catchments are listed in Table 5.3. THe result shows that all dynamical model parameters obtained through simultaneous calibration for the 96 MOPEX catchments worked well for both German catchments. But for the Rottweil catch-

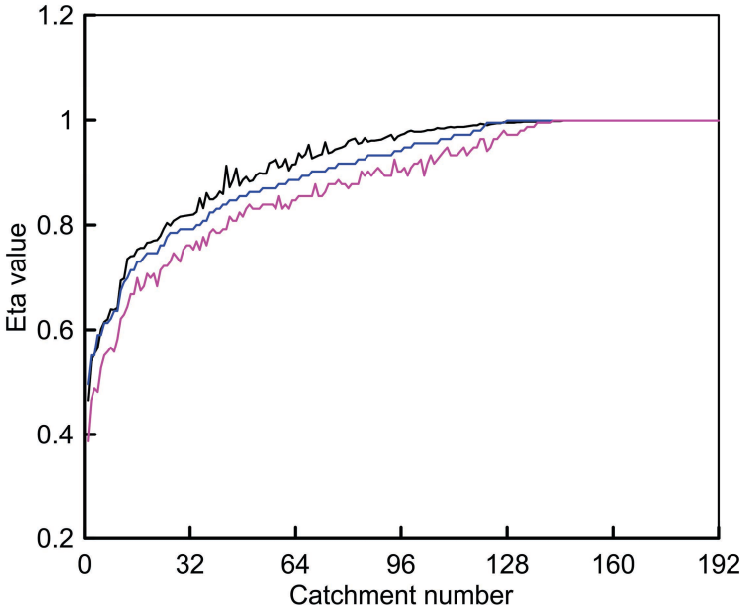

Figure 5.15: Distribution of the parameter η for three randomly selected common parameter vectors obtained via HBV using NS performance measure for 192 selected catchments.

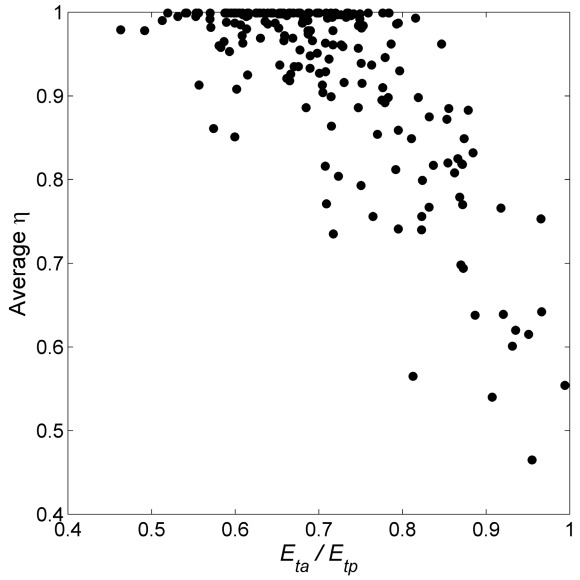

Figure 5.16: Scatterplots of mean η and ratio of actual evapotranspiration to potential evapotranspiraton for 192 selected catchments.

ment, model performance is worse than for the Fils catchment at Süssen. This indicates, that there is some skill in the transferred parameters, but the differences are substantial. Figure 5.17 shows part of the observed and the modeled hydrographs of HBV using the NS perfor-

mance measure. For these three catchment, the transfer is reasonable and the dynamics of the discharge are similar to the U.S. case.

Table 5.3: Mean model performances of the German and Chinese catchments using the common parameter sets calibrated by the 96 MOPEX catchments.

Model	HBV			HYMOD		
Measure	NS	GK	NS+LNS	NS	GK	NS+LNS
Rottweil, Neckar	0.47	0.90	0.52	0.48	0.92	0.55
Süssen, Fils	0.58	0.97	0.68	0.58	0.96	0.65
Chengcun	0.65	0.96	0.51	0.43	0.93	0.48

For the Chengcun catchment, the results are less encouraging when compared to the individual calibration results. The models show some skill, but model performance is worse than for the German catchments. This means that there is some skill in the transferred parameters, but the differences are substantial. A comparison of the observed to the modeled hydrographs in Figure 5.17 shows this clearly. However note that the climatic conditions of this catchment are very different from those of the 96 MOPEX catchments used for parameter transfer. The climate of the Chengcun catchment is warmer and wetter than that in the selected U.S. catchments. This experiment demonstrated that a single set of dynamical model parameters is unlikely to be good everywhere. On the other hand, even very distant and different catchments may behave similarly.

5.7 Discussion

5.7.1 Robust parameter sets

The three experiments were carried out in a way that a set of parameters (usually represented by 10 000 individual parameter sets) was used. This leads to a considerable fluctuation of the results. Modelers often prefer to use one single parameter vector. If a single parameter vector is desired, then according to Bárdossy and Singh [2008], the deepest parameter set (which represents the most central point in the whole parameter vectors) is the most likely candidate to be robust. This study also indicates, that the deepest parameter set performs slightly better than the mean of the parameter sets considered.

5.7.2 Variability and estimation of η

As defined, the water balance related parameter η is specific for each catchment and each model parameter vector. Therefore, each individual catchment has a large variation in η for the calibrated 10 000 parameter sets. And for the same set of good parameters that match different water balances well, different catchments always require very different η values

(a) Rottweil catchment

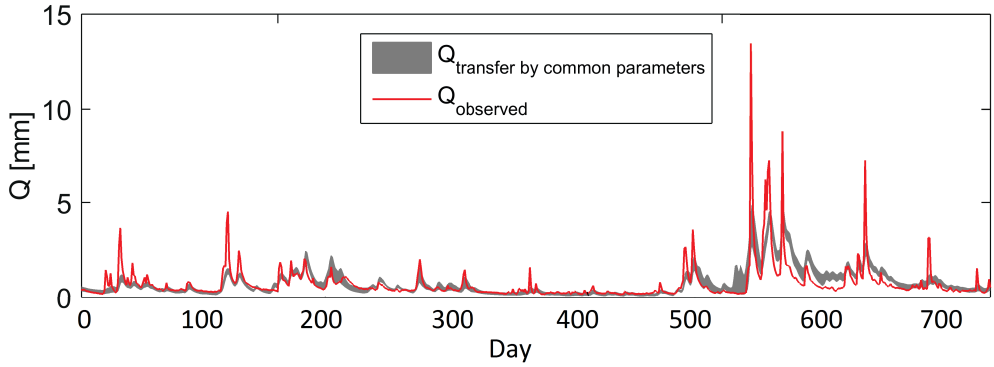

(b) Fils catchment at Süssen

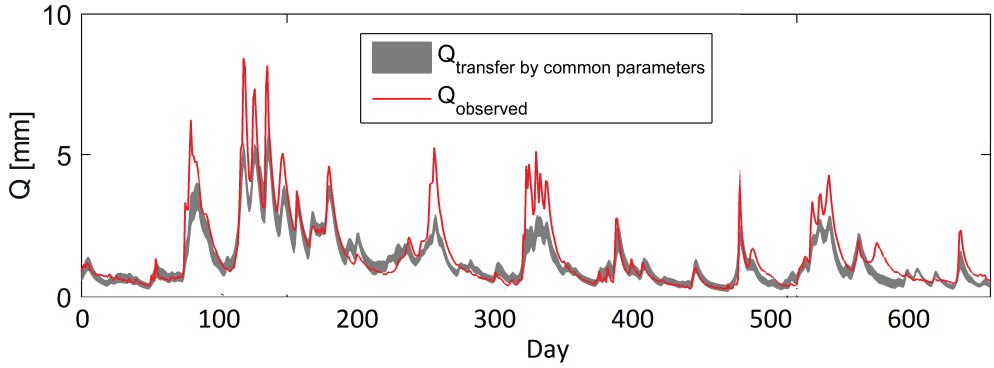

(c) Chengcun catchment

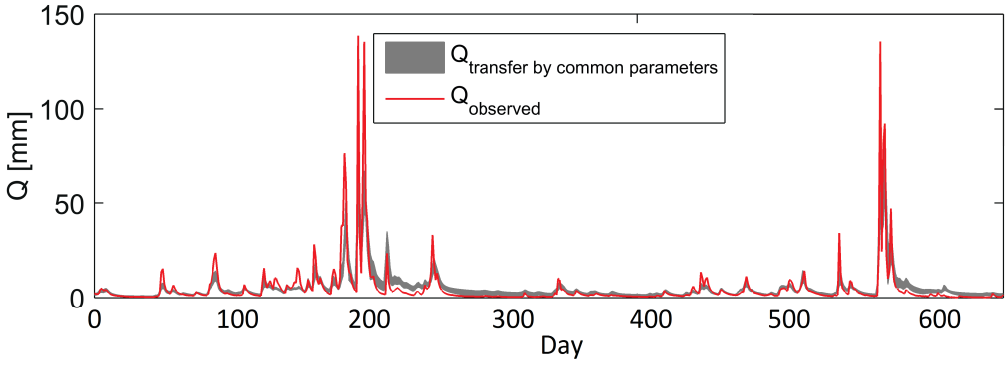

Figure 5.17: Observed (red) and modeled (gray) discharges for Rottweil, Süssen and Chengcun catchments. Modeling was performed using the common parameter sets of the 96 MOPEX catchments obtained by calibration using HBV for NS.

to control actual evapotranspiration. Parameter η is estimated because it controls the water balance and can be estimated at other catchments. The remaining parameters (the dynamic ones) are regionally calibrated (all catchments are given the same parameter set). Therefore

only η varies between catchments. As η is specific for each parameter vector, regionalization of η directly is not feasible and η remains different for different parameter vectors after regionalization. In the numerical experiments, in order to estimate the water balance parameter η, the long-term discharge volumes were treated as known variables for both gauged and ungauged catchments. For application in a practical system, the long-term discharge volumes have to be estimated for ungauged catchments. The estimation of parameter η is a limitation of the presented simultaneous calibration approach. Regionalization of long-term discharge volumes is a prerequisite for the application in ungauged basins. For the study area, the discharge coefficients which relate discharge volumes to (known) precipitation show a quite smooth spatial behavior as shown on Figure 2.3 in Chapter 2. Thus the regionalization of this parameter does not seem to be an extremely complicated task in this particular region. According to the previous analysis of η, for each common dynamical parameter set, one can have a possible estimator of η for a certain catchment based on the regionalization of discharge coefficients. The potential application of this approach in other regions needs to be investigated in future work.

5.7.3 Prediction in ungauged basins

The results of this study supported the general finding of Ricard et al. [2012] and Gaborit et al. [2015], where the simultaneous calibration lead to weaker model performance than the individual one for both the calibration and the validation time period. The loss of model performance in validation is smaller than that in calibration. When applied to ungauged catchments, the simultaneous calibration shows more robustness than the individual one. Simultaneous calibration of models in geographical space offers a good possibility for the runoff prediction in ungauged basins. Compared with traditional regionalization method, only the water balance parameter η has to be estimated based on the regionalization of discharge coefficients.

It was examined from the hydrographs that high flows are often underestimated and low flows are probably overestimated. This kind of phenomenon has also been detected in previous regional calibration studies [Ricard et al., 2012; Gaborit et al., 2015]. This behavior is mainly due to the uncertainty of model structure and the low spatial and temporal resolutions of both models and input variables [Gaborit et al., 2015].

5.8 Conclusions

In this chapter, the transfer ability of the dynamical parameters of hydrological models was investigated. In order to cope with the clear differences in water balances due to water or energy limitations, a new model parameter η controlling the actual evapotranspiration was introduced. This parameter is determined for each vector of other model parameters by adjusting the long-term water balances. This parameter was not transferred, only the other parameters controlling flow dynamics and short-term water balances were assumed to be shared by many catchments. In order to assure the generality of the results, three different

lumped hydrological models were used in combination with three different performance measures in four numerical experiments on a large number of catchments. The following conclusions can be drawn:

- Hydrological models are often overfitted during calibration. The parameters are sometimes more specific for the calibration time period and their relation to catchment properties seems to be unclear. This makes parameter transfers or parameter regionalization based on individual calibration difficult.
- In the second experiment, a common calibration strategy was introduced and tested on a small number (15) of catchments. For the common calibration an overall objective function which considers all catchments simultaneously and allows little compensation is required. Compromise programming offers a good possibility for this purpose. This methodology was able to identify parameter sets which work reasonably well for all catchments. Testing the parameters on an independent time period shows that common parameters perform as well as those obtained using individual calibration. The transfer of the common parameters to model ungauged catchments works well. Note that the water balance parameters have to be estimated individually for the ungauged catchments.
- Extending the number of catchments covering a gigantic spatial scale (continental) still allows a reasonable common calibration and transfer of the dynamical parameters. The performance on this scale is weaker than on the smaller sizes, but a transfer to other ungauged catchments is still possible.
- Parameters obtained via continental scale calibration are transferable to model catchments on other continents. This shows that there is a partly common behavior of most catchments. However, note that the performance of these common parameters is significantly worse than what can be obtained using individual calibration.
- The fact that many catchments share common parameters which describe their dynamical behavior does not mean that they really do have the same dynamical behavior. The model output highly depends on the parameter η which varies from catchment to catchment and also correlated to the other model parameters describing dynamic behavior.
- The results of the experiments were similar for all three hydrological models applied independently of the choice of the performance measures. Note however, that the common parameters corresponding to the different performance measures differ considerably. A common behavior is dependent on how one evaluates the performance of the models.
- The performance of the joint parameters depends strongly on the selection of the catchments used to assess them. The optimal choice of the appropriate catchments was not investigated in the framework of this research. The second experiment suggests that a reasonable geographic proximity of the catchments might be a good choice for common calibration.

Common parameters offer a good possibility for the prediction of ungauged catchments. Only one single parameter η which controls the long-term water balances has to be estimated individually. This, however, can be done using other modeling approaches including regionalization methods.

In this study, all the models were tested on the daily time scale. The results show, that many catchments behave similarly as the same dynamical parameter sets could perform reasonable for all of them. This means that hydrological behavior on the daily scale is mainly dominated by precipitation characteristics and actual evapotranspiration. Differences in catchment properties seem to rather have significant effects on smaller temporal scales (e.g., hourly). Results also indicate that the differences in catchment properties cannot be captured well by simple lumped model parameters.

6 Model Calibration under Non-stationary Conditions

This chapter tests the transferability of model performance under climate change conditions and presents the approaches of improving the quality of model parameter transfer.

6.1 Introduction

As climate change becomes a major issue in both science and society, the impacts of climate change on hydrology have been extensively investigated over the past two decades [Vaze and Teng, 2011; Vaze et al., 2011; Coron et al., 2012]. Previous studies have shown that climate change may have a significant influence on the water availability and hydrological circulations [Rind et al., 1992]. Floods and droughts are the greatest potential natural disasters that "stimulates" other factors such as economics, social life, agriculture and others to adapt to changes in climate behavior [Barnett and Adger, 2007]. It is really important for hydrologists to be able to predict the potential impact of climate change on catchment behaviors and therefore develop sustainable water management strategies. The statement "hydrological non-stationarity" has been widely used to describe climate and runoff variability evident in different time periods within a long hydroclimate time series to changes in rainfall-runoff relationships and catchment characteristics [Chiew et al., 2014; Vaze et al., 2015]. Milly et al. [2007] initiated significant discussions and an increased focus towards research on hydrological non-stationarity.

The hydrological process may be considered as non-stationary under the changing climate and land use conditions. As described in Chapter 3, the model parameters of the conceptual hydrological models are not directly measurable. The unknown parameters are usually adjusted in a calibration procedure to reproduce the measured signals from the observed hydrometeorological data and catchment characteristics. The identification of conceptual model parameters highly relies on the observed data sets that are used for model calibration. This kind of "stationarity" assumption challenges the sufficiency for predicting further changes or time variability, as the final objective for hydrological modeling is not repeating what was observed. As an applicable rainfall-runoff model, it should well capture the essential features of the catchment process and therefore be transferable to various conditions. A considerable number of studies have shown that the model parameters estimation during different calibration time period might be significantly different. It limits the transferability of hydrological models under non-stationary conditions [Bastola et al., 2011; Li et al., 2012].

This chapter investigates the transferability of model parameters in time within different climate conditions, and approaches are developed to overcome the hydrological model extrapolation problem. The effects of incorporating bias constraints into calibration routines when model parameters are used for prediction runoff in different weather conditions are also tested. The dissimilarity of climate indicators for the different time periods was measured using pairwise copula density. Two new model calibration methods were introduced to improve the transferability of model parameters. To cope with the instability of model parameters calibrated on catchments in non-stationary conditions, the idea of simultaneous calibration on streamflow records for the period with different climate characteristics was investigated. In addition, a weather-based weight function is implemented to adjust the calibration period to future climate conditions.

6.2 Methodology

The HBV model and HYMOD model were used to investigate the influence of climate conditions. These two conceptual models have been applied for climate change impact assessments in a significant number of basins around the world [Merz et al., 2011; Najafi et al., 2011].

The Nash-Sutcliffe efficiency (NS) [Nash and Sutcliffe, 1970] and the combination of Nash-Sutcliffe and bias constraint (NSB) [Viney et al., 2009] (see Chapter 3 for the Equations) were taken as objective function for evaluating the model calibration and validation performance. For each catchment, both HBV and HYMOD were calibrated for five different ten years lasting sub-periods. The ROPE algorithm was used for model parameters identification.

The 10 000 calibrated model parameter vectors for each sub-period were used to simulate the discharge series over the remaining four sub-periods. Afterwards, the simulated model performance was compared with the corresponding calibrated model performance to investigate the temporal transferability of model parameters under different climate conditions.

In this study, empirical copula density was applied to detect the dissimilarity of observational data series for different sub-periods. The simultaneous calibration in temporal space approach and the weight function method were introduced in the model calibration process to enhance the transferability of model parameters under different climate conditions. The general ideas of these methods are presented in the following.

6.2.1 Pairwise Empirical Copula Density

First, the concept of copula , empirical copula density estimation and the indicators that used to define the copula-based dissimilarity measures are introduced. In probability theory, copula is a distribution function on the multi-dimensional unit cube [Sklar, 1973]. In copula function, the marginal distribution of each variable is uniform on [0, 1]. A n dimensional copula C can be expressed as:

$$C : [0, 1]^n \rightarrow [0, 1] \tag{6.1}$$

$$C(u^{(i)}) = 0 \qquad if \qquad u^{(i)} = (, u_1, ..., u(i-1), 0, , u_{i+1}, ..., , u_n) \tag{6.2}$$

$$C(u^{(i)}) = u_i \qquad if \qquad u^{(i)} = (1, ..., u_i, 1, ..., 1) \tag{6.3}$$

For every hyperrectangle, the corresponding probability should be non-negative:

$$\sum_{i=0}^{2^n-1} (-1)^{n-\sum_{i=1}^{n} j_i} C(u_1 + j_1\Delta_1, ..., u_n + j_n\Delta_n) \geq 0 \tag{6.4}$$

$$if \quad 0 \leq u_i \leq u_i + \Delta_i \leq 1 \quad and \quad i = \sum_{k=0}^{n-1} j_k 2^k$$

Copulas are widely used to capture the dependence structure for the random variables that join multivariate distribution functions to single dimension distribution functions [Samaniego et al., 2010]. The applications of copula functions in the multi-dimensional case can be found in Nelsen [1999]; Bárdossy [2006]; Li [2010] and Sugimoto [2014].

In practice, the marginal distribution functions for the given multi-dimensional variables are usually not known in advance. The empirical copulas are defined as frequencies of observations similar to empirical distribution functions and can flexibly be calculated from a given sample [Sugimoto, 2014]. Therefore, the empirical copulas, which can be seen as the empirical distribution of the rank-transformed data, is often used instead of original copulas. Here we take a bivariate copula (u, v) as an example. (R_i, S_i) denotes the ranks for the random sample (X_i, Y_i) for $i = 1, 2, ..., n$, and the empirical copula can be calculated by the following formula:

$$c_n(u, v) = \frac{1}{n} \sum_{i=1}^{n} I(\frac{R_i}{n+1} \leq u, \frac{S_i}{n+1} \leq v) \tag{6.5}$$

Where n is the number of the data set and I is an indicator function.

The concept of empirical copula frequency can be defined [Nelsen, 1999]:

$$c_n(\frac{i}{n}, \frac{j}{n}) = \begin{cases} \frac{1}{n} & \text{if} \quad (R_i, S_j) \quad \text{is an element of the sample} \\ 0 & \text{else} \end{cases} \tag{6.6}$$

For the given case (u, v), the empirical copula density between these two variables for a regular $n \times n$ lattice can be estimated by counting the number of points in each lattice [Nelsen, 1999; Bárdossy, 2006]:

$$c^*(\frac{2i-1}{2k}, \frac{2j-1}{2k}) = \frac{1}{n} \left| (R_i, S_j); \frac{i-1}{k} < u < \frac{i}{k}, \frac{j-1}{k} < v < \frac{j}{k} \right| \tag{6.7}$$

Here k is the total number of lattices, i and j are the indices of lattices for u and v coordinates, respectively.

Samaniego et al. [2010] used the empirical copula functions to define catchments dissimilarity measures by a pair of streamflow time series at different catchment. In this study, the Antecedent Precipitation Index (API) and the corresponding discharge series for the

study catchment were taken as indices for measuring the dissimilarity between different sub-periods.

API is usually calculated for rainstorms to determine the antecedent moisture conditions prior to the corresponding flood event. The *API* value is calculated as:

$$API(t) = API(t-1) + \alpha P(t) \tag{6.8}$$

Here α is a memory constant. For a selected rainstorm, the *API* value on any given day (*API(t)*) is equal to the parameter α multiplied by the *API* on the previous day (*API(t-1)*) plus the effective precipitation on that day (P(t)). According to the references, the memory constant α reported in the range between 0.8 and 0.9 for the MOPEX catchments.

As discussed before, for a specific catchment, the copula density between the *API* and observed runoff depth is usually not known. Therefore, the empirical copula density of these two variables has to be estimated from the historical data sample. An empirical copula of *API* and *Q* is an estimate of the distribution function with uniform marginals that synthesize the dependence of soil moisture condition and daily runoff depth at the same time during the period $t = 1, ..., T$.

6.2.2 Simultaneous Calibration

In this chapter, the common calibration approach was used to calibrate models simultaneously for several sub-periods with different climate conditions. The objective of this method was expected to identify parameter sets which perform simultaneously well for each sub-period. A detailed description of the simultaneous calibration strategy can be found in Section 5.4.

6.2.3 Weather Adjustment with Weight Function

According to the previous model calibration experiments, for a particular catchment, the model parameters calibrated during different time periods are often not constant over time. Parameters calibrated during different weather conditions indicate large differences. They cause problems for model parameter transition and climate change impact assessments. Here we propose the idea of adjusting the weather for the calibration time period to the receiver period to improve the temporal transferability of model parameters. A weight function [Gonzalez and Wu, 1999] is incorporated into the objective function to give the time periods that have similar weather conditions as the receiver periods higher "weight". Therefore, the annual precipitation for each year was compared with the average value over the decade, if the period with annual precipitation is less than the average value, this period represents a relatively "dry" year and for all the "wet" years state the annual precipitation greater than the mean value. Before the procedure of model calibration, the mean annual precipitation for the donor sub-period and receiver sub-period are compared. If the average annual precipitation for the receiver sub-period is bigger than the donor sub-period, representing the "wet" years within the donor sub-period are more similar to the general weather of the receiver sub-period and vice versa.

Take the NS model performance as an example. Here we emphasized the data record that has similar climate conditions as the validation period using weighting function:

$$NS_w = 1 - \frac{\sum_{t=1}^{T} w_t(Q_o(t) - Q_m(t))^2}{\sum_{t=1}^{T} w_t(Q_o(t) - \bar{Q}_o)^2} \tag{6.9}$$

Here $w(t)$ is the weight for data record on a given day t. For the calibration time period that has similar climate as the validation period, a relatively high weight (generally greater than 1) was taken for evaluating the model performance. Meanwhile, for the calibration year that has very different value for the annual precipitation, a small weight was applied for calculating the model performance.

6.3 Case Study

6.3.1 Variability of Climatic data

This study was tested on a number of 50 MOPEX catchments with more than 50 years of reliable data. Figure 6.1 shows the locations of the streamgauges for the study catchments. These catchments are ranging in size from 189 km^2 to 8 689 km^2 with a median value of 1 844 km^2. More details for the MOPEX catchments can be found in Chapter 2.

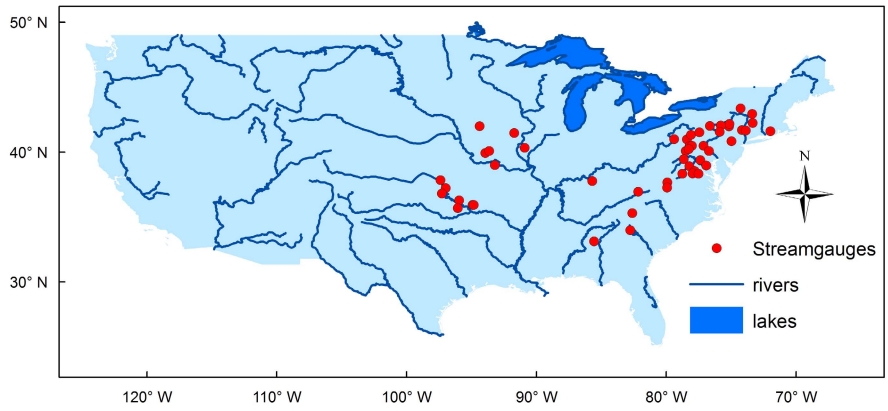

Figure 6.1: Location of the streamgauges for the 50 selected MOPEX catchments.

Table 6.1 lists the median, maximum and minimum values of basic catchment properties for the selected catchments, as well as Table 6.2 summarizes the meteorological conditions [Falcone et al., 2010]. The tables indicate that these 50 catchments differ greatly in both catchment characteristics and climate conditions. The long-term average annual precipitation displays a gradual decrease from the east coast to the central region. There is an apparent decline in the average air temperature from about 16.0 ^{0}C in the south part to about 5.6 ^{0}C

in the north along with an increase in the percentage of snowfall during cold seasons. The annual potential evapotranspiration ranges from 660 mm to 1 397 mm and the annual runoff ranges from 95 mm to 1 201 mm. The runoff coefficient which represents the ratio of annual flow to annual precipitation varies from 0.12 to 0.63.

Table 6.1: Median, maximum and minimum values of the catchment characteristics for the 50 selected MOPEX catchments.

	Drainage area (km^2)	Shape factor	Field capacity	Percent of relative humidity	Average porosity	Base flow index	Snow proportion (%)
Median	1844.1	0.12	0.33	67.40	0.40	0.44	14.5
Max	8686.9	0.45	0.38	73.17	0.48	0.69	38.0
Min	189.1	0.06	0.22	63.05	0.24	0.10	2.6

Table 6.2: Median, maximum and minimum values of the meteorological conditions for the 50 selected MOPEX catchments.

	Mean annual precipitaion (mm)	Average temperature (^oC)	Annual potential evapotranspiration (mm)	Annual runoff (mm)	Runoff coefficient
Median	1019.8	10.8	831.8	426.9	0.36
Max	1943.3	16.0	1396.6	1200.6	0.63
Min	763.2	5.6	660.4	94.8	0.12

As a first step, the historical data series for each catchment from 1950 to 1999 was taken to investigate the non-stationarity of climate conditions. The total 50 years data set was split up into five sub-periods. Each sub-period contains consecutive ten-year daily data. It is assumed that ten-year data record are sufficiently long time series to capture hydrological behavior, and the catchment conditions remain unchanged [Refsgaard and Storm, 1996]. The first hydrological year of each sub-period was considered as a warm up period in modeling and did not take account for model performance evaluation. In order to have a more accurate assessment of the data set, the analysis of climate variations only using the data period that considered for model performance evaluation. Figure 6.2 summarizes the average annual precipitation over each sub-period for all 50 catchments, note that the catchment numbers are sorted by the value of mean annual precipitation. This graph demonstrates the obvious fluctuating climatic conditions for different catchments at various time period. The average annual precipitation for all 50 catchments varies from 673 mm/yr to 2 150 mm/yr. The annual precipitation is considerable variable for different sub-periods. The differences for the relatively wet catchments (with a high value of annual precipitation) are greater than for the dry ones. For the 40 fairly wet catchments, the climate conditions show similar temporal trends. The average annual precipitation has significantly increased by almost 250 mm/yr from the the 60S to the 70S. The difference of mean annual precipitation be-

tween the driest decade (50S) and the wettest decade (90S) are around 170 mm/yr for the ten relatively dry catchments. The annual precipitation value shows a slight increase with the increasing of the decade for these ten dry catchments that are located on the west region of the study domain.

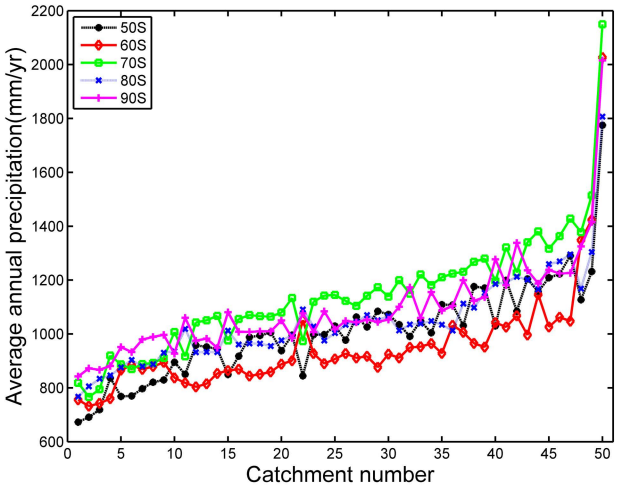

Figure 6.2: Ten-year average annual precipitation for the 50 selected MOPEX catchments.

Figure 6.3 shows the corresponding result of average air temperature. The temporal trend of air temperature seems not as clear as that of precipitation. It can be concluded from this figure that for most of the catchments, the average temperature decreased from the warmest decade 50S to the coldest period 60S by nearly 0.6 ^{0}C.

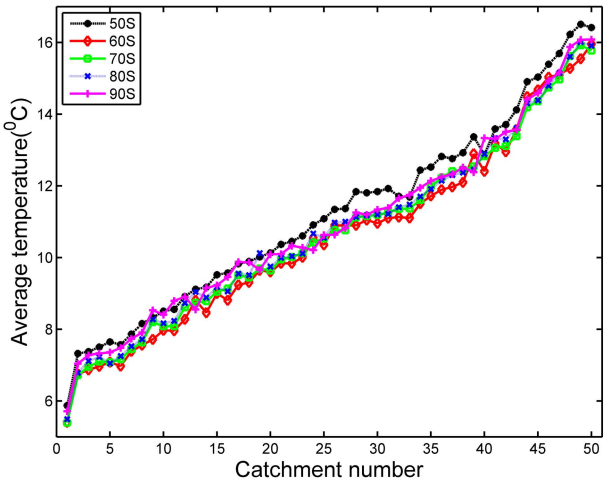

Figure 6.3: Ten-year average air temperature for the 50 selected MOPEX catchments.

6.3.2 Calibration Results

Figure 6.4 shows a typical example of the model calibration and validation results using NS as performance criteria. The color coded matrices express the mean value of the objective function NS for the 10 000 parameter vectors of catchment 01321000 for HBV and HYMOD model, respectively. Firstly, HBV and HYMOD models perform differently for the same historical data set. For most of the sub-periods, HBV leads to better model performance because of the more flexible representation of the model structure. Besides, from the color-coded matrices, we can see that the model performance varies for different sub-periods, and the performance of the transferred parameter vectors shows a sharply varying picture. While in some cases the different sub-periods seem to share parameter vectors with reasonably good performance, in other cases, the transfer lead to weak performance. Moreover, the matrix for a specific sub-period is not symmetrical. For example, all the calibrated parameters are actually good for the sub-period 90S, but the parameters identified by sub-period 90S lead to relatively weak performance for the 80S for both HBV and HYMOD. We also found that some parameter sets perform well for all sub-periods, while others are not transferable. The main reason for the asymmetry of the parameter transition matrix is that each catchment has different climate forcing during different sub-periods and this leads to very different model parameter sets. The calibrated parameter sets are highly influenced by the climate conditions during the calibration periods.

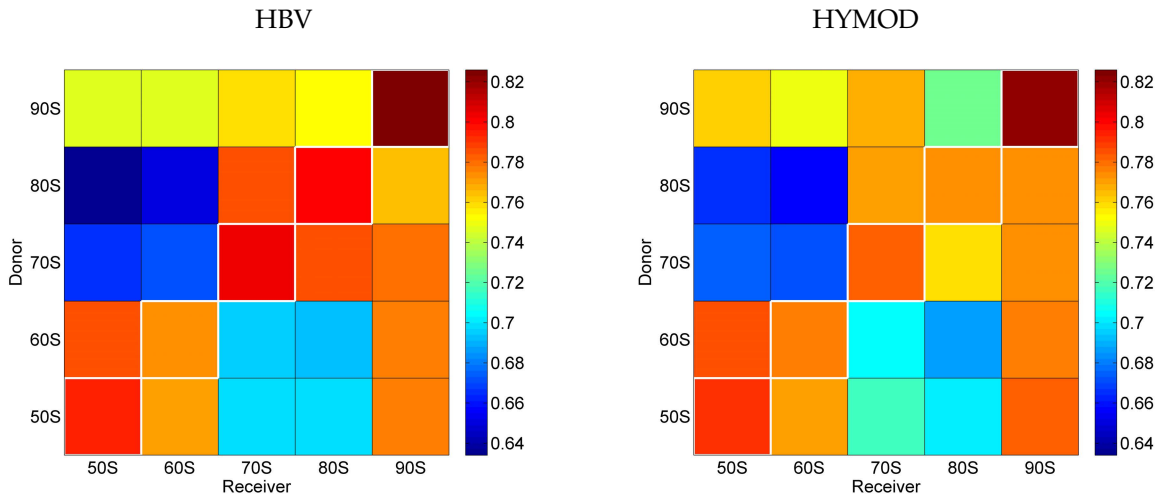

Figure 6.4: Color-coded matrices for the mean NS model performance for calibration and cross-validation period for catchment 01321000.

The left part of Figure 6.5 shows the cumulative distribution function of NS model performance for all model calibration results, while the right part of Figure 6.5 shows the corresponding results of the absolute value of bias. It can be seen clearly from the curves that for the same data sets, HBV and HYMOD show different model performance. In general, HBV performs better than HYMOD because it contains more flexible parameters. This figure also compares the difference of using different objective functions (NS, NSB) for model calibration. For both models, the best NS efficiencies are obtained for the objective function that maximizes efficiency only and has no bias constraint. When considering the bias constraint,

the NS model performances are slightly decreased. However, with the bias constraints, the water balance could be apparently improved for both HBV and HYMOD as the bias errors are significantly smaller than the unconstrained case.

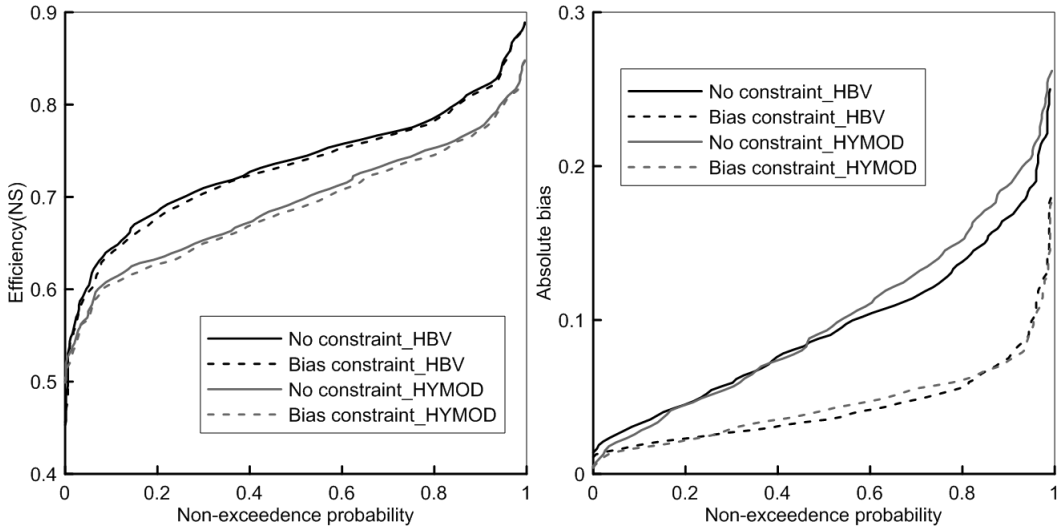

Figure 6.5: Cumulative distribution of NS coefficient (left) and absolute bias value(right) for HBV (black) and HYMOD (grey) model calibration. Models were calibrated using two different objective functions: non constraint (solid line) and bias constraint (dash line).

The spatial mean model performances that used NSB as the objective function for different sub-periods are summarized in Figure 6.6. For both HBV and HYMOD, the average NS efficiencies for the dry period (60S) are slightly worse than the performances calibrated on other sub-periods. The losses in NS performance of the HBV model are greater than that of the HYMOD. This is mainly because, during the dry period, there might be limited flood events for the models to capture the fundamental characteristics of the rainfall-runoff behaviors for the catchment.

6.3.3 Validation Results

For every sub-period, there are four sets of simulation results when transferring parameter sets from other sub-periods. Therefore, for in total 50 catchments, it results in 1 000 sets of simulation results. Figure 6.7 shows the cumulative distribution of the simulated NS coefficient and absolute biases for both HBV and HYMOD. From the cumulative probability plots, we could see clearly that the statistics for both efficiency NS and absolute biases are poorer for validation than for calibration. The cross validation efficiency NS for non-constraint cases tends to be greater than the bias constraint cases. But the differences are lighter than the calibration results. The water volume error could be effectively reduced by using bias constraints. From the right side of the Non-exceedence probability curves for the absolute bias, we could see that some of the simulation results lead to significant bias error (close to 0.5) for using bias constraint as well as the non-constraint cases. It represents that for a few

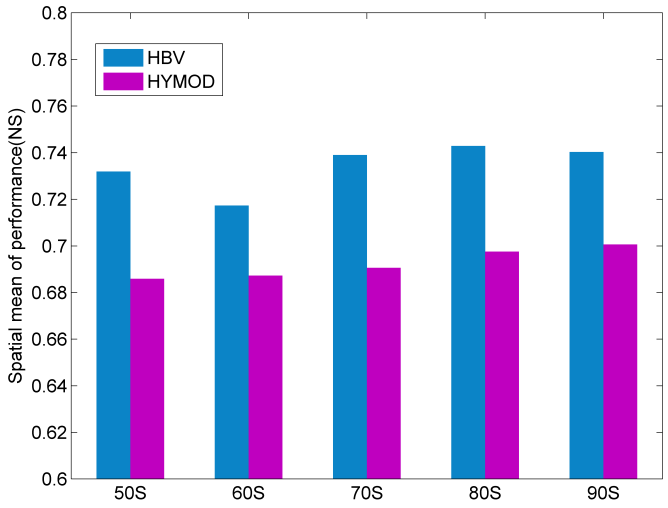

Figure 6.6: Mean NS model performance over 50 catchments for five calibration period for HBV (blue) and HYMOD (pink) using NSB as objective function.

catchments, the model validation leads to a relatively big problem for the water balance as well as to lower efficiency values in the simulation.

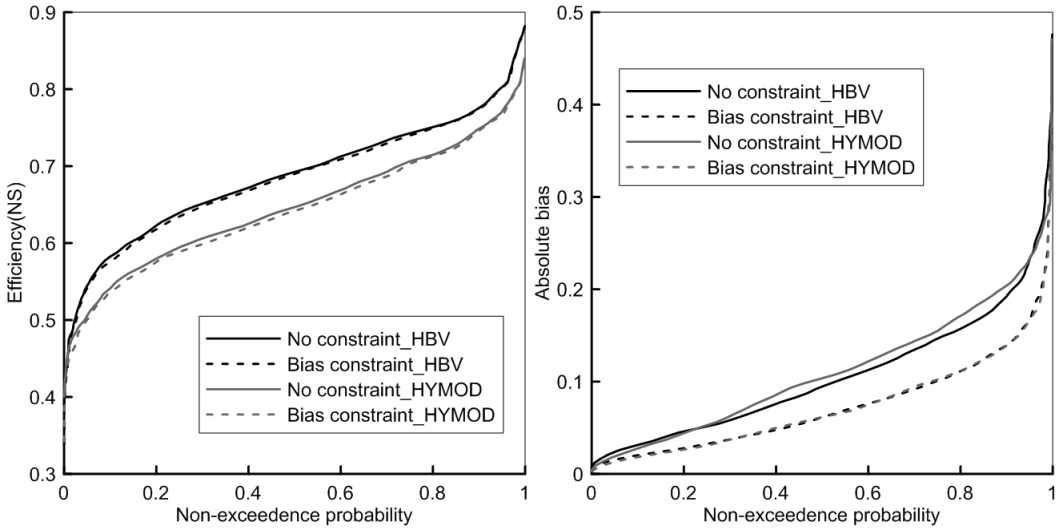

Figure 6.7: Cumulative distribution of NS coefficient (left) and absolute bias value(right) for HBV (black) and HYMOD (grey) model validation. Models were calibrated using two different objective functions: non constraint (solid line) and bias constraint (dash line).

The calibration and validation results of this study supported the finding of [Viney et al., 2009], where the incorporation of bias constraint with NS efficiency strategy frequently leads to slightly poorer NS performance than the unconstrained case. However, the biases can be

significantly reduced with the bias constraint. This provides support for incorporating bias constraints into the model calibration process. In the following study, the NS efficiency combined with bias constraint(NSB) was taken as the objective function for model evaluation.

6.3.4 Transferability and Climate Change Indicators

In order to investigate the transferability of parameters under changed climatic conditions, the transfer performance has been normalized with respect to the model calibration performance for the data period. The percentage difference between the normalized model performance and the maximum possible value (1) denotes the accuracy of the simulated model performance. The smaller the value, the worse the transferred quality. A value of zero represents the simulation result is as good as the model calibration. Figure 6.8 shows the percentage reduction in efficiency NS for all sub-periods and Figure 6.9 shows the absolute value of the simulated biases, respectively. Here the percentage reduction in model performance is plotted against the percentage difference in average annual precipitation in the validation period relative to the calibration period, and the average annual precipitation of the calibration period is taken as the denominator [Vaze et al., 2010]. All the scatters on the left side of the y-axis represent the simulated performance where the precipitation in the simulation sub-period is lower than in the calibration sub-period and vice versa. As expected, the simulation results are very similar for both HBV and HYMOD because of the similar model structure. Figure 6.8 shows that in a few number of simulations (HBV: 5 % and HYMOD: 2%), the simulation NS values are close to the individual calibration results, which demonstrates the calibrated model parameters are well transferred to the receiver sub-periods. The lines of best fit in this figure show the clear correlation between the differences in weather conditions for the calibration and validation sub-periods and the reduction in model efficiency NS. With the increasing of difference in rainfall conditions between calibration and validation sub-periods, the reduction in model performance usually becomes higher. Figure 6.9 indicates that the mean value of the absolute biases are significantly higher if there are a larger difference between precipitation in the calibration and validation sub-periods. It also indicates that the absolute biases are usually greater when the model parameters calibrated in a high precipitation sub-period is used to model the discharge in a low precipitation sub-period than when the parameters calibrated in a low precipitation sub-period is used to model the discharge in a high precipitation sub-period. It can be found from the figure that some simulations for the relatively wet sub-periods by transferring parameters from the dry ones lead to significant water balance error.

Figure 6.10 plots the percentage reduction in model efficiency NS against the difference in the rate of runoff and precipitation between the validation and calibration sub-periods, Figure 6.11 plots the absolute bias, respectively. The ratio of runoff (Q) and precipitation (P) represents the long-term water balance separation between water being released from the catchments as streamflow and as evapotranspiration [Milly, 1994; Sawicz et al., 2011]. The correlation between the transferability of model parameters and the ratio of runoff and precipitation seems stronger than if one considers annual precipitation as the indicator. Reduction in model performance become higher for a larger difference between the Q/P values

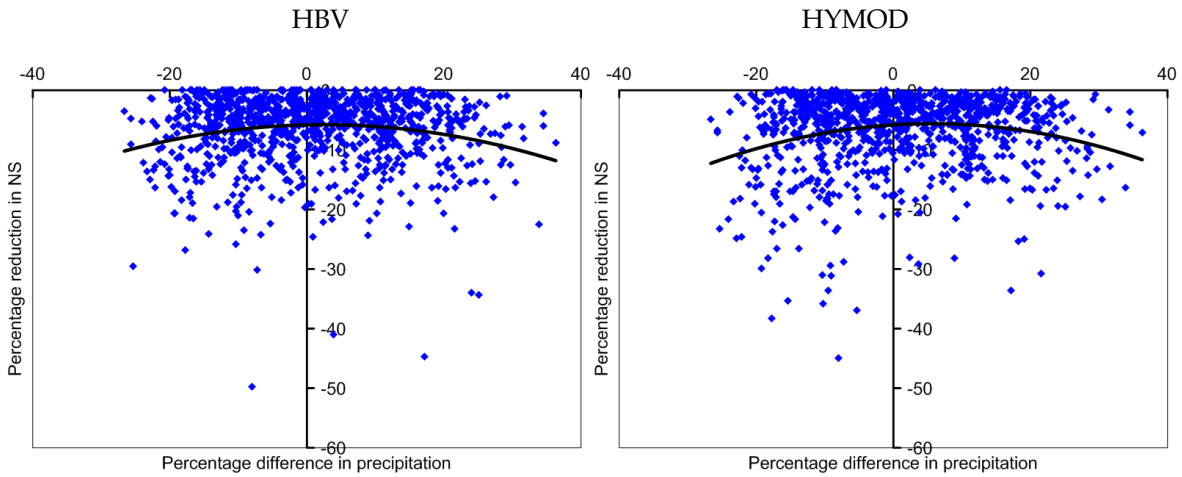

Figure 6.8: Scatterplots of percentage reduction in transfer model performance (NS) against percentage difference in precipitation between the validation and calibration sub-periods for HBV (left) and HYMOD (right).

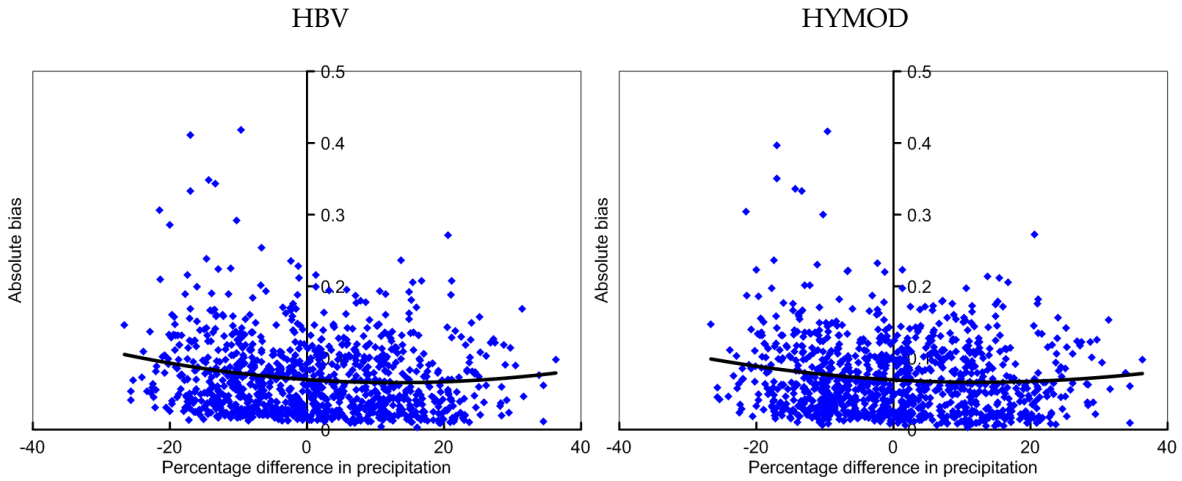

Figure 6.9: Scatterplots of absolute biases for validation periods against percentage difference in precipitation between the validation and calibration sub-periods for HBV (left) and HYMOD (right).

in calibration and validation periods. If the *Q/P* values are very different, the simulated qualities are generally poor.

The correlations between model performance and the difference between average air temperature in calibration and simulation sup-periods are plotted in Figure 6.12 for the percentage reduction in model performance and Figure 6.13 for absolute bias, respectively. The percentage difference in air temperature is calculated such that the mean temperature for the calibration sub-period is taken as the denominator. The negative value on the x-axis represent the transfer results that the temperature in the simulation sub-period is lower than in the validation period and vice versa. The air temperature for the study catchments are relatively stable over the time period, and the relationship between the reduction in model

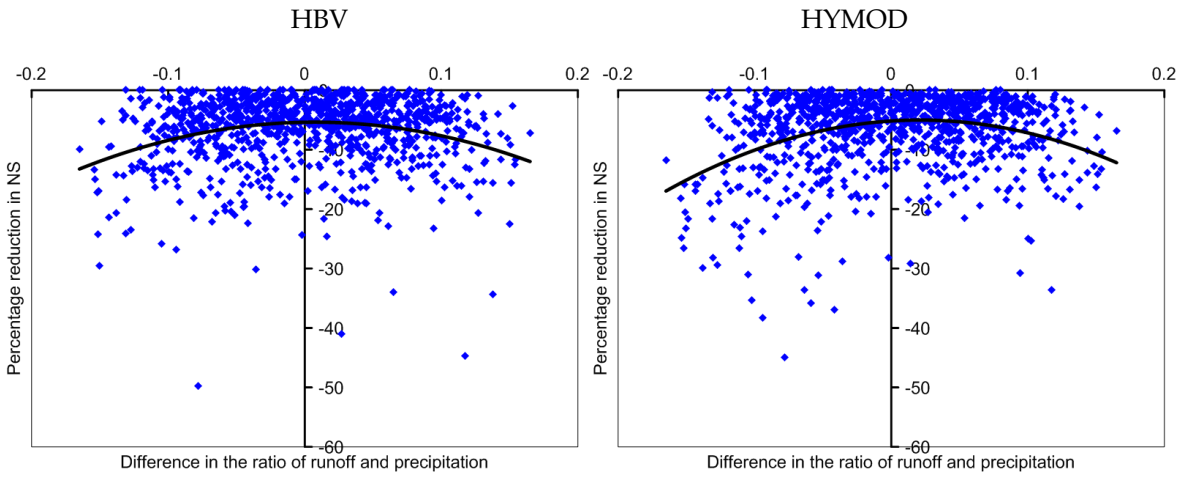

Figure 6.10: Scatterplots of percentage reduction in validation performance against difference in the ratio of runoff and precipitation between the validation and calibration sub-periods for HBV (left) and HYMOD (right).

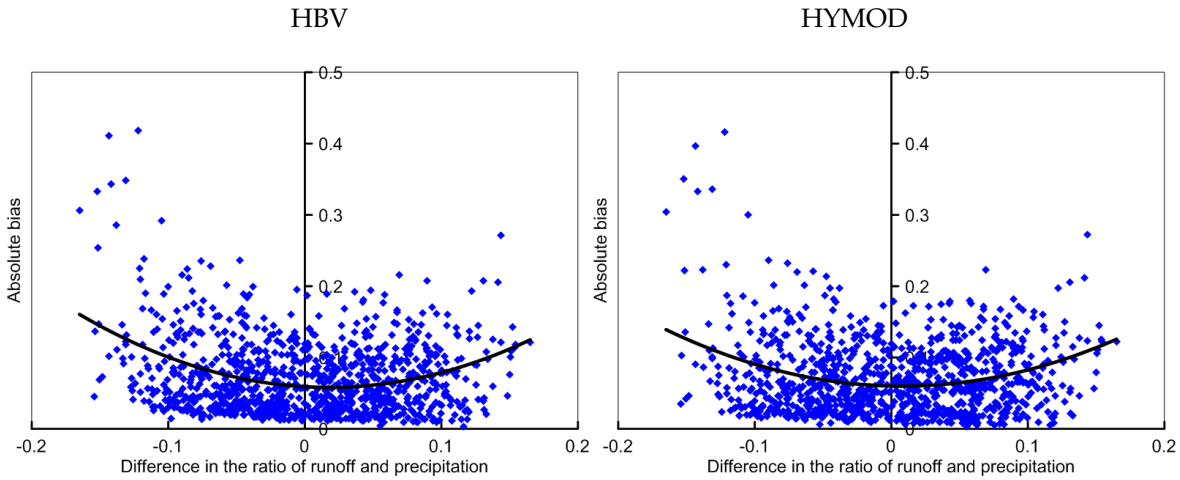

Figure 6.11: Scatterplots of absolute biases for validation periods against difference in the ratio of runoff and precipitation between the validation and calibration sub-periods for HBV (left) and HYMOD (right).

efficiencies and the changes in temperature conditions are very feeble. If the percentage difference in temperature becomes greater than 6%, the absolute bias shows slight increases.

In order to provide more insight of the temporal transferability of model parameters, the transfer results for 10 000 individual parameter sets have been investigated. Figure 6.14 shows an example of the validation results for catchment 01649500. The left histogram shows the validation performance of sub-period 70S by transferring parameters calibrated using the historical data of sub-period 50S. As a comparison, the calibration result is shown in the figure for reference. The simulated model efficiency for the 70S is similar to the calibration results, only about 5% of these 10 000 parameter sets are slightly worse. We can conclude that the parameters calibrated on the 50S are suitable for performing the rainfall-

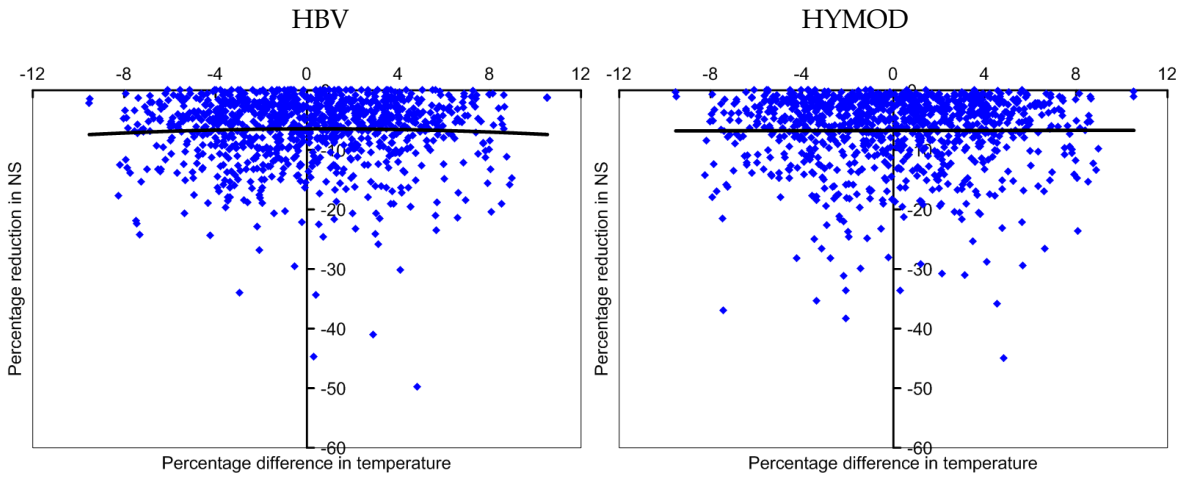

Figure 6.12: Scatterplots of percentage reduction in validation performance against percentage difference in temperature between the validation and calibration sub-periods for HBV (left) and HYMOD (right).

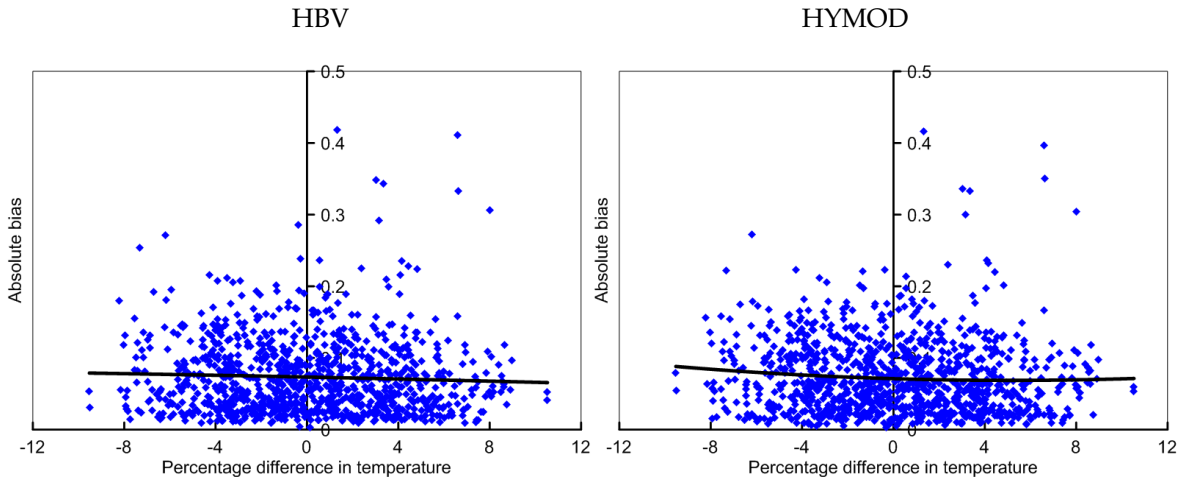

Figure 6.13: Scatterplots of absolute biases for validation periods against percentage difference in temperature between the validation and calibration sub-periods for HBV (left) and HYMOD (right).

runoff response of the 70S. However, the simulated model efficiency of the 50S by transferring parameter sets from the 70S is not as good as expected. The 10 000 individual parameter sets lead to a considerable fluctuation of the results. Only 3% of the parameter sets calibrated on the 70S are reliable for the 50S. For a few number of parameter sets, the reduction even reaches down to 0.3. This is mainly because of the difference weather conditions for these two sub-periods. The annual precipitation for sub-period 70S is greater than for the 50S, and more parameter sets could reasonably perform the rainfall-runoff process than for the dry periods. This study indicates that the calibration procedure should be performed very carefully if the modelers choose to use single parameter vectors for model application.

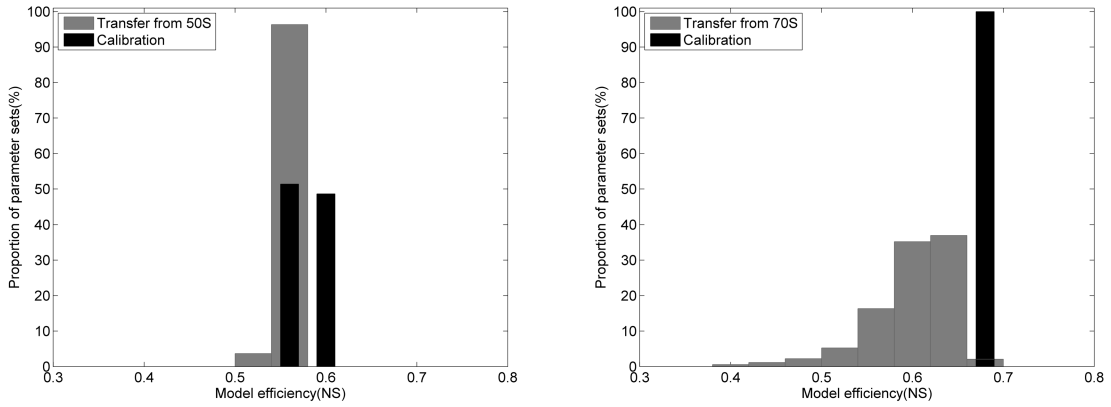

Figure 6.14: Histogram of transferred NS efficiency (gray) of HBV for catchment 01649500 for the sub-periods of 70S (left) and 50S (right). The individual calibrated NS model performances (black) were shown as the reference.

6.3.5 Transferability and Dissimilarity of Sub-periods

Figure 6.15 shows an example of the bivariate empirical copula density of API and runoff depth for four different sub-periods for catchment 01562000. The distance $L_{i,j}$ of copula density for two different sub-periods i and j was calculated as:

$$L_{i,j} = \sum_{l=1}^{n} \sum_{k=1}^{n} [C_{n-l,n-k}(i) - C_{n-l,n-k}(j)]^2 \tag{6.10}$$

Here the distance value represents the level of dissimilarity between two different sub-periods. A high value of L indicates greater dissimilarity in the hydrological response. This kind of dissimilarity was estimated for all sub-periods that involved in this study. Figure 6.16 plots the transfer model efficiency NS against the difference in empirical copula densities of API and runoff depth between the calibration and validation sub-periods for all study catchments. The results indicate that with the increasing of the distance between the bivariate empirical copula densities, the model validation leads to worse model performance. It can be seen clearly from the plots that the model performance displays dramatically decrease if the distance values are greater than 400.

6.3.6 Long Time Period Transition

For all the study catchments, the HBV model was calibrated using 40-year data series, and the parameter sets were then applied to the remaining sub-period. Figure 6.17 shows the transfer NS model performance for each sub-period. The transfer results from the ten-year data based calibration are plotted in the illustration as a comparison. For all the sub-periods, the long time data based calibration usually leads to a better-transfer model performance than the short one. The long time calibration data covers various climate conditions for the

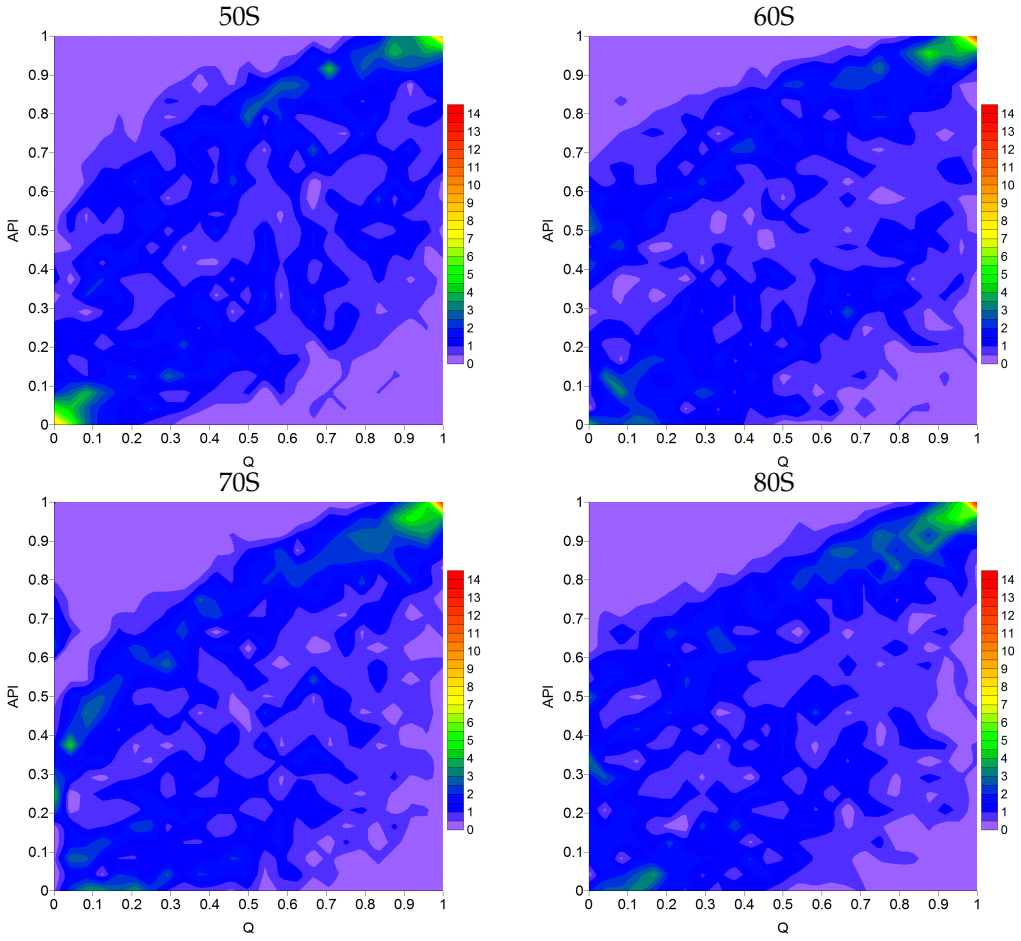

Figure 6.15: An example of empirical copula density of API (y-axis) and Q(x-axis) for four sub-periods for catchment 01562000.

rainfall-runoff process and can reduce the uncertainty of model parameters. The models are better constrained when they use 40-year data compared to using ten-year data. The simulation results indicate that the effect of calibration data length and variability on the transferability of model parameters.

6.3.7 Common Transition

Simultaneous calibration was taken for the driest sub-period 60S and the wettest sub-period 70S for both HBV and HYMOD. Firstly, the model performances for the individual and common calibration were compared. The individual calibration approach logically leads to better model performance than the common calibration, following the finding in Chapter 5. The mean NS performance over the all study catchments for sub-period 60S drops from 0.75 to 0.72 for HBV model and from 0.71 to 0.68 for HYMOD model, respectively.

When one applies the models for the validation sub-periods 90S, for the individual cali-

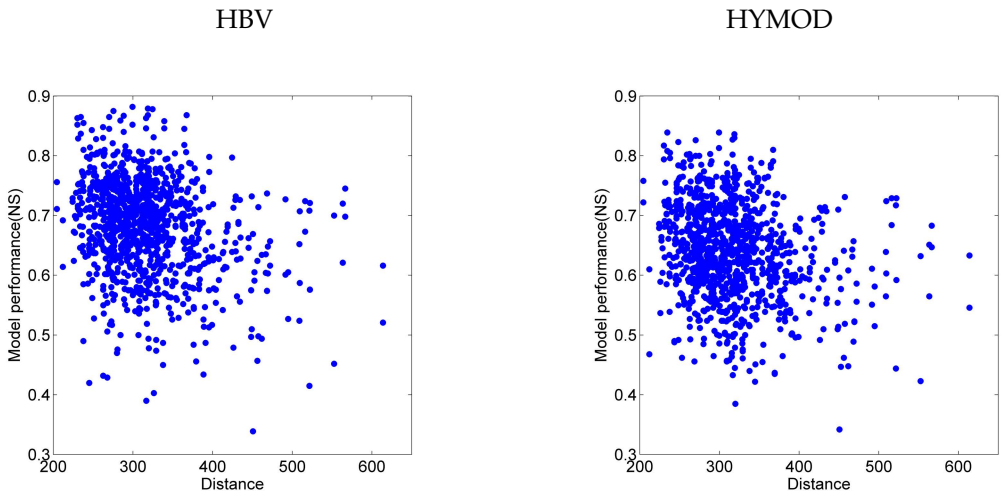

Figure 6.16: Scatterplot of transfer model performance (NS) against distance of bivariate copula densities between the validation and calibration sub-periods for HBV (left) and HYMOD (right).

brated model parameters, the average model performance is around 0.67. While for the common calibration, the mean value increases to 0.51. It indicates the robustness of the commonly calibrated parameter sets.

As shown in Figure 6.2, the 60S are generally the driest sub-periods and the 70S are the wettest sub-periods for most of the study catchments. This assumed that the data set of these two decades could cover most of the weather conditions of other sub-periods. Figure 6.18 shows the average simulation efficiency NS for the rest three sub-periods by using the parameter sets calibrated on common calibration against the case of using individually calibrated parameter sets. The results indicate that the simulated efficiency are slightly better for the common parameters, especially for HYMOD. For the minimum NS coefficient for all the 10 000 parameter sets, as shown in Figure 6.19, it could be well improved if simulated by the common parameter sets were used instead of individual parameter sets. For about 60% of HBV and 57% of HYMOD, the common parameters lead to model efficiency NS where the minimum values are better than that obtained by individual calibration parameters.

Figure 6.20 shows the absolute bias values of using common parameter sets comparing with the one obtained from individual parameter sets. As expected, the absolute biases for the commonly calibrated parameters are lower than for the individual ones. For example, the mean absolute bias over all catchments drops from 0.07 to 0.06 for HBV and from 0.06 to 0.05 for HYMOD, respectively. However, the absolute biases show opposite tendency for the donor sub-period of the 60S and the 70S. For some simulation runs, the transfer absolute bias increase if using 60S data set for model calibration and decrease if using the data period of 70S for model calibration. This might be due to the different weather conditions for these two decades.

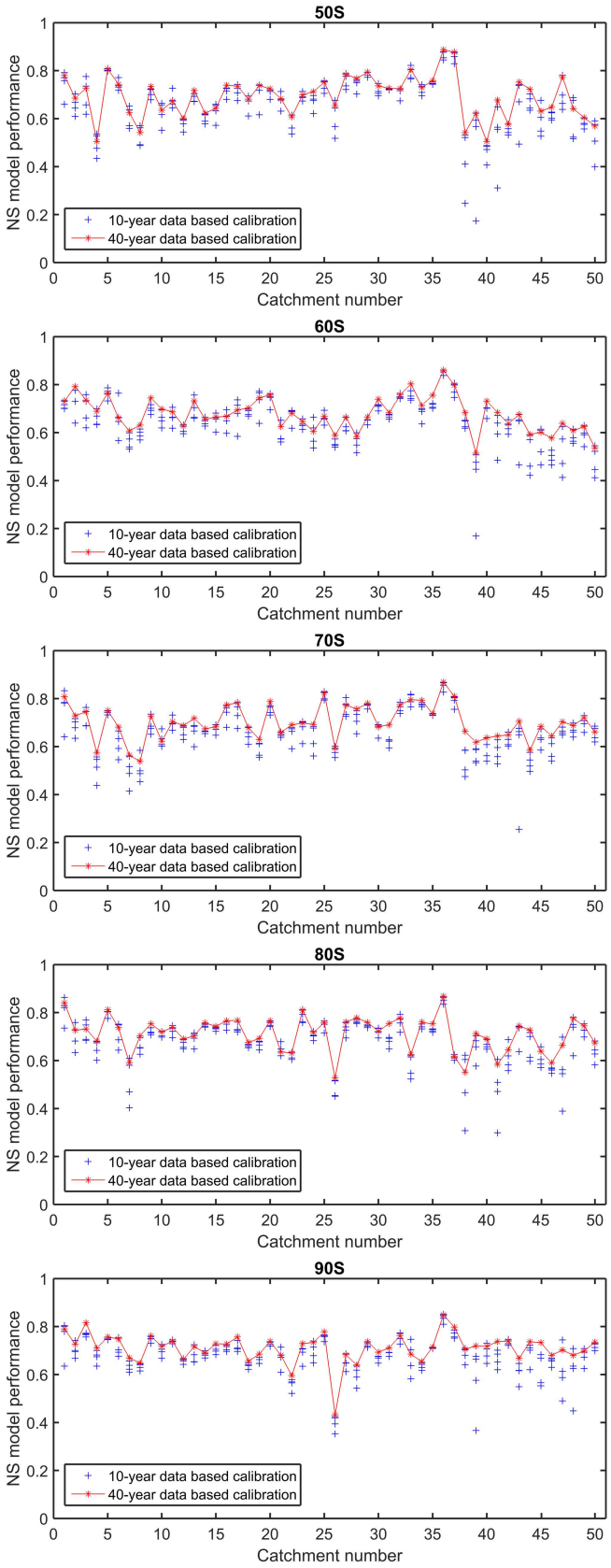

Figure 6.17: Transferred NS coefficient of HBV model for 50 MOPEX catchments for five sub-periods. Model parameters were calibrated using NSB as performance criteria based on 10-year (blue) and 40-year (red) data records, respectively.

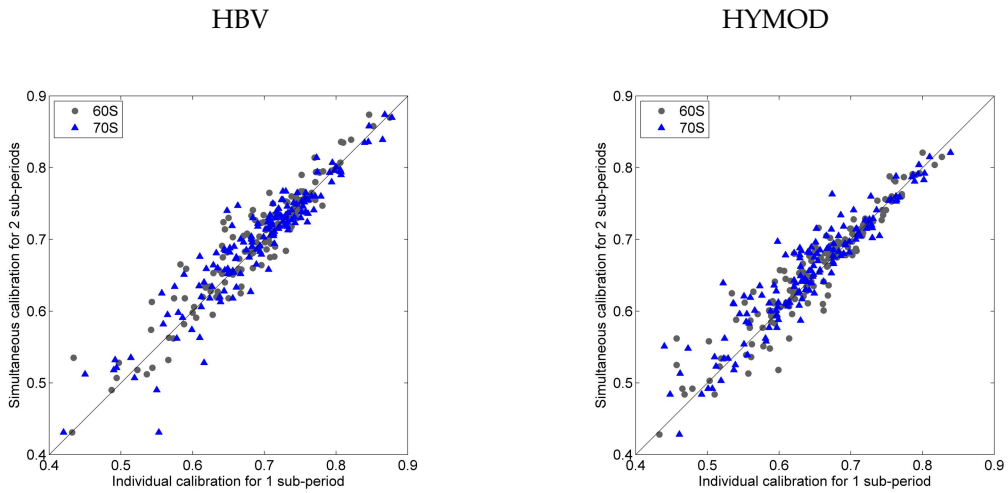

Figure 6.18: Mean NS model performance for 50 MOPEX catchments for the sub-period 60S (gray circles) and the 70S (blue triangles) for HBV (left) and HYMOD (right). Model parameters were estimated by individual calibration for one sub-period and simultaneous calibration for two sub-periods, respectively.

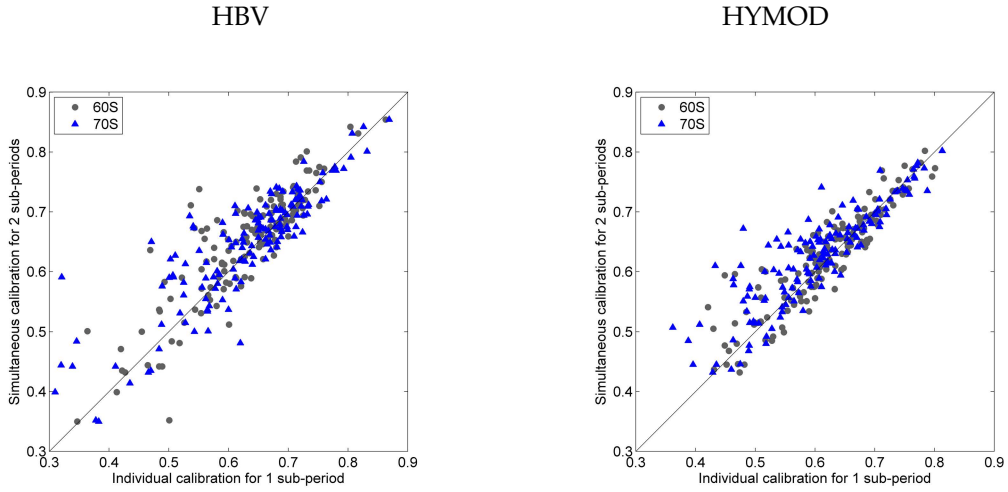

Figure 6.19: Minimum NS model performance for 50 MOPEX catchments for the sub-period 60S (gray circles) and the 70S (blue triangles) for HBV (left) and HYMOD (right). Model parameters were estimated by individual calibration for one sub-period and simultaneous calibration for two sub-periods, respectively.

6.3.8 Weather Adjustment

The weight function approach was applied for the sub-periods with a large difference in mean annual precipitation to detect the change of model performance and the transferability of model parameters. The sub-periods with the percentage difference in annual precipitation greater than 20% were considered in this study. For a total of 27 simulations, the annual precipitation for the receiver sub-period is 20% smaller than the one for the donor sub-

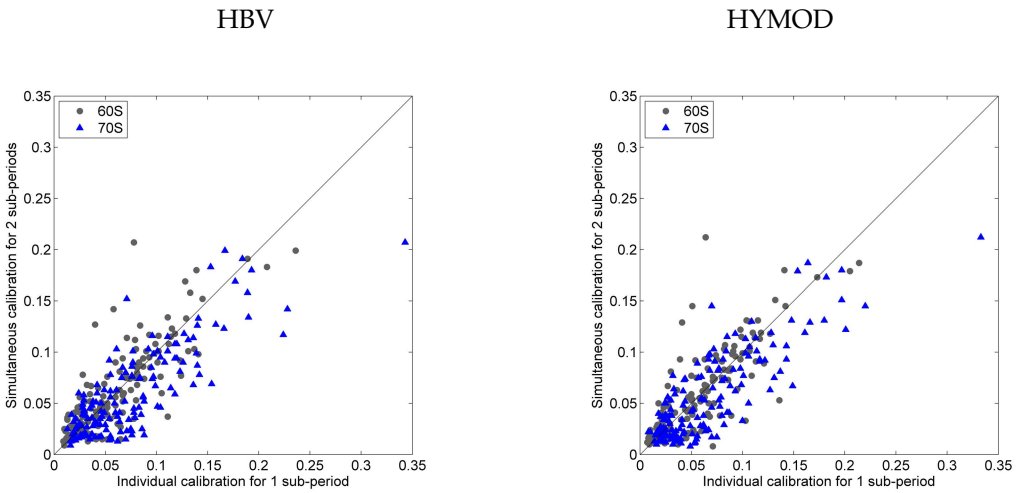

Figure 6.20: Absolute biases for 50 MOPEX catchments for the sub-period 60S (gray circles) and the 70S (blue triangles) for HBV (left) and HYMOD (right). Model parameters were estimated by individual calibration for one sub-period and simultaneous calibration for two sub-periods, respectively.

period. For a total of 74 simulations, the annual precipitation for the receiver sub-period is 20% greater than the donor sub-period with respect to the donor sub-period. For all these donor sub-periods, HBV model was recalibrated based on weight function to adjust the climate conditions similar to the receiver sub-periods. For comparison, two different weight function were used in this study. For case 1, value $w(t) = 1.2$ was applied to the years where the weather is similar to the weather of the receivers, $w(t) = 0.8$ was given to the so-called dissimilar years. For case 2, a higher weight $w(t) = 1.5$ was applied to the similar years and $w(t) = 0.7$ was used for dissimilar years.

Figure 6.21 shows the simulation results for the receiver sub-periods where the annual precipitation is much lower than for the donor sub-periods by using two different weight functions. The individual transferred results are also presented as comparison. The result shows that for 9 out of 27 simulations, the NS efficiency slightly increases if applying weight function into calibration strategy. The higher the weight for the similar years, the better the simulation results are. However, a total of 7 simulations show decreasing NS performance with the increasing weight for the period has similar climate conditions, while for 11 simulations the weight functions did not affect the simulation results.

Figure 6.22 shows the results for the receiver sub-periods where the rainfall is greater than for the donor sub-periods. The change of NS coefficient seems smaller than the application for the opposite way. For 10 out of 74 simulations, the model performance improved slightly by using weight functions and one-third of the simulations do not show clear change. However, for at least 16 simulations, the model performance decreases if weight function are incorporated in the model calibration procedure.

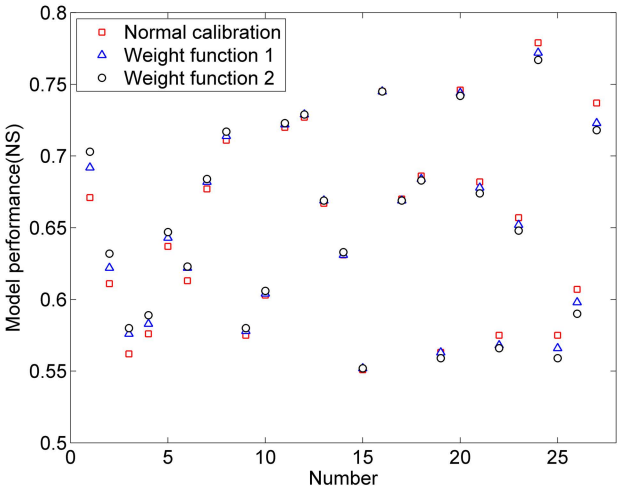

Figure 6.21: Mean NS model performance for the relatively dry sub-periods by transferring model parameters from wet sub-periods.

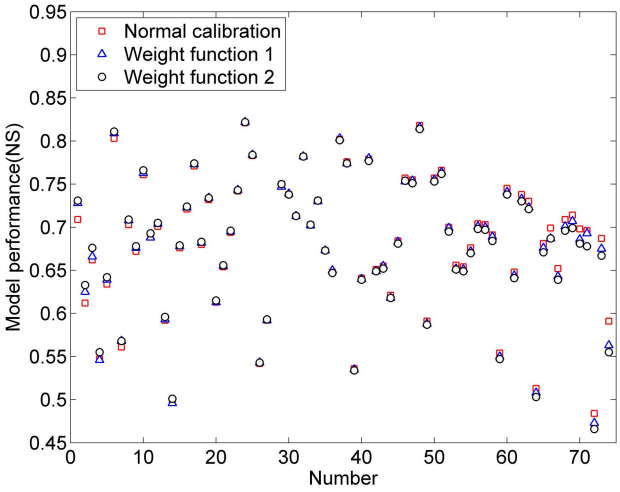

Figure 6.22: Mean NS model performance for the relatively wet sub-periods by transferring parameters from dry sub-periods.

6.4 Conclusions

In this chapter, the transferability of model parameter sets under different climate conditions was investigated. The result shows that model parameters are strongly influenced by the climatic conditions of the calibration period. The sub-period calibration and cross-validation approaches indicate that the variability of climate conditions often leads to different parameters for the same catchment. The incorporation of bias constraint with NS efficiency strategy could achieve better water balances compared to the unconstrained one when model parameters are subsequently used for very different climate conditions.

The transferability of model parameters highly depends on the data set used for model calibration which can be detected by the dissimilarity of climate characteristics using copula density. To cope with the instability of model parameters calibrated on catchments in non-stationary conditions, two model calibration strategies, the common calibration of multi sub-periods and the climate condition based weight function were applied. The transfer quantities could be slightly improved by these approaches.

7 Influence of Data Quantity and Quality on Model Parameterization

This chapter investigates the influences of calibration data length and data quality on model parameterization and presents approaches for parameter estimation in data-limited catchments.

7.1 Introduction

As discussed before, conceptual rainfall-runoff model parameters highly depend on the data series that are used to calibrate the models [Yapo et al., 1996; Beven, 2011]. Previous studies [Duan et al., 1994; Yapo et al., 1996] have indicated that the data selected for model calibration should be "representative" of the various phenomena experienced by the catchments. Some people have attempted to satisfy this requirement by using as large a data set as possible. However, observations of continuous hydrometeological data for model calibration and validation are available only at a small fraction of the basins. The application of hydrological models is often limited due to the lack of observation data.

In this chapter, a number of catchments were calibrated using different length of data periods and the transferability of the calibrated model parameters was tested in two different validation time periods. The objective of this study is to evaluate the influences of data quality and quantity on model parameterization, to investigate how much observational data are sufficient or necessary to obtain a good model calibration, and to find a solution to reduce the uncertainty of model parameters in data-limited regions.

7.2 Methodology

In the research presented in this chapter, the lumped HBV model was selected to simulate the rainfall-runoff behaviors of the 15 MOPEX catchments that have been described in Section 2.1. The combination of Nash-Sutcliffe efficiency and log-bias constraint (NSB) was taken as model performance criterion (see Equation 3.22). As usual, each calibration obtains 10 000 parameter sets that perform very similar by using the ROPE algorithm.

In this chapter, two numerical experiments were carried out on the selected 15 catchments, using a 40-year record of historical data from 1950 to 1989. The 40-year data set was split into calibration (1950-1969) and validation (1970-1989) periods as shown in Figure 7.1.

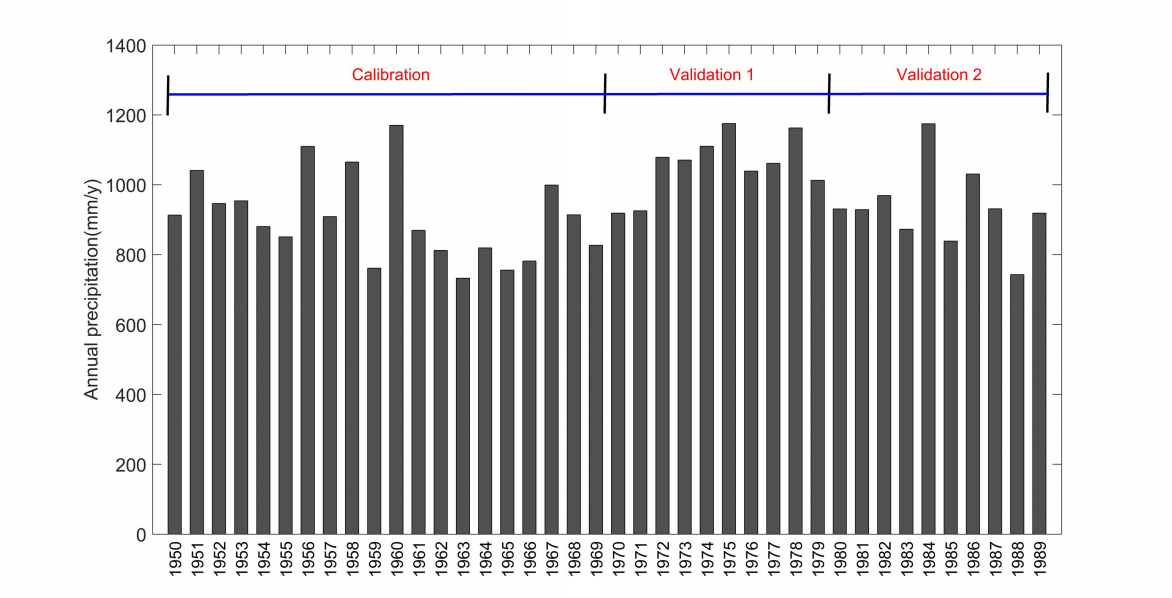

Figure 7.1: Separation of historical data: calibration (1950-1969), validation 1 (1970-1979) and validation 2 (1980-1989).

In numerical experiment 1, the HBV model was simulated using data lengths of 1, 2, 5, and 10 consecutive hydrological years from the period 1950-1969. This results in 20, 10, 4 and 2 calibration runs for every catchment. In each calibration, one-year data before the selected period was taken as a warm up time period to minimize initialization error. Nevertheless, the calculation of the objective function does not consider this warm up year. All the calibrated parameters were used to verify two distinct validation time periods (1970-1979,1980-1989) to investigate the transferability and sensitivity of model parameters.

In numerical experiment 2, in order to reduce the uncertainty of parameter estimation for catchments with limited historical data, the common calibration is proposed to calibrate models simultaneously for the target catchment and the neighboring catchment. Here it is assumed that the calibration for the target catchment uses only one-year historical data as a "data-limited" catchment. This kind of approach is expected to use extra information from similar catchments to identify robust parameters for the data-limited catchments. The neighboring catchment for common calibration was selected based on the geographical distance between the streamgauges of the catchments. Table 7.1 lists the spatial proximity catchment and the corresponding geographical distance for all 15 catchments. The ten-year data from the nearest catchment for the period 1950-1959 was selected to conduct simultaneous calibration with the target catchment using only one-year historical data. The model calibration was carried out for the time period 1950 to 1969 and resulted in 20 simulations for each "data-limited" catchment.

Table 7.1: The selection of the nearest catchment and the corresponding distance.

No	Catchment	The nearest catchment	Distance(km^2)
1	01548500	01611500	228
2	01606500	03180500	76
3	01611500	01606500	99
4	01663500	01664000	15
5	01664000	01663500	15
6	01667500	01664000	25
7	02016000	02018000	19
8	02018000	02016000	19
9	02030500	01667500	80
10	03114500	03155500	46
11	03155500	03114500	46
12	03164000	03173000	73
13	03173000	03164000	73
14	03180500	03186500	60
15	03186500	03180500	60

7.3 Results

7.3.1 The Impact of Data Variability

Figure 7.2 plots the model performance of calibration based on a one-year data set and the corresponding evaluated model performance for the validation period 1970-1979. For most of the cases, the calibrated model performance is bigger than for the validation runs. This also indicates that the parameter calibrated with higher efficiency usually result in better performances than the ones calibrated with lower efficiency.

Figure 7.3 compares the model performance for the two different validation time periods 1970-1979 and 1980-1989 using the parameters estimated based on one-year data. The transfer model performances for these two time periods are very similar. The correlation coefficient of the model performance is about 0.80. This high correlation of the validation performance for different data sets indicates the stability of the calibration parameters. It can be seen from the plots that the low-performance calibrations are relatively more sensitive to the particular validation period.

The bar chart shown in Figure 7.4 represents the individual calibration performance for the period 1970-1979 for all 15 catchments. The models always perform differently for different catchments which is assumed to be due to input and output errors. In order to compare the transferred model performance for different catchments, all the transfer model performances using parameters calibrated on different lengths of data were normalized by the individual calibration performance for the target period. The higher the value represents the better the parameter for transfer. A value of 100% means a perfect prediction. The upper

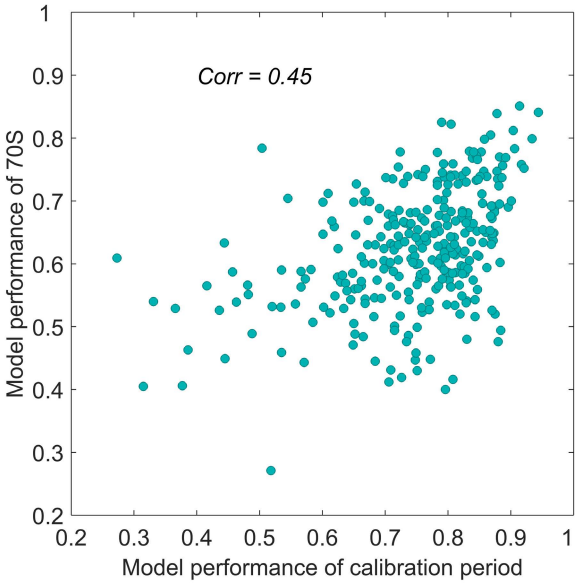

Figure 7.2: Correlation of NS model performance for one-year data based calibration period and the validation period 1970-1979.

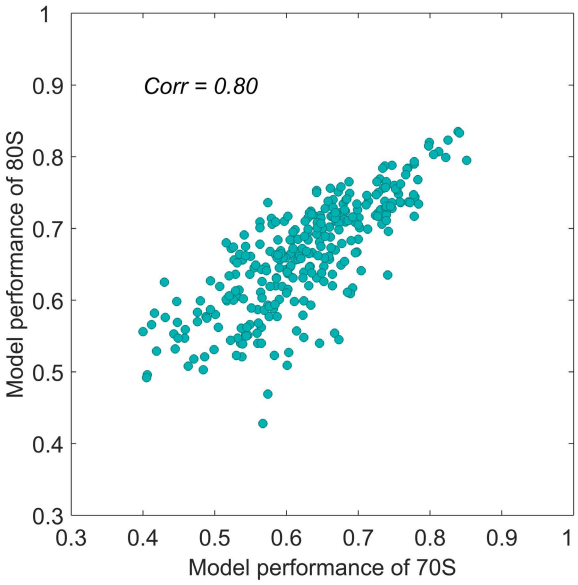

Figure 7.3: Correlation of NS model performance for two different validation period: 1970-1979 and 1980-1989. HBV model parameters were calibrated based on one-year data.

part of Figure 7.4 shows the relative model performance of 15 catchments by transferring the one-year-based calibrated model parameters to the time period 1970-1979. We can see clearly that the model parameters obtained by one-year calibration perform differently for each catchment. Most of the parameters estimated by one-year data could capture more than 60% of the model performance for the ten-year validation. For catchment 12 and 15, all the parameters calibrated on one-year data perform well because the relative model performances are bigger than 80%.

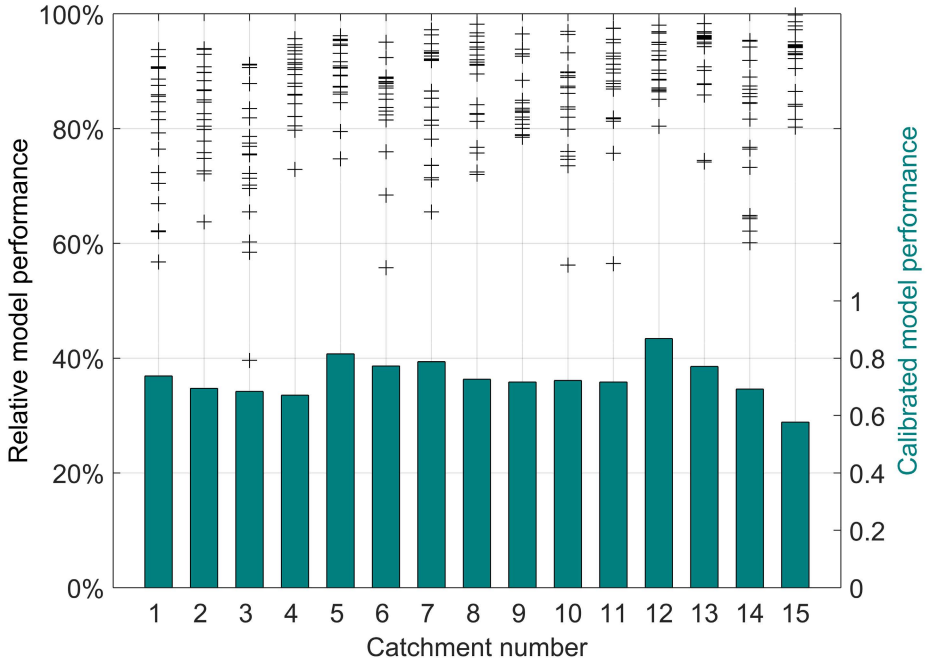

Figure 7.4: Mean NS model performance of individual calibration (bar chat) and the relative NS model performance for the transfer of the one-year based calibrated model parameters (scatterplots) for the sub-period 1970-1979. The relative model performance was normalized by the individual calibration performance for the corresponding sub-period.

Figure 7.5 compares the mean model performance for the validation period 1970-1979 when different lengths of data were used for calibration. As expected, the validation performance increases with the increase of length of data used for calibration for most of the catchments. The sensitivity of data length for parameter estimation varies for different catchments. For example, the average model performance seems very similar for using 1, 2, 5 and 10 years data for parameter estimates for catchment 9 and 15. However, for catchment 1, 5 and 11, the validation performance improves a lot if more years were selected for model calibration. For the 10 years data based model calibration, 11 out of 15 catchments obtain more than 90% relative model performance for the validation period. This indicates that 10-year data are sufficient good for a model calibration for most of the study catchments.

For the one-year data based model calibrations, the influences of data quality to the trans-

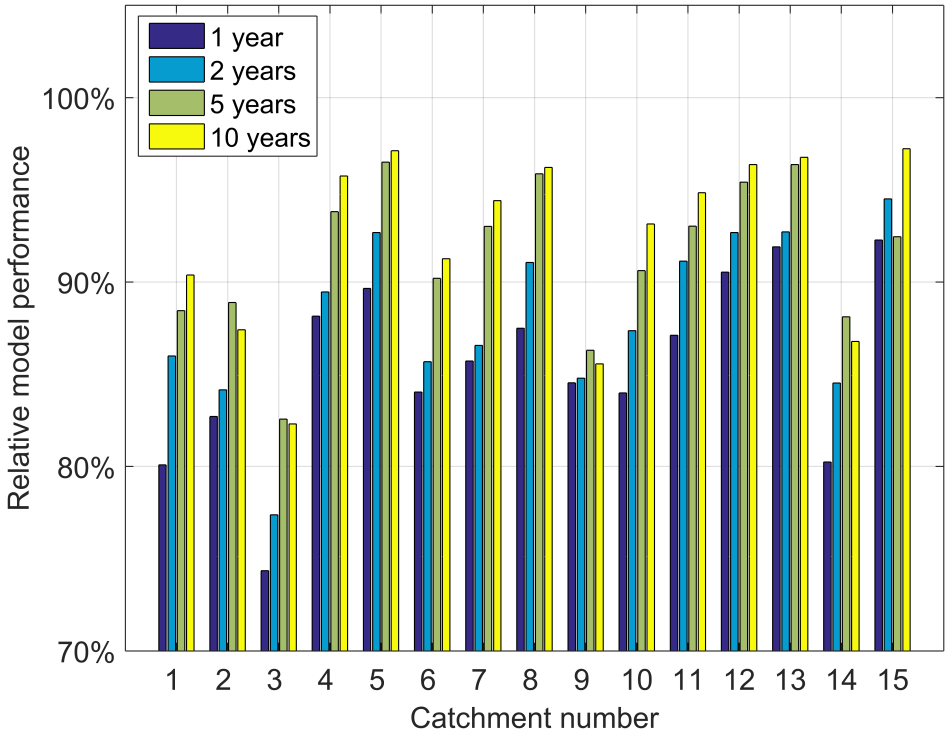

Figure 7.5: Comparison of relative NS model performance for 15 study catchments for the sub-period 1970-1979 for transferred parameters from different length of data based model calibration.

ferability of model parameters were investigated. Figure 7.6 shows the correlation of the transfer model performance for the validation period 1970-1979 with the observed runoff during the calibration period. The left part of Figure 7.6 plots the correlation with peak flow and the right part plots the correlation with 10% high flow value. We can see clearly from the scatterplots that most of the poorly transferred parameters are estimated by the dataset with relatively small peak flow. However, the correlation with 10% high flow values is not as clear as the correlation with peak flow.

The relationship between the peak flow and the calibrated model parameters was also explored. The result shows that for one-year based model calibration, the peak flow value has relatively high impact on threshold water lever *HL* and near surface flow storage constant *K0* as shown in Figure 7.7. In HBV model structure, these two parameters are highly related to surface runoff. A low value of peak flow during the calibration procedure limits the information for the model parameter estimation and the models are not able to capture the essential features of the catchments. Therefore, the model parameters could not be transferred to different conditions.

Figure 7.8 shows an example of the distribution of the parameters *HL* and *K0* that were calibrated using the different lengths of data series. Both parameters display definite changes

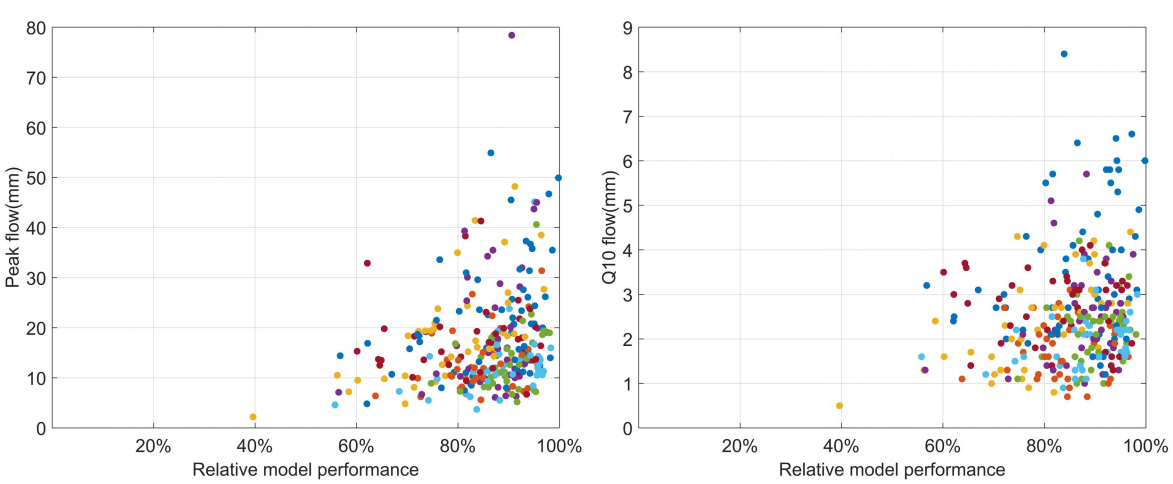

Figure 7.6: Correlation of the transferred NS model performance for the sub-period 1970-1979 with the observed peak flow (left) and the 10% high flow value during the calibration periods.

with the increasing of data length used for model calibration. The uncertainty of model parameters could be significantly reduced if more information was involved in the calibration routine. Figure 7.9 shows the corresponding transferred model performance for the period 1970-1979. By increasing the length of data from one-year to two-year, the model performances improved notably. But when the data used for calibration was increased from 5 to 10 years, the result was somewhat unexpected as the performance decreased. This may be due to the observational errors and specific features in the calibration period, since the adjustment of the model can be very specific to the observation period leading to an overestimation of model parameters.

7.3.2 Application in Data-limited Catchments

For all 15 catchments, the simultaneous calibration was performed for the target catchment with one-year data and with ten-year data from 1950-1959 for the nearest catchment. Firstly, the model performances for the individual and for the common calibration were compared. The NS model performance for the common calibration is relatively lower than the individual one for the target catchment. Both of these parameter sets were used to simulate the model for two validation periods. The result shows that for the period 1970-1979, the mean model performance of the individual parameter sets over all study catchment is about 0.62 while for the common calibration the average value increases to 0.64, indicating the robustness of the common calibration. Figure 7.10 compares the transfer model performance of individually calibrated model parameters based on one-year data and the common calibration with a neighboring catchment for the validation periods. The scatterplots show that by using the information from a neighboring catchment, the model might obtain much more reliable parameter estimations. For about 65% of the validation period 1970-1979 and 64%

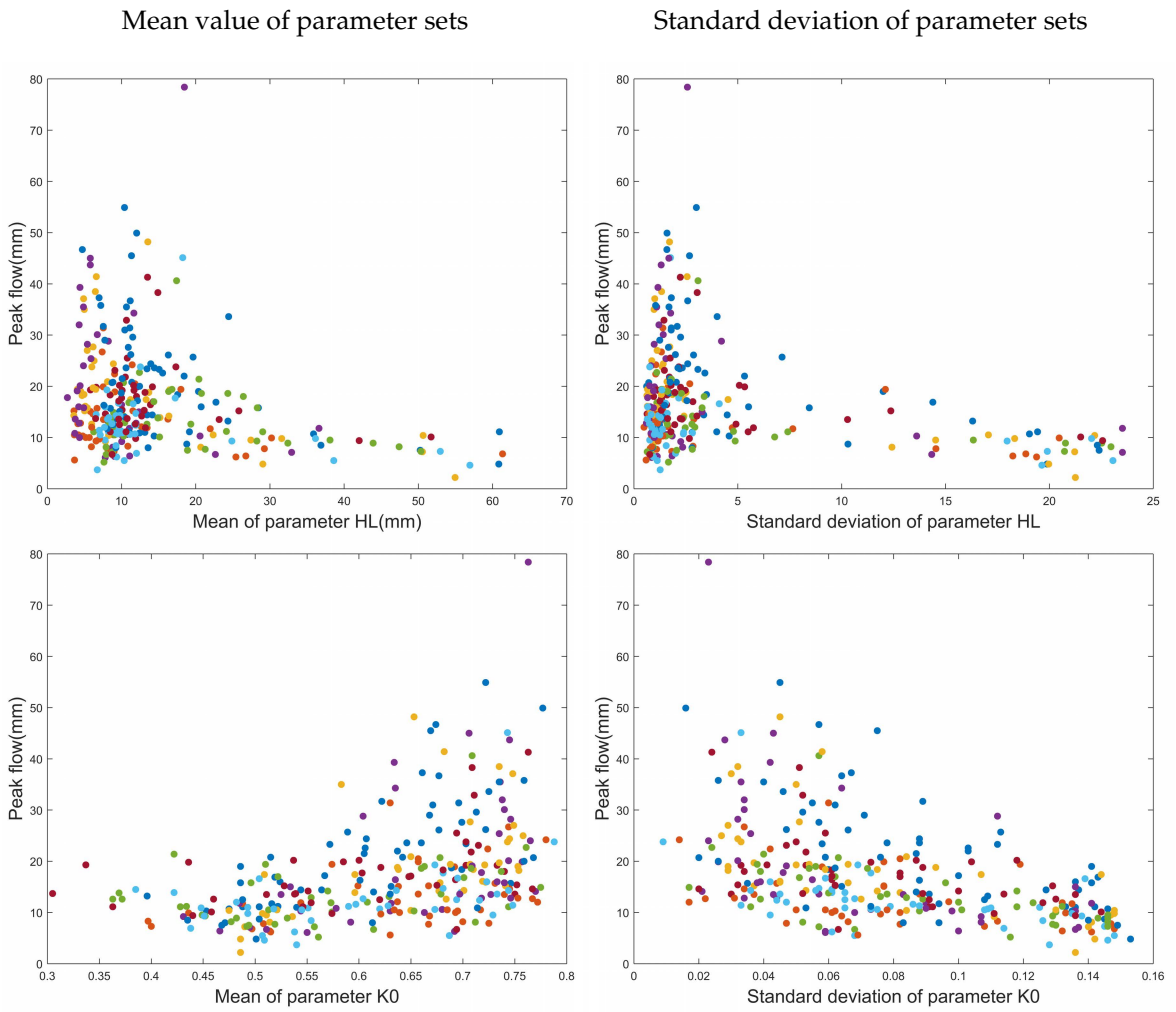

Figure 7.7: Correlation of peak flow value with the parameter threshold water lever HL (upper) and near surface flow storage constant K0 (lower). The left side of the scatterplots shows the mean value of parameter sets and the right side illustrates the standard deviation value, respectively.

of the validation period 1980-1989, the common parameters lead to a model efficiency NS where the average values are better than those obtained by individual calibration parameters. Simultaneous calibration with a neighboring catchment offers a good way for model calibration and prediction in data-limited catchments.

This chapter only shows the result of using single neighboring catchment for common calibration. In our study, simultaneous calibration with multi neighboring catchments was also tested. Unfortunately, none of the simulation results shows improvement when compared with the single adjacent catchment approach.

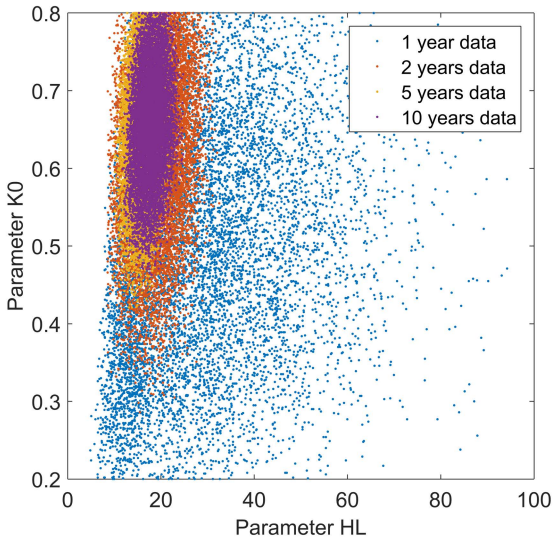

Figure 7.8: Scatterplots for two HBV parameters (HL and K0) obtained using different length of data for catchment 01611500 .

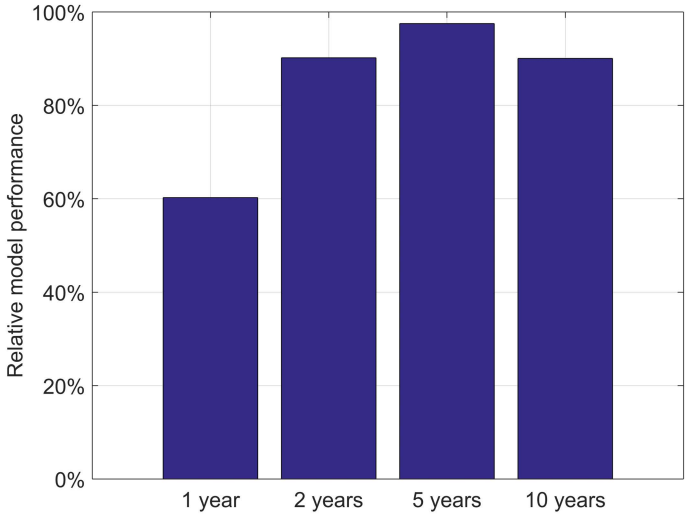

Figure 7.9: Transferred NS model performance for catchment 01611500 for the sub-period 1970-1979. Parameters were calibrated using different length of data, all the model performances were normalized by the individual calibration result for 1970-1979.

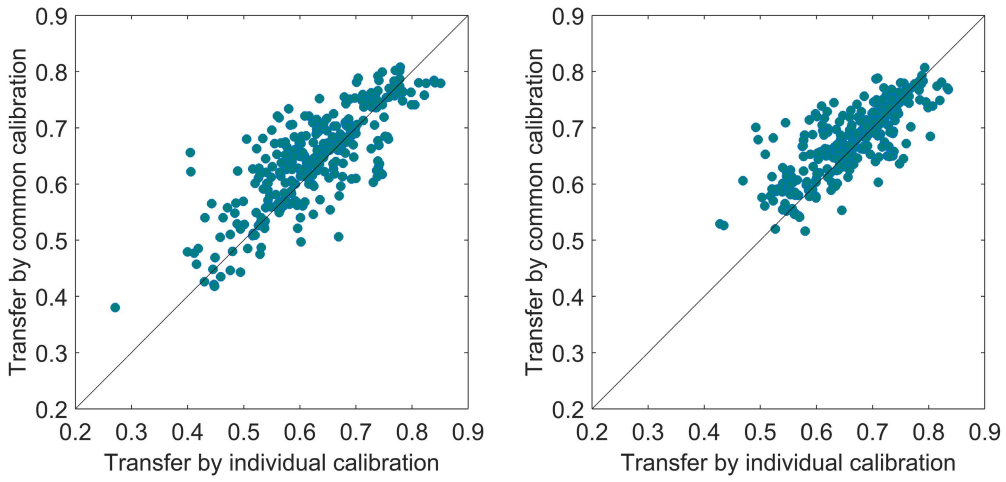

(a) 1970-1979 (b) 1980-1989

Figure 7.10: Mean NS model performance of transfer parameters from individual calibration and common calibration for the sub-period 1970-1979 (left) and 1980-1989 (right), respectively.

7.4 Conclusions

In this chapter, the HBV model was calibrated based on different lengths of data sets and different time periods. The result shows that the transferability of model parameters increases with the increasing of the length of data used for calibration for most of the catchments. The sensitivity of data length for parameter estimation varies between different catchments. In general, a 5-10 year data set is necessary to obtain a good model calibration. Results also show that flood events have significant influence on model parameter identification, especially for the parameters that correlate to the generating of surface runoff. For the model calibration in data-limited catchments, simultaneous calibration with a similar catchment might lead to more reliable parameter estimations than only using the limited data.

8 Summary and Outlook

8.1 Summary

This thesis addresses a major concern of the transferability of conceptual hydrological model parameters both on the spatial and temporal scales.

Due to observational errors and specific features in the calibration period, the adjustment of the model can be very specific to the observation period leading to an overcalibration. To overcome such limitations, a simultaneous calibration approach is introduced to identify parameter sets that perform well for all catchments within the modeled domain. A new model parameter η controlling the actual evapotranspiration was introduced to cope with the clear differences in water balances due to water or energy limitations. Three hydrological models were used in combination with three different performance measures in four numerical experiments on a large number of catchments. The individual calibration and transfer results indicate that models are often overfitted during calibration. The parameters are sometimes more specific for the calibration time period and their relation to catchment properties seems to be unclear. This makes parameter transfers or parameter regionalization based on individual calibration difficult. The common spatial calibration strategy, which explicitly assumed that catchments share dynamical parameters, was tested on a number of 15 catchments and 96 catchments, respectively. The common calibration provides an efficient way to identify parameter sets which work reasonably for all catchments within the modeled domain. Testing the parameters on an independent time period shows that common parameters perform comparably well as those obtained using individual calibration. The transfer of the common parameters to model ungauged catchments works well. The performance of common parameters on a small number (15) of catchments was better than on a big number (96) of catchments covering a large spatial scale. It indicates that the performance of the common parameters depends strongly on the selection of the catchments used to assess them, and a reasonable geographic proximity of the catchments might be a good choice for common calibration. The results of the experiments were similar for all three hydrological models applied independently of the choice of the performance measures. Note however, that the common parameters corresponding to the different performance measures differ considerably. The common behavior is dependent on how one evaluates the performance of the models. The fact that many catchments share common parameters which describe their dynamical behavior does not mean that they really do have the same dynamical behavior. The model output highly depends on the parameter η which varies from catchment to catchment and also as a function of the other model parameters describing dynamical behavior. Common parameters offer a good possibility for the prediction of ungauged catchments,

because then only the parameter η which controls the long-term water balances has to be estimated individually. This however can be done using other modeling approaches including regionalization methods.

The rainfall-runoff behavior for a specific catchment may be considered as non-stationary under the changing climate and land use conditions. Parameter estimates for different calibration time periods might be significantly different. This limits the applications of hydrological models under non-stationary conditions. In this study, the transferability of model parameter sets under different climate conditions is investigated. The result shows that model parameters are strongly influenced by the climatic conditions of the calibration time period. The sub-period calibration and cross-validation approaches indicate that the variability of climate conditions often leads to different parameters for the same catchment. The incorporation of bias constraint with NS efficiency strategy could achieve better water balances than the unconstrained one when model parameters are subsequently used for very different climate conditions. The transferability of model parameters highly depends on the data set that is used for model calibration which can be detected by the dissimilarity of climate characteristics using copula density. To cope with the instability of model parameters under non-stationary conditions, two model calibration strategies, the common calibration for multi sub-periods and the weather adjustment with weight function are tested on the HBV model. These approaches tend slightly to improve the model performance for most of the simulations as compared to traditional calibration, although the benefit is small.

The reliability of hydrological models is highly influenced by the quality and quantity of data sets used for parameter identification. This influences of data quantity and quality on model parameterization are also investigated in this study. The model was calibrated based on different lengths of data sets and different time periods. The result indicates that the transferability of model parameters increases with the increasing of data length used for calibration for most of the study catchments. The sensitivity of data length for parameter estimation varies for different catchments. In general, a length of data ranging from five years to ten years is sufficient to calibrate a particular rainfall-runoff process. The result also shows that the flood events have significant influence on model parameter estimation, especially for the surface runoff correlated parameters. As observations of continuous hydrometeological data for model calibration and validation are available only at a small fraction of the basins, the application of hydrological models is often limited due to the lack of observation data. The common calibration approach was presented by using information from spatial proximity catchments. The result shows that for more than half of the simulations, the model performance and transfer quantity can be slightly improved by using information from similar catchments. However, for one-third of the simulations, the model parameters calibrated by simultaneous calibration leads to worse model performances than the one by individual calibration.

8.2 Outlook

For applying the simultaneous calibration approach in geographical space, the long-term discharge volumes have to be estimated for ungauged catchments. This problem is not ex-

plicitly treated in this study. The estimation of parameter η is a limitation of the presented simultaneous calibration approach. Regionalization of long-term discharge volumes is a prerequisite for the application in ungauged basins. For the MOPEX catchments involved in this study, the discharge coefficients which relate discharge volumes to (known) precipitation show a quite smooth spatial behavior. Thus, the regionalization of this parameter seems not to be an extremely complicated task in this particular region. The potential application of this approach in other regions needs to be investigated in future work.

In this study, all the models were tested on the daily time scale. Differences in catchment properties have significant effects on smaller temporal scales (e.g. hourly). Results also indicate that the differences in catchment properties cannot be captured well by simple lumped model parameters.

This study only tests the lumped conceptual models. The model performance and transferability for different temporal and spatial resolutions may be considered.

In this study, only the changes in climate conditions have been investigated. The land cover information should also be considered as "non-stationary" in hydrological model simulations.

Bibliography

Abrahart, R. J., See, L., et al. (2002). Multi-model data fusion for river flow forecasting: an evaluation of six alternative methods based on two contrasting catchments. *Hydrology and Earth System Sciences Discussions*, 6(4):655–670.

Ahmed, S. and De Marsily, G. (1987). Comparison of geostatistical methods for estimating transmissivity using data on transmissivity and specific capacity. *Water resources research*, 23(9):1717–1737.

Ali, G., Tetzlaff, D., Soulsby, C., McDonnell, J. J., and Capell, R. (2012). A comparison of similarity indices for catchment classification using a cross-regional dataset. *Advances in Water Resources*, 40:11–22.

Andréassian, V., Le Moine, N., Perrin, C., Ramos, M.-H., Oudin, L., Mathevet, T., Lerat, J., and Berthet, L. (2012). All that glitters is not gold: the case of calibrating hydrological models. *Hydrological Processes*, 26(14):2206–2210.

Archfield, S. and Vogel, R. (2010). Map correlation method: Selection of a reference streamgage to estimate daily streamflow at ungaged catchments. *Water Resources Research*, 46(10).

Arsenault, R., Poulin, A., Côté, P., and Brissette, F. (2013). Comparison of stochastic optimization algorithms in hydrological model calibration. *Journal of Hydrologic Engineering*, 19(7):1374–1384.

Bárdossy, A. (2006). Copula-based geostatistical models for groundwater quality parameters. *Water Resources Research*, 42(11).

Bárdossy, A. (2007). Calibration of hydrological model parameters for ungauged catchments. *Hydrology and Earth System Sciences*, 11(2).

Bárdossy, A., Huang, Y., and Wagener, T. (2016). Simultaneous calibration of hydrological models in geographical space. *Hydrology and Earth System Sciences*, 20(7):2913–2928.

Bárdossy, A. and Singh, S. K. (2008). Robust estimation of hydrological model parameters. *Hydrology and Earth System Sciences*, 12(6):1273–1283.

Barnett, J. and Adger, W. N. (2007). Climate change, human security and violent conflict. *Political geography*, 26(6):639–655.

Bastola, S., Murphy, C., and Sweeney, J. (2011). Evaluation of the transferability of hydrological model parameters for simulations under changed climatic conditions. *Hydrology & Earth System Sciences Discussions*, 8(3).

Bergström, S. and Forsman, A. (1973). Development of a conceptual deterministic rainfall-runoff model. *Nordic Hydrology*, 4:174–190.

Beven, K. and Freer, J. (2001). Equifinality, data assimilation, and uncertainty estimation in mechanistic modelling of complex environmental systems using the glue methodology. *Journal of hydrology*, 249(1):11–29.

Beven, K. J. (2000). Uniqueness of place and process representations in hydrological modelling. *Hydrology and Earth System-Sciences*, 4(2):203–213.

Beven, K. J. (2005). Rainfall-runoff modeling: Introduction. *Encyclopedia of hydrological sciences*.

Beven, K. J. (2011). *Rainfall-runoff modelling: the primer*. John Wiley & Sons.

Blöschl, G. (2013). *Runoff prediction in ungauged basins: synthesis across processes, places and scales*. Cambridge University Press.

Boyle, D. P., Gupta, H. V., Sorooshian, S., Koren, V., Zhang, Z., and Smith, M. (2001). Toward improved streamflow forecasts: Value of semidistributed modeling. *Water Resources Research*, 37 (11):2749–2759.

Brooks, P. D., Troch, P. A., Durcik, M., Gallo, E., and Schlegel, M. (2011). Quantifying regional scale ecosystem response to changes in precipitation: Not all rain is created equal. *Water Resources Research*, 47(10).

Chiew, F., Potter, N., Vaze, J., Petheram, C., Zhang, L., Teng, J., and Post, D. (2014). Observed hydrologic non-stationarity in far south-eastern australia: implications for modelling and prediction. *Stochastic Environmental Research and Risk Assessment*, 28(1):3–15.

Chiew, F., Teng, J., Vaze, J., Post, D., Perraud, J., Kirono, D., and Viney, N. (2009). Estimating climate change impact on runoff across southeast australia: Method, results, and implications of the modeling method. *Water Resources Research*, 45(10).

Clarke, R. (1973). A review of some mathematical models used in hydrology, with observations on their calibration and use. *Journal of hydrology*, 19(1):1–20.

Coron, L., Andreassian, V., Perrin, C., Lerat, J., Vaze, J., Bourqui, M., and Hendrickx, F. (2012). Crash testing hydrological models in contrasted climate conditions: An experiment on 216 australian catchments. *Water Resources Research*, 48(5).

Das, T., Bárdossy, A., Zehe, E., and He, Y. (2008). Comparison of conceptual model performance using different representations of spatial variability. *Journal of Hydrology*, 356(1):106–118.

Duan, Q., Schaake, J., Andrassian, V., Franks, S., Goteti, G., Gupta, H., Gusev, Y., Habets, F., Hall, A., Hay, L., Hogue, T., Huang, M., Leavesley, G., Liang, X., Nasonova, O., Noilhan, J., Oudin, L., Sorooshian, S., Wagener, T., and Wood, E. (2006). Model parameter estimation experiment (mopex): An overview of science strategy and major results from the second and third workshops. *Journal of Hydrology*, 320(1?):3 – 17. The model parameter estimation experiment {MOPEX} {MOPEX} workshop.

Duan, Q., Sorooshian, S., and Gupta, V. K. (1994). Optimal use of the sce-ua global optimization method for calibrating watershed models. *Journal of hydrology*, 158(3):265–284.

Falcone, J. A., Carlisle, D. M., Wolock, D. M., and Meador, M. R. (2010). Gages: A stream gage database for evaluating natural and altered flow conditions in the conterminous united states: Ecological archives e091-045. *Ecology*, 91(2):621–621.

Farnsworth, R. K. and Thompson, E. S. (1983). *Mean monthly, seasonal, and annual pan evaporation for the United States*. US Department of Commerce, National Oceanic and Atmospheric Administration, National Weather Service.

Fernandez, W., Vogel, R., and Sankarasubramanian, A. (2000). Regional calibration of a watershed model. *Hydrological Sciences Journal*, 45(5):689–707.

Gaborit, É., Ricard, S., Lachance-Cloutier, S., Anctil, F., Turcotte, R., and Polat, A. (2015). Comparing global and local calibration schemes from a differential split-sample test perspective. *Canadian Journal of Earth Sciences*, 52(11):990–999.

Gharari, S. (2016). *On the role of model structure in hydrological modeling: Understanding models*. TU Delft, Delft University of Technology.

Gonzalez, R. and Wu, G. (1999). On the shape of the probability weighting function. *Cognitive psychology*, 38(1):129–166.

Götzinger, J. (2007). *Distributed conceptual hydrological modelling-simulation of climate, land use change impact and uncertainty analysis*. Ph.D. dissertation No. 164, University of Stuttgart.

Grigg, D. (1965). The logic of regional systems 1. *Annals of the Association of American Geographers*, 55(3):465–491.

Gupta, H. V., Kling, H., Yilmaz, K. K., and Martinez, G. F. (2009). Decomposition of the mean squared error and nse performance criteria: Implications for improving hydrological modelling. *Journal of Hydrology*, 377(1):80–91.

Gupta, H. V., Sorooshian, S., and Yapo, P. O. (1998). Toward improved calibration of hydrologic models: Multiple and noncommensurable measures of information. *Water Resources Research*, 34(4):751–763.

Gupta, R., Gigras, P., Mohapatra, H., Goswami, V. K., and Chauhan, B. (2003). Microbial α-amylases: a biotechnological perspective. *Process Biochemistry*, 38(11):1599–1616.

Hamon, W. R. (1963). *Computation of direct runoff amounts from storm rainfall*. publisher not identified.

Hartmann, G. M. (2007). *Investigation of evapotranspiration concepts in hydrological modelling for climate change impact assessment*. Ph.D. dissertation No. 161, University of Stuttgart.

He, Y. (2008). Application of a non-parametric classification scheme to catchment hydrology. *Ph.D. dissertation No. 172, University of Stuttgart*.

Hrachowitz, M., Savenije, H., Blöschl, G., McDonnell, J., Sivapalan, M., Pomeroy, J., Arheimer, B., Blume, T., Clark, M., Ehret, U., et al. (2013). A decade of predictions in ungauged basins (pub)a review. *Hydrological sciences journal*, 58(6):1198–1255.

Kaczmarek, Z., Strzepek, K. M., Somlyódy, L., and Priazhinskaya, V. (1996). *Water resources management in the face of climatic/hydrologic uncertainties*, volume 18. Springer Science & Business Media.

Kollat, J., Reed, P., and Wagener, T. (2012). When are multiobjective calibration trade-offs in hydrologic models meaningful? *Water Resources Research*, 48(3).

Kottek, M., Grieser, J., Beck, C., Rudolf, B., and Rubel, F. (2006). World map of the köppen-geiger climate classification updated. *Meteorologische Zeitschrift*, 15(3):259–263.

Kraußе, T., für das International Hydrological Programme der Unesco und das Hydrology, D. N., and der WMO, W. R. P. (2013a). *Robust parameter estimation-chances for hydrologic modelling in uncertain conditions*. IHP-HWRP Secretariat.

Kraußе, T., für das International Hydrological Programme der Unesco und das Hydrology, D. N., and der WMO, W. R. P. (2013b). *Robust parameter estimation-chances for hydrologic modelling in uncertain conditions*. IHP-HWRP Secretariat.

Li, C., Zhang, L., Wang, H., Zhang, Y., Yu, F., Yan, D., and Verhoest, N. (2012). The transferability of hydrological models under nonstationary climatic conditions. *Hydrology & Earth System Sciences*, 16(4).

Li, J. (2010). *Application of copulas as a new geostatistical tool*. Ph.D. dissertation No. 187, University of Stuttgart.

Liu, R. Y. et al. (1990). On a notion of data depth based on random simplices. *The Annals of Statistics*, 18(1):405–414.

Liu, R. Y., Parelius, J. M., Singh, K., et al. (1999). Multivariate analysis by data depth: descriptive statistics, graphics and inference,(with discussion and a rejoinder by liu and singh). *The annals of statistics*, 27(3):783–858.

Liu, R. Y., Serfling, R. J., and Souvaine, D. L. (2006). *Data depth: robust multivariate analysis, computational geometry, and applications*, volume 72. American Mathematical Soc.

Madsen, H. (2000). Automatic calibration of a conceptual rainfall–runoff model using multiple objectives. *Journal of hydrology*, 235(3):276–288.

Madsen, H., Wilson, G., and Ammentorp, H. C. (2002). Comparison of different automated strategies for calibration of rainfall-runoff models. *Journal of Hydrology*, 261(1):48–59.

Mahalanobis, P. C. (1936). On the generalized distance in statistics. *Proceedings of the National Institute of Sciences (Calcutta)*, 2:49–55.

McDonnell, J. and Woods, R. (2004). On the need for catchment classification. *Journal of Hydrology*, 299(1-2):2–3.

McIntyre, N., Lee, H., Wheater, H., Young, A., and Wagener, T. (2005). Ensemble predictions of runoff in ungauged catchments. *Water Resources Research*, 41(12):n/a–n/a.

Merz, R., Parajka, J., and Blschl, G. (2011). Time stability of catchment model parameters: Implications for climate impact analyses. *Water Resources Research*, 47(2):n/a–n/a.

Milly, P., Julio, B., Malin, F., Robert, M., Zbigniew, W., Dennis, P., and Ronald, J. (2007). Stationarity is dead. *Ground Water News & Views*, 4(1):6–8.

Milly, P. C. D. (1994). Climate, soil water storage, and the average annual water balance. *Water Resources Research*, 30(7):2143–2156.

Moore, R. J. (1985). The probability-distributed principle and runoff production at point and basin scales. *Hydrological Sciences Journal*, 30(2):273–297.

Najafi, M., Moradkhani, H., and Jung, I. (2011). Assessing the uncertainties of hydrologic model selection in climate change impact studies. *Hydrological Processes*, 25(18):2814–2826.

Nash, J. and Sutcliffe, J. (1970). River flow forecasting through conceptual models. 1. a discussion of principles. *Journal of Hydrology*, 10:282–290.

Nelsen, R. B. (1999). An introduction to copulas, volume 139 of lecture notes in statistics.

Oudin, L., Andréassian, V., Perrin, C., Michel, C., and Le Moine, N. (2008). Spatial proximity, physical similarity, regression and ungaged catchments: A comparison of regionalization approaches based on 913 french catchments. *Water Resources Research*, 44(3).

Oudin, L., Kay, A., Andréassian, V., and Perrin, C. (2010). Are seemingly physically similar catchments truly hydrologically similar? *Water Resources Research*, 46(11).

Parajka, J., Blöschl, G., and Merz, R. (2007). Regional calibration of catchment models: Potential for ungauged catchments. *Water Resources Research*, 43(6).

Penman, H. L. (1948). Natural evaporation from open water, bare soil and grass. *Proceedings of the Royal Society of London. Series A. Mathematical and Physical Sciences*, 193(1032):120–145.

Rango, A. and Martinec, J. (1995). Revisiting the degree-day method for snowmelt computations1. *JAWRA Journal of the American Water Resources Association*, 31(4):657–669.

Razavi, T. and Coulibaly, P. (2012). Streamflow prediction in ungauged basins: review of regionalization methods. *Journal of Hydrologic Engineering*, 18(8):958–975.

Refsgaard, J. C. and Storm, B. (1996). Construction, calibration and validation of hydrological models. In *Distributed hydrological modelling*, pages 41–54. Springer.

Ricard, S., Bourdillon, R., Roussel, D., and Turcotte, R. (2012). Global calibration of distributed hydrological models for large-scale applications. *Journal of Hydrologic Engineering*, 18(6):719–721.

Rind, D., Rosenzweig, C., and Goldberg, R. (1992). Modelling the hydrological cycle in assessments of climate change. *Nature*.

Samaniego, L. (2003). *Hydrological Consequences of Land Use/Land Cover and Climatic Changes in Mesoscale Catchments*. Ph.D. dissertation No. 118, University of Stuttgart.

Samaniego, L., Bárdossy, A., and Kumar, R. (2010). Streamflow prediction in ungauged catchments using copula-based dissimilarity measures. *Water resources research*, 46(2).

Sawicz, K., Kelleher, C., Wagener, T., Troch, P., Sivapalan, M., and Carrillo, G. (2014). Characterizing hydrologic change through catchment classification. *Hydrology and Earth System Sciences*, 18(1):273–285.

Sawicz, K., Wagener, T., Sivapalan, M., Troch, P., and Carrillo, G. (2011). Catchment classification: empirical analysis of hydrologic similarity based on catchment function in the eastern usa. *Hydrology and Earth System Sciences*, 15(9).

Schaefli, B. and Gupta, H. (2007). Do nash values have value? *Hydrological Processes*, 21(15):2075–2080.

Serfling, R. (2006). Depth functions in nonparametric multivariate inference. *DIMACS Series in Discrete Mathematics and Theoretical Computer Science*, 72:1.

Shamseldin, A. Y. (1997). Application of a neural network technique to rainfall-runoff modelling. *Journal of Hydrology*, 199(3):272–294.

Singh, S. K. (2010). *Robust parameter estimation in gauged and ungauged basins*. Ph.D. dissertation No. 198, University of Stuttgart.

Singh, V. P. et al. (1995). *Computer models of watershed hydrology.* Water Resources Publications.

Sivakumar, B. and Singh, V. (2012). Hydrologic system complexity and nonlinear dynamic concepts for a catchment classification framework. *Hydrology and Earth System Sciences*, 16(11):4119–4131.

Sivapalan, M. (2003). Prediction in ungauged basins: a grand challenge for theoretical hydrology. *Hydrological Processes*, 17(15):3163–3170.

Sklar, A. (1973). Random variables, joint distribution functions, and copulas. *Kybernetika*, 9(6):449–460.

Sugimoto, T. (2014). *Copula based stochastic analysis of discharge time series*. Ph.D. dissertation No. 232, University of Stuttgart.

Toth, E. (2013). Catchment classification based on characterisation of streamflow and precipitation time series. *Hydrology and Earth System Sciences*, 17(3):1149–1159.

Tukey, J. W. (1975). Mathematics and the picturing of data. In *Proceedings of the international congress of mathematicians*, volume 2, pages 523–531.

Vaze, J., Chiew, F., Hughes, D., and Andréassian, V. (2015). Preface: Hs02-hydrologic nonstationarity and extrapolating models to predict the future. *Proceedings of the International Association of Hydrological Sciences*, 371:1.

Vaze, J., Davidson, A., Teng, J., and Podger, G. (2011). Impact of climate change on water availability in the macquarie-castlereagh river basin in australia. *Hydrological Processes*, 25(16):2597–2612.

Vaze, J., Post, D., Chiew, F., Perraud, J.-M., Viney, N., and Teng, J. (2010). Climate non-stationarity–validity of calibrated rainfall–runoff models for use in climate change studies. *Journal of hydrology*, 394(3):447–457.

Vaze, J. and Teng, J. (2011). Future climate and runoff projections across new south wales, australia: results and practical applications. *Hydrological Processes*, 25(1):18–35.

Vencálek, O. (2011). Concept of data depth and its applications. *Acta Universitatis Palackianae Olomucensis. Facultas Rerum Naturalium. Mathematica*, 50(2):111–119.

Viney, N., Perraud, J., Vaze, J., Chiew, F., Post, D., and Yang, A. (2009). The usefulness of bias constraints in model calibration for regionalisation to ungauged catchments. In *18th World IMACS Congress and MODSIM09 International Congress on Modelling and Simulation*, pages 13–17. Modelling and Simulation Society of Australia and New Zealand and International Association for Mathematics and Computers in Simulation: Cairns.

Wagener, T., Boyle, D. P., Lees, M. J., Wheater, H. S., Gupta, H. V., and Sorooshian, S. (2001). A framework for development and application of hydrological models. *Hydrology and Earth System Sciences*, 5(1):13–26.

Wagener, T., Sivapalan, M., Troch, P., and Woods, R. (2007). Catchment classification and hydrologic similarity. *Geography Compass*, 1(4):901–931.

Wheater, H., Jakeman, A., and Beven, K. (1993). Progress and directions in rainfall-runoff modelling. *Wiley, pp. 101-13*.

Yao, C., Li, Z., Yu, Z., and Zhang, K. (2012). A priori parameter estimates for a distributed, grid-based xinanjiang model using geographically based information. *Journal of Hydrology*, 468:47–62.

Yapo, P. O., Gupta, H. V., and Sorooshian, S. (1996). Automatic calibration of conceptual rainfall-runoff models: sensitivity to calibration data. *Journal of Hydrology*, 181(1):23–48.

Yapo, P. O., Gupta, H. V., and Sorooshian, S. (1998). Multi-objective global optimization for hydrologic models. *Journal of hydrology*, 204(1):83–97.

Zeleny, M. (1981). *Multiple Criteria Decision Making*. McGraw-Hill, New York, USA.

Zhao, R. J. and Liu, X. R. (1995). *The Xinanjiang model. In: Computer Models of Watershed Hydrology*. Water Resources Publications, Littleton, Colorado, USA.

Zuo, Y. and Serfling, R. (2000). General notions of statistical depth function. *Annals of statistics*, pages 461–482.

Institut für Wasser- und Umweltsystemmodellierung
Universität Stuttgart, Germany
Yingchunhuang2010@gmail.com

Yingchun Huang

PERSONAL DATA

January 5, 1984

Longyan, China

EDUCATION

Dr. -Ing., Hydrology and Geohydrology, 2016

Institute for Modelling Hydraulic and Environmental Systems

University of Stuttgart, Germany

M.Sc., Hydrology and Water Resources, 2010

College of Hydrology and Water Resources

Hohai University, China

B.Sc., Hydrology and Water Resources Engineering, 2007

College of Hydrology and Water Resources

Hohai University, China

RESEARCH EXPERIMENCE

10/2010 – 10/2016	Research Assistant in the Institute for Modeling Hydraulic and Environmental Systems, University of Stuttgart
01/2012 - 12/2013	Research Assistant at University of Giessen. Participated in the project: Impacts of Land Use and Management Practices on Water Resources under Climate Change in the Hai He Basin, China
06/2009 - 09/2010	Participated in the project: Novel Early Flood Warning and Risk Assessment system, funded by the Innovation China-UK (ICUK) program
03/2009 - 09/2009	Participated in the project: Real Flood Forecasting System of Dongtiao basin, funded by Zhejiang Design Institute of Water Conservancy and Hydroelectric Power
09/2007 - 03/ 2009	Participated in the project: Flood Forecasting in the Nanjing Reach of Yangtze River and Chu River, funded by Nanjing Water Conservancy Bureau
05/2006 - 03/2007	Participated in the project: Relationship between Phreatic Evaporation and Water Table Depth, funded by Hohai University

Institut für Wasser- und Umweltsystemmodellierung
Universität Stuttgart

Pfaffenwaldring 61
70569 Stuttgart (Vaihingen)
Telefon (0711) 685 - 64717/64749/64752/64679
Telefax (0711) 685 - 67020 o. 64746 o. 64681
E-Mail: iws@iws.uni-stuttgart.de
http://www.iws.uni-stuttgart.de

Verzeichnis der Mitteilungshefte

1 Röhnisch, Arthur: *Die Bemühungen um eine Wasserbauliche Versuchsanstalt an der Technischen Hochschule Stuttgart*, und
Fattah Abouleid, Abdel: *Beitrag zur Berechnung einer in lockeren Sand gerammten, zweifach verankerten Spundwand*, 1963

2 Marotz, Günter: *Beitrag zur Frage der Standfestigkeit von dichten Asphaltbelägen im Großwasserbau*, 1964

3 Gurr, Siegfried: *Beitrag zur Berechnung zusammengesetzter ebener Flächentragwerke unter besonderer Berücksichtigung ebener Stauwände, mit Hilfe von Randwert- und Lastwertmatrizen*, 1965

4 Plica, Peter: *Ein Beitrag zur Anwendung von Schalenkonstruktionen im Stahlwasserbau*, und

Petrikat, Kurt: *Möglichkeiten und Grenzen des wasserbaulichen Versuchswesens*, 1966

5 Plate, Erich: *Beitrag zur Bestimmung der Windgeschwindigkeitsverteilung in der durch eine Wand gestörten bodennahen Luftschicht*,
und
Röhnisch, Arthur; Marotz, Günter: *Neue Baustoffe und Bauausführungen für den Schutz der Böschungen und der Sohle von Kanälen, Flüssen und Häfen; Gestehungskosten und jeweilige Vorteile*, sowie
Unny, T.E.: *Schwingungsuntersuchungen am Kegelstrahlschieber*, 1967

6 Seiler, Erich: *Die Ermittlung des Anlagenwertes der bundeseigenen Binnenschiffahrtsstraßen und Talsperren und des Anteils der Binnenschiffahrt an diesem Wert*, 1967

7 *Sonderheft anläßlich des 65. Geburtstages von Prof. Arthur Röhnisch mit Beiträgen von* Benk, Dieter; Breitling, J.; Gurr, Siegfried; Haberhauer, Robert; Honekamp, Hermann; Kuz, Klaus Dieter; Marotz, Günter; Mayer-Vorfelder, Hans-Jörg; Miller, Rudolf; Plate, Erich J.; Radomski, Helge; Schwarz, Helmut; Vollmer, Ernst; Wildenhahn, Eberhard; 1967

8 Jumikis, Alfred: *Beitrag zur experimentellen Untersuchung des Wassernachschubs in einem gefrierenden Boden und die Beurteilung der Ergebnisse*, 1968

9 Marotz, Günter: *Technische Grundlagen einer Wasserspeicherung im natürlichen Untergrund*, 1968

10 Radomski, Helge: *Untersuchungen über den Einfluß der Querschnittsform wellenförmiger Spundwände auf die statischen und rammtechnischen Eigenschaften*, 1968

11 Schwarz, Helmut: *Die Grenztragfähigkeit des Baugrundes bei Einwirkung vertikal gezogener Ankerplatten als zweidimensionales Bruchproblem*, 1969

12 Erbel, Klaus: *Ein Beitrag zur Untersuchung der Metamorphose von Mittelgebirgsschneedecken unter besonderer Berücksichtigung eines Verfahrens zur Bestimmung der thermischen Schneequalität*, 1969

13 Westhaus, Karl-Heinz: *Der Strukturwandel in der Binnenschiffahrt und sein Einfluß auf den Ausbau der Binnenschiffskanäle*, 1969

14 Mayer-Vorfelder, Hans-Jörg: *Ein Beitrag zur Berechnung des Erdwiderstandes unter Ansatz der logarithmischen Spirale als Gleitflächenfunktion*, 1970

15 Schulz, Manfred: *Berechnung des räumlichen Erddruckes auf die Wandung kreiszylindrischer Körper*, 1970

16 Mobasseri, Manoutschehr: *Die Rippenstützmauer. Konstruktion und Grenzen ihrer Standsicherheit*, 1970

17 Benk, Dieter: *Ein Beitrag zum Betrieb und zur Bemessung von*

Hochwasserrückhaltebecken, 1970

18 Gàl, Attila: *Bestimmung der mitschwingenden Wassermasse bei überströmten Fischbauchklappen mit kreiszylindrischem Staublech*, 1971, vergriffen

19 Kuz, Klaus Dieter: *Ein Beitrag zur Frage des Einsetzens von Kavitationserscheinungen in einer Düsenströmung bei Berücksichtigung der im Wasser gelösten Gase*, 1971, vergriffen

20 Schaak, Hartmut: *Verteilleitungen von Wasserkraftanlagen*, 1971

21 *Sonderheft zur Eröffnung der neuen Versuchsanstalt des Instituts für Wasserbau der Universität Stuttgart mit Beiträgen von* Brombach, Hansjörg; Dirksen, Wolfram; Gàl, Attila; Gerlach, Reinhard; Giesecke, Jürgen; Holthoff, Franz-Josef; Kuz, Klaus Dieter; Marotz, Günter; Minor, Hans-Erwin; Petrikat, Kurt; Röhnisch, Arthur; Rueff, Helge; Schwarz, Helmut; Vollmer, Ernst; Wildenhahn, Eberhard; 1972

22 Wang, Chung-su: *Ein Beitrag zur Berechnung der Schwingungen an Kegelstrahlschiebern*, 1972

23 Mayer-Vorfelder, Hans-Jörg: *Erdwiderstandsbeiwerte nach dem Ohde-Variationsverfahren*, 1972

24 Minor, Hans-Erwin: *Beitrag zur Bestimmung der Schwingungsanfachungsfunktionen überströmter Stauklappen*, 1972, vergriffen

25 Brombach, Hansjörg: *Untersuchung strömungsmechanischer Elemente (Fluidik) und die Möglichkeit der Anwendung von Wirbelkammerelementen im Wasserbau*, 1972, vergriffen

26 Wildenhahn, Eberhard: *Beitrag zur Berechnung von Horizontalfilterbrunnen*, 1972

27 Steinlein, Helmut: *Die Eliminierung der Schwebstoffe aus Flußwasser zum Zweck der unterirdischen Wasserspeicherung, gezeigt am Beispiel der Iller*, 1972

28 Holthoff, Franz Josef: *Die Überwindung großer Hubhöhen in der Binnenschiffahrt durch Schwimmerhebewerke*, 1973

29 Röder, Karl: *Einwirkungen aus Baugrundbewegungen auf trog- und kastenförmige Konstruktionen des Wasser- und Tunnelbaues*, 1973

30 Kretschmer, Heinz: *Die Bemessung von Bogenstaumauern in Abhängigkeit von der Talform*, 1973

31 Honekamp, Hermann: *Beitrag zur Berechnung der Montage von Unterwasserpipelines*, 1973

32 Giesecke, Jürgen: *Die Wirbelkammertriode als neuartiges Steuerorgan im Wasserbau*, und
Brombach, Hansjörg: *Entwicklung, Bauformen, Wirkungsweise und Steuereigenschaften von Wirbelkammerverstärkern*, 1974

33 Rueff, Helge: *Untersuchung der schwingungserregenden Kräfte an zwei hintereinander angeordneten Tiefschützen unter besonderer Berücksichtigung von Kavitation*, 1974

34 Röhnisch, Arthur: *Einpreßversuche mit Zementmörtel für Spannbeton - Vergleich der Ergebnisse von Modellversuchen mit Ausführungen in Hüllwellrohren*, 1975

35 *Sonderheft anläßlich des 65. Geburtstages von Prof. Dr.-Ing. Kurt Petrikat mit Beiträgen von*: Brombach, Hansjörg; Erbel, Klaus; Flinspach, Dieter; Fischer jr., Richard; Gàl, Attila; Gerlach, Reinhard; Giesecke, Jürgen; Haberhauer, Robert; Hafner Edzard; Hausenblas, Bernhard; Horlacher, Hans-Burkhard; Hutarew, Andreas; Knoll, Manfred; Krummet, Ralph; Marotz, Günter; Merkle, Theodor; Miller, Christoph; Minor, Hans-Erwin; Neumayer, Hans; Rao, Syamala; Rath, Paul; Rueff, Helge; Ruppert, Jürgen; Schwarz, Wolfgang; Topal-Gökceli, Mehmet; Vollmer, Ernst; Wang, Chung-su; Weber, Hans-Georg; 1975

36 Berger, Jochum: *Beitrag zur Berechnung des Spannungszustandes in rotationssymmetrisch belasteten Kugelschalen veränderlicher Wandstärke unter Gas- und Flüssigkeitsdruck durch Integration schwach singulärer Differentialgleichungen*, 1975

37 Dirksen, Wolfram: *Berechnung instationärer Abflußvorgänge in gestauten Gerinnen mittels Differenzenverfahren und die Anwendung auf Hochwasserrückhaltebecken*, 1976

38 Horlacher, Hans-Burkhard: *Berechnung instationärer Temperatur- und Wärmespannungsfelder in langen mehrschichtigen Hohlzylindern*, 1976

39 Hafner, Edzard: *Untersuchung der hydrodynamischen Kräfte auf Baukörper im Tiefwasserbereich des Meeres*, 1977, ISBN 3-921694-39-6

40 Ruppert, Jürgen: *Über den Axialwirbelkammerverstärker für den Einsatz im Wasserbau*, 1977, ISBN 3-921694-40-X

41 Hutarew, Andreas: *Beitrag zur Beeinflußbarkeit des Sauerstoffgehalts in Fließgewässern an Abstürzen und Wehren*, 1977, ISBN 3-921694-41-8, vergriffen

42 Miller, Christoph: *Ein Beitrag zur Bestimmung der schwingungserregenden Kräfte an unterströmten Wehren*, 1977, ISBN 3-921694-42-6

43 Schwarz, Wolfgang: *Druckstoßberechnung unter Berücksichtigung der Radial- und Längsverschiebungen der Rohrwandung*, 1978, ISBN 3-921694-43-4

44 Kinzelbach, Wolfgang: *Numerische Untersuchungen über den optimalen Einsatz variabler Kühlsysteme einer Kraftwerkskette am Beispiel Oberrhein*, 1978, ISBN 3-921694-44-2

45 Barczewski, Baldur: *Neue Meßmethoden für Wasser-Luftgemische und deren Anwendung auf zweiphasige Auftriebsstrahlen*, 1979, ISBN 3-921694-45-0

46 Neumayer, Hans: *Untersuchung der Strömungsvorgänge in radialen Wirbelkammerverstärkern*, 1979, ISBN 3-921694-46-9

47 Elalfy, Youssef-Elhassan: *Untersuchung der Strömungsvorgänge in Wirbelkammerdioden und -drosseln*, 1979, ISBN 3-921694-47-7

48 Brombach, Hansjörg: *Automatisierung der Bewirtschaftung von Wasserspeichern*, 1981, ISBN 3-921694-48-5

49 Geldner, Peter: *Deterministische und stochastische Methoden zur Bestimmung der Selbstdichtung von Gewässern*, 1981, ISBN 3-921694-49-3, vergriffen

50 Mehlhorn, Hans: *Temperaturveränderungen im Grundwasser durch Brauchwassereinleitungen*, 1982, ISBN 3-921694-50-7, vergriffen

51 Hafner, Edzard: *Rohrleitungen und Behälter im Meer*, 1983, ISBN 3-921694-51-5

52 Rinnert, Bernd: *Hydrodynamische Dispersion in porösen Medien: Einfluß von Dichteunterschieden auf die Vertikalvermischung in horizontaler Strömung*, 1983, ISBN 3-921694-52-3, vergriffen

53 Lindner, Wulf: *Steuerung von Grundwasserentnahmen unter Einhaltung ökologischer Kriterien*, 1983, ISBN 3-921694-53-1, vergriffen

54 Herr, Michael; Herzer, Jörg; Kinzelbach, Wolfgang; Kobus, Helmut; Rinnert, Bernd: *Methoden zur rechnerischen Erfassung und hydraulischen Sanierung von Grundwasserkontaminationen*, 1983, ISBN 3-921694-54-X

55 Schmitt, Paul: *Wege zur Automatisierung der Niederschlagsermittlung*, 1984, ISBN 3-921694-55-8, vergriffen

56 Müller, Peter: *Transport und selektive Sedimentation von Schwebstoffen bei gestautem Abfluß*, 1985, ISBN 3-921694-56-6

57 El-Qawasmeh, Fuad: *Möglichkeiten und Grenzen der Tropfbewässerung unter besonderer Berücksichtigung der Verstopfungsanfälligkeit der Tropfelemente*, 1985, ISBN 3-921694-57-4, vergriffen

58 Kirchenbaur, Klaus: *Mikroprozessorgesteuerte Erfassung instationärer Druckfelder am Beispiel seegangsbelasteter Baukörper*, 1985, ISBN 3-921694-58-2

59 Kobus, Helmut (Hrsg.): *Modellierung des großräumigen Wärme- und Schadstofftransports im Grundwasser*, Tätigkeitsbericht 1984/85 (DFG-Forschergruppe an den Universitäten Hohenheim, Karlsruhe und Stuttgart), 1985, ISBN 3-921694-59-0, vergriffen

60 Spitz, Karlheinz: *Dispersion in porösen Medien: Einfluß von Inhomogenitäten und Dichteunterschieden*, 1985, ISBN 3-921694-60-4, vergriffen

61 Kobus, Helmut: *An Introduction to Air-Water Flows in Hydraulics*, 1985, ISBN 3-921694-61-2

62 Kaleris, Vassilios: *Erfassung des Austausches von Oberflächen- und Grundwasser in horizontalebenen Grundwassermodellen*, 1986, ISBN 3-921694-62-0

63 Herr, Michael: *Grundlagen der hydraulischen Sanierung verunreinigter Porengrundwasserleiter*, 1987, ISBN 3-921694-63-9

64 Marx, Walter: *Berechnung von Temperatur und Spannung in Massenbeton infolge Hydratation*, 1987, ISBN 3-921694-64-7

65 Koschitzky, Hans-Peter: *Dimensionierungskonzept für Sohlbelüfter in Schußrinnen zur Vermeidung von Kavitationsschäden*, 1987, ISBN 3-921694-65-5

66 Kobus, Helmut (Hrsg.): *Modellierung des großräumigen Wärme- und Schadstofftransports im Grundwasser*, Tätigkeitsbericht 1986/87 (DFG-Forschergruppe an den Universitäten Hohenheim, Karlsruhe und Stuttgart) 1987, ISBN 3-921694-66-3

67 Söll, Thomas: *Berechnungsverfahren zur Abschätzung anthropogener Temperaturanomalien im Grundwasser*, 1988, ISBN 3-921694-67-1

68 Dittrich, Andreas; Westrich, Bernd: *Bodenseeufererosion, Bestandsaufnahme und Bewertung*, 1988, ISBN 3-921694-68-X, vergriffen

69 Huwe, Bernd; van der Ploeg, Rienk R.: *Modelle zur Simulation des Stickstoffhaushaltes von Standorten mit unterschiedlicher landwirtschaftlicher Nutzung*, 1988, ISBN 3-921694-69-8, vergriffen

70 Stephan, Karl: *Integration elliptischer Funktionen*, 1988, ISBN 3-921694-70-1

71 Kobus, Helmut; Zilliox, Lothaire (Hrsg.): *Nitratbelastung des Grundwassers, Auswirkungen der Landwirtschaft auf die Grundwasser- und Rohwasserbeschaffenheit und Maßnahmen zum Schutz des Grundwassers*. Vorträge des deutsch-französischen Kolloquiums am 6. Oktober 1988, Universitäten Stuttgart und Louis Pasteur Strasbourg (Vorträge in deutsch oder französisch, Kurzfassungen zweisprachig), 1988, ISBN 3-921694-71-X

72 Soyeaux, Renald: *Unterströmung von Stauanlagen auf klüftigem Untergrund unter Berücksichtigung laminarer und turbulenter Fließzustände*,1991, ISBN 3-921694-72-8

73 Kohane, Roberto: *Berechnungsmethoden für Hochwasserabfluß in Fließgewässern mit überströmten Vorländern*, 1991, ISBN 3-921694-73-6

74 Hassinger, Reinhard: *Beitrag zur Hydraulik und Bemessung von Blocksteinrampen in flexibler Bauweise*, 1991, ISBN 3-921694-74-4, vergriffen

75 Schäfer, Gerhard: *Einfluß von Schichtenstrukturen und lokalen Einlagerungen auf die Längsdispersion in Porengrundwasserleitern*, 1991, ISBN 3-921694-75-2

76 Giesecke, Jürgen: *Vorträge, Wasserwirtschaft in stark besiedelten Regionen; Umweltforschung mit Schwerpunkt Wasserwirtschaft*, 1991, ISBN 3-921694-76-0

77 Huwe, Bernd: *Deterministische und stochastische Ansätze zur Modellierung des Stickstoffhaushalts landwirtschaftlich genutzter Flächen auf unterschiedlichem Skalenniveau*, 1992, ISBN 3-921694-77-9, vergriffen

78 Rommel, Michael: *Verwendung von Kluftdaten zur realitätsnahen Generierung von Kluftnetzen mit anschließender laminar-turbulenter Strömungsberechnung*, 1993, ISBN 3-92 1694-78-7

79 Marschall, Paul: *Die Ermittlung lokaler Stofffrachten im Grundwasser mit Hilfe von Einbohrloch-Meßverfahren*, 1993, ISBN 3-921694-79-5, vergriffen

80 Ptak, Thomas: *Stofftransport in heterogenen Porenaquiferen: Felduntersuchungen und stochastische Modellierung*, 1993, ISBN 3-921694-80-9, vergriffen

81 Haakh, Frieder: *Transientes Strömungsverhalten in Wirbelkammern,* 1993, ISBN 3-921694-81-7

82 Kobus, Helmut; Cirpka, Olaf; Barczewski, Baldur; Koschitzky, Hans-Peter: *Versucheinrichtung zur Grundwasser und Altlastensanierung VEGAS, Konzeption und Programmrahmen*, 1993, ISBN 3-921694-82-5

83 Zang, Weidong: *Optimaler Echtzeit-Betrieb eines Speichers mit aktueller Abflußregenerierung*, 1994, ISBN 3-921694-83-3, vergriffen

84 Franke, Hans-Jörg: *Stochastische Modellierung eines flächenhaften Stoffeintrages und Transports in Grundwasser am Beispiel der Pflanzenschutzmittelproblematik*, 1995, ISBN 3-921694-84-1

85 Lang, Ulrich: *Simulation regionaler Strömungs- und Transportvorgänge in Karstaquiferen mit Hilfe des Doppelkontinuum-Ansatzes: Methodenentwicklung und Parameteridentifikation*, 1995, ISBN 3-921694-85-X, vergriffen

86 Helmig, Rainer: *Einführung in die Numerischen Methoden der Hydromechanik*, 1996, ISBN 3-921694-86-8, vergriffen

87 Cirpka, Olaf: *CONTRACT: A Numerical Tool for Contaminant Transport and Chemical Transformations - Theory and Program Documentation* -, 1996, ISBN 3-921694-87-6

88 Haberlandt, Uwe: *Stochastische Synthese und Regionalisierung des Niederschlages für Schmutzfrachtberechnungen*, 1996, ISBN 3-921694-88-4

89 Croisé, Jean: *Extraktion von flüchtigen Chemikalien aus natürlichen Lockergesteinen mittels erzwungener Luftströmung*, 1996, ISBN 3-921694-89-2, vergriffen

90 Jorde, Klaus: *Ökologisch begründete, dynamische Mindestwasserregelungen bei Ausleitungskraftwerken*, 1997, ISBN 3-921694-90-6, vergriffen

91 Helmig, Rainer: *Gekoppelte Strömungs- und Transportprozesse im Untergrund - Ein Beitrag zur Hydrosystemmodellierung-*, 1998, ISBN 3-921694-91-4, vergriffen

92 Emmert, Martin: *Numerische Modellierung nichtisothermer Gas-Wasser Systeme in porösen Medien,* 1997, ISBN 3-921694-92-2

93 Kern, Ulrich: *Transport von Schweb- und Schadstoffen in staugeregelten Fließgewässern am Beispiel des Neckars*, 1997, ISBN 3-921694-93-0, vergriffen

94 Förster, Georg: *Druckstoßdämpfung durch große Luftblasen in Hochpunkten von Rohrleitungen 1997*, ISBN 3-921694-94-9

95 Cirpka, Olaf: *Numerische Methoden zur Simulation des reaktiven Mehrkomponententransports im Grundwasser*, 1997, ISBN 3-921694-95-7, vergriffen

96 Färber, Arne: *Wärmetransport in der ungesättigten Bodenzone: Entwicklung einer thermischen In-situ-Sanierungstechnologie*, 1997, ISBN 3-921694-96-5

97 Betz, Christoph: *Wasserdampfdestillation von Schadstoffen im porösen Medium: Entwicklung einer thermischen In-situ-Sanierungstechnologie*, 1998, ISBN 3-921694-97-3

98 Xu, Yichun: *Numerical Modeling of Suspended Sediment Transport in Rivers*, 1998, ISBN 3-921694-98-1, vergriffen

99 Wüst, Wolfgang: *Geochemische Untersuchungen zur Sanierung CKW-kontaminierter Aquifere mit Fe(0)-Reaktionswänden,* 2000, ISBN 3-933761-02-2

100 Sheta, Hussam: *Simulation von Mehrphasenvorgängen in porösen Medien unter Einbeziehung von Hysterese-Effekten*, 2000, ISBN 3-933761-03-4

101 Ayros, Edwin: *Regionalisierung extremer Abflüsse auf der Grundlage statistischer Verfahren*, 2000, ISBN 3-933761-04-2, vergriffen

102 Huber, Ralf: *Compositional Multiphase Flow and Transport in Heterogeneous Porous Media*, 2000, ISBN 3-933761-05-0

103 Braun, Christopherus: *Ein Upscaling-Verfahren für Mehrphasenströmungen in porösen Medien*, 2000, ISBN 3-933761-06-9

104 Hofmann, Bernd: *Entwicklung eines rechnergestützten Managementsystems zur Beurteilung von Grundwasserschadensfällen*, 2000, ISBN 3-933761-07-7

105 Class, Holger: *Theorie und numerische Modellierung nichtisothermer Mehrphasenprozesse in NAPL-kontaminierten porösen Medien,* 2001, ISBN 3-933761-08-5

106 Schmidt, Reinhard: *Wasserdampf- und Heißluftinjektion zur thermischen Sanierung kontaminierter Standorte*, 2001, ISBN 3-933761-09-3

107 Josef, Reinhold:, *Schadstoffextraktion mit hydraulischen Sanierungsverfahren unter Anwendung von grenzflächenaktiven Stoffen*, 2001, ISBN 3-933761-10-7

108 Schneider, Matthias: *Habitat- und Abflussmodellierung für Fließgewässer mit unscharfen Berechnungsansätzen*, 2001, ISBN 3-933761-11-5

109 Rathgeb, Andreas: *Hydrodynamische Bemessungsgrundlagen für Lockerdeckwerke an überströmbaren Erddämmen*, 2001, ISBN 3-933761-12-3

110 Lang, Stefan: *Parallele numerische Simulation instätionärer Probleme mit adaptiven Methoden auf unstrukturierten Gittern*, 2001, ISBN 3-933761-13-1

111 Appt, Jochen; Stumpp Simone: *Die Bodensee-Messkampagne 2001, IWS/CWR Lake Constance Measurement Program 2001*, 2002, ISBN 3-933761-14-X

112 Heimerl, Stephan: *Systematische Beurteilung von Wasserkraftprojekten,* 2002, ISBN 3-933761-15-8, vergriffen

113 Iqbal, Amin: *On the Management and Salinity Control of Drip Irrigation,* 2002, ISBN 3-933761-16-6

114 Silberhorn-Hemminger, Annette: *Modellierung von Kluftaquifersystemen: Geostatistische Analyse und deterministisch-stochastische Kluftgenerierung,* 2002, ISBN 3-933761-17-4

115 Winkler, Angela: *Prozesse des Wärme- und Stofftransports bei der In-situ-Sanierung mit festen Wärmequellen,* 2003, ISBN 3-933761-18-2

116 Marx, Walter: *Wasserkraft, Bewässerung, Umwelt - Planungs- und Bewertungsschwerpunkte der Wasserbewirtschaftung,* 2003, ISBN 3-933761-19-0

117 Hinkelmann, Reinhard: *Efficient Numerical Methods and Information-Processing Techniques in Environment Water,* 2003, ISBN 3-933761-20-4

118 Samaniego-Eguiguren, Luis Eduardo: *Hydrological Consequences of Land Use / Land Cover and Climatic Changes in Mesoscale Catchments*, 2003, ISBN 3-933761-21-2

119 Neunhäuserer, Lina: *Diskretisierungsansätze zur Modellierung von Strömungs- und Transportprozessen in geklüftet-porösen Medien*, 2003, ISBN 3-933761-22-0

120 Paul, Maren: *Simulation of Two-Phase Flow in Heterogeneous Poros Media with Adaptive Methods*, 2003, ISBN 3-933761-23-9

121 Ehret, Uwe: *Rainfall and Flood Nowcasting in Small Catchments using Weather Radar*, 2003, ISBN 3-933761-24-7

122 Haag, Ingo: *Der Sauerstoffhaushalt staugeregelter Flüsse am Beispiel des Neckars - Analysen, Experimente, Simulationen -,* 2003, ISBN 3-933761-25-5

123 Appt, Jochen: *Analysis of Basin-Scale Internal Waves in Upper Lake Constance,* 2003, ISBN 3-933761-26-3

124 Hrsg.: Schrenk, Volker; Batereau, Katrin; Barczewski, Baldur; Weber, Karolin und Koschitzky, Hans-Peter: *Symposium Ressource Fläche und VEGAS - Statuskolloquium 2003, 30. September und 1. Oktober 2003,* 2003, ISBN 3-933761-27-1

125 Omar Khalil Ouda: *Optimisation of Agricultural Water Use: A Decision Support System for the Gaza Strip,* 2003, ISBN 3-933761-28-0

126 Batereau, Katrin: *Sensorbasierte Bodenluftmessung zur Vor-Ort-Erkundung von Schadensherden im Untergrund*, 2004, ISBN 3-933761-29-8

127 Witt, Oliver: *Erosionsstabilität von Gewässersedimenten mit Auswirkung auf den Stofftransport bei Hochwasser am Beispiel ausgewählter Stauhaltungen des Oberrheins*, 2004, ISBN 3-933761-30-1

128 Jakobs, Hartmut: *Simulation nicht-isothermer Gas-Wasser-Prozesse in komplexen Kluft-Matrix-Systemen*, 2004, ISBN 3-933761-31-X

129 Li, Chen-Chien: *Deterministisch-stochastisches Berechnungskonzept zur Beurteilung der Auswirkungen erosiver Hochwasserereignisse in Flussstauhaltungen,* 2004, ISBN 3-933761-32-8

130 Reichenberger, Volker; Helmig, Rainer; Jakobs, Hartmut; Bastian, Peter; Niessner, Jennifer: *Complex Gas-Water Processes in Discrete Fracture-Matrix Systems: Up-scaling, Mass-Conservative Discretization and Efficient Multilevel Solution,* 2004, ISBN 3-933761-33-6

131 Hrsg.: Barczewski, Baldur; Koschitzky, Hans-Peter; Weber, Karolin; Wege, Ralf: *VEGAS - Statuskolloquium 2004,* Tagungsband zur Veranstaltung am 05. Oktober 2004 an der Universität Stuttgart, Campus Stuttgart-Vaihingen, 2004, ISBN 3-933761-34-4

132 Asie, Kemal Jabir: *Finite Volume Models for Multiphase Multicomponent Flow through Porous Media*. 2005, ISBN 3-933761-35-2

133 Jacoub, George: *Development of a 2-D Numerical Module for Particulate Contaminant Transport in Flood Retention Reservoirs and Impounded Rivers,* 2004, ISBN 3-933761-36-0

134 Nowak, Wolfgang: *Geostatistical Methods for the Identification of Flow and Transport Parameters in the Subsurface,* 2005, ISBN 3-933761-37-9

135 Süß, Mia: *Analysis of the influence of structures and boundaries on flow and transport processes in fractured porous media*, 2005, ISBN 3-933761-38-7

136 Jose, Surabhin Chackiath: *Experimental Investigations on Longitudinal Dispersive Mixing in Heterogeneous Aquifers,* 2005, ISBN: 3-933761-39-5

137 Filiz, Fulya: *Linking Large-Scale Meteorological Conditions to Floods in Mesoscale Catchments,* 2005, ISBN 3-933761-40-9

138 Qin, Minghao: *Wirklichkeitsnahe und recheneffiziente Ermittlung von Temperatur und Spannungen bei großen RCC-Staumauern*, 2005, ISBN 3-933761-41-7

139 Kobayashi, Kenichiro: *Optimization Methods for Multiphase Systems in the Subsurface - Application to Methane Migration in Coal Mining Areas*, 2005, ISBN 3-933761-42-5

140 Rahman, Md. Arifur: *Experimental Investigations on Transverse Dispersive Mixing in Heterogeneous Porous Media,* 2005, ISBN 3-933761-43-3

141 Schrenk, Volker: *Ökobilanzen zur Bewertung von Altlastensanierungsmaßnahmen,* 2005, ISBN 3-933761-44-1

142 Hundecha, Hirpa Yeshewatesfa: *Regionalization of Parameters of a Conceptual Rainfall-Runoff Model*, 2005, ISBN: 3-933761-45-X

143 Wege, Ralf: *Untersuchungs- und Überwachungsmethoden für die Beurteilung natürlicher Selbstreinigungsprozesse im Grundwasser,* 2005, ISBN 3-933761-46-8

144 Breiting, Thomas: *Techniken und Methoden der Hydroinformatik - Modellierung von komplexen Hydrosystemen im Untergrund*, 2006, 3-933761-47-6

145 Hrsg.: Braun, Jürgen; Koschitzky, Hans-Peter; Müller, Martin: *Ressource Untergrund: 10 Jahre VEGAS: Forschung und Technologieentwicklung zum Schutz von Grundwasser und Boden,* Tagungsband zur Veranstaltung am 28. und 29. September 2005 an der Universität Stuttgart, Campus Stuttgart-Vaihingen, 2005, ISBN 3-933761-48-4

146 Rojanschi, Vlad: *Abflusskonzentration in mesoskaligen Einzugsgebieten unter Berücksichtigung des Sickerraumes,* 2006, ISBN 3-933761-49-2

147 Winkler, Nina Simone: *Optimierung der Steuerung von Hochwasserrückhaltebecken-systemen,* 2006, ISBN 3-933761-50-6

148 Wolf, Jens: *Räumlich differenzierte Modellierung der Grundwasserströmung alluvialer Aquifere für mesoskalige Einzugsgebiete*, 2006, ISBN: 3-933761-51-4

149 Kohler, Beate: *Externe Effekte der Laufwasserkraftnutzung*, 2006, ISBN 3-933761-52-2

150 Hrsg.: Braun, Jürgen; Koschitzky, Hans-Peter; Stuhrmann, Matthias: *VEGAS-Statuskolloquium 2006,* Tagungsband zur Veranstaltung am 28. September 2006 an der Universität Stuttgart, Campus Stuttgart-Vaihingen, 2006, ISBN 3-933761-53-0

151 Niessner, Jennifer: *Multi-Scale Modeling of Multi-Phase - Multi-Component Processes in Heterogeneous Porous Media*, 2006, ISBN 3-933761-54-9

152 Fischer, Markus: *Beanspruchung eingeerdeter Rohrleitungen infolge Austrocknung bindiger Böden,* 2006, ISBN 3-933761-55-7

153 Schneck, Alexander: *Optimierung der Grundwasserbewirtschaftung unter Berücksichtigung der Belange der Wasserversorgung, der Landwirtschaft und des Naturschutzes*, 2006, ISBN 3-933761-56-5

154 Das, Tapash: *The Impact of Spatial Variability of Precipitation on the Predictive Uncertainty of Hydrological Models,* 2006, ISBN 3-933761-57-3

155 Bielinski, Andreas: *Numerical Simulation of CO_2 sequestration in geological formations*, 2007, ISBN 3-933761-58-1

156 Mödinger, Jens: *Entwicklung eines Bewertungs- und Entscheidungsunterstützungssystems für eine nachhaltige regionale Grundwasserbewirtschaftung*, 2006, ISBN 3-933761-60-3

157 Manthey, Sabine: *Two-phase flow processes with dynamic effects in porous media - parameter estimation and simulation,* 2007, ISBN 3-933761-61-1

158 Pozos Estrada, Oscar: *Investigation on the Effects of Entrained Air in Pipelines,* 2007, ISBN 3-933761-62-X

159 Ochs, Steffen Oliver: *Steam injection into saturated porous media – process analysis including experimental and numerical investigations*, 2007, ISBN 3-933761-63-8

160 Marx, Andreas: *Einsatz gekoppelter Modelle und Wetterradar zur Abschätzung von Niederschlagsintensitäten und zur Abflussvorhersage, 2007,* ISBN 3-933761-64-6

161 Hartmann, Gabriele Maria: *Investigation of Evapotranspiration Concepts in Hydrological Modelling for Climate Change Impact Assessment*, 2007, ISBN 3-933761-65-4

162 Kebede Gurmessa, Tesfaye: *Numerical Investigation on Flow and Transport Characteristics to Improve Long-Term Simulation of Reservoir Sedimentation*, 2007, ISBN 3-933761-66-2

163 Trifković, Aleksandar: *Multi-objective and Risk-based Modelling Methodology for Planning, Design and Operation of Water Supply Systems*, 2007, ISBN 3-933761-67-0

164 Götzinger, Jens: *Distributed Conceptual Hydrological Modelling - Simulation of Climate, Land Use Change Impact and Uncertainty Analysis*, 2007, ISBN 3-933761-68-9

165 Hrsg.: Braun, Jürgen; Koschitzky, Hans-Peter; Stuhrmann, Matthias: *VEGAS – Kolloquium 2007,* Tagungsband zur Veranstaltung am 26. September 2007 an der Universität Stuttgart, Campus Stuttgart-Vaihingen, 2007, ISBN 3-933761-69-7

166 Freeman, Beau: *Modernization Criteria Assessment for Water Resources Planning; Klamath Irrigation Project, U.S.*, 2008, ISBN 3-933761-70-0

167 Dreher, Thomas: *Selektive Sedimentation von Feinstschwebstoffen in Wechselwirkung mit wandnahen turbulenten Strömungsbedingungen*, 2008, ISBN 3-933761-71-9

168 Yang, Wei: *Discrete-Continuous Downscaling Model for Generating Daily Precipitation Time Series*, 2008, ISBN 3-933761-72-7

169 Kopecki, Ianina: *Calculational Approach to FST-Hemispheres for Multiparametrical Benthos Habitat Modelling,* 2008*,* ISBN 3-933761-73-5

170 Brommundt, Jürgen: *Stochastische Generierung räumlich zusammenhängender Niederschlagszeitreihen*, 2008, ISBN 3-933761-74-3

171 Papafotiou, *Alexandros: Numerical Investigations of the Role of Hysteresis in Heterogeneous Two-Phase Flow Systems*, 2008, ISBN 3-933761-75-1

172 He, Yi: *Application of a Non-Parametric Classification Scheme to Catchment Hydrology*, 2008, ISBN 978-3-933761-76-7

173 Wagner, Sven: *Water Balance in a Poorly Gauged Basin in West Africa Using Atmospheric Modelling and Remote Sensing Information*, 2008, ISBN 978-3-933761-77-4

174 Hrsg.: Braun, Jürgen; Koschitzky, Hans-Peter; Stuhrmann, Matthias; Schrenk, Volker: *VEGAS-Kolloquium 2008 Ressource Fläche III*, Tagungsband zur Veranstaltung am 01. Oktober 2008 an der Universität Stuttgart, Campus Stuttgart-Vaihingen, 2008, ISBN 978-3-933761-78-1

175 Patil, Sachin: *Regionalization of an Event Based Nash Cascade Model for Flood Predictions in Ungauged Basins*, 2008, ISBN 978-3-933761-79-8

176 Assteerawatt, Anongnart: *Flow and Transport Modelling of Fractured Aquifers based on a Geostatistical Approach,* 2008, ISBN 978-3-933761-80-4

177 Karnahl, Joachim Alexander: *2D numerische Modellierung von multifraktionalem Schwebstoff- und Schadstofftransport in Flüssen*, 2008, ISBN 978-3-933761-81-1

178 Hiester, Uwe: *Technologieentwicklung zur In-situ-Sanierung der ungesättigten Bodenzone mit festen Wärmequellen,* 2009, ISBN 978-3-933761-82-8

179 Laux, Patrick: *Statistical Modeling of Precipitation for Agricultural Planning in the Volta Basin of West Africa,* 2009, ISBN 978-3-933761-83-5

180 Ehsan, Saqib: *Evaluation of Life Safety Risks Related to Severe Flooding,* 2009, ISBN 978-3-933761-84-2

181 Prohaska, Sandra: *Development and Application of a 1D Multi-Strip Fine Sediment Transport Model for Regulated Rivers,* 2009, ISBN 978-3-933761-85-9

182 Kopp, Andreas: *Evaluation of CO_2 Injection Processes in Geological Formations for Site Screening,* 2009, ISBN 978-3-933761-86-6

183 Ebigbo, Anozie: *Modelling of biofilm growth and its influence on CO_2 and water (two-phase) flow in porous media,* 2009, ISBN 978-3-933761-87-3

184 Freiboth, Sandra: *A phenomenological model for the numerical simulation of multiphase multicomponent processes considering structural alterations of porous media*, 2009, ISBN 978-3-933761-88-0

185 Zöllner, Frank: *Implementierung und Anwendung netzfreier Methoden im Konstruktiven Wasserbau und in der Hydromechanik*, 2009, ISBN 978-3-933761-89-7

186 Vasin, Milos: *Influence of the soil structure and property contrast on flow and transport in the unsaturated zone*, 2010, ISBN 978-3-933761-90-3

187 Li, Jing: *Application of Copulas as a New Geostatistical Tool*, 2010, ISBN 978-3-933761-91-0

188 AghaKouchak, Amir: *Simulation of Remotely Sensed Rainfall Fields Using Copulas*, 2010, ISBN 978-3-933761-92-7

189 Thapa, Pawan Kumar: *Physically-based spatially distributed rainfall runoff modelling for soil erosion estimation*, 2010, ISBN 978-3-933761-93-4

190 Wurms, Sven: *Numerische Modellierung der Sedimentationsprozesse in Retentionsanlagen zur Steuerung von Stoffströmen bei extremen Hochwasserabflussereignissen*, 2011, ISBN 978-3-933761-94-1

191 Merkel, Uwe: *Unsicherheitsanalyse hydraulischer Einwirkungen auf Hochwasserschutzdeiche und Steigerung der Leistungsfähigkeit durch adaptive Strömungsmodellierung*, 2011, ISBN 978-3-933761-95-8

192 Fritz, Jochen: *A Decoupled Model for Compositional Non-Isothermal Multiphase Flow in Porous Media and Multiphysics Approaches for Two-Phase Flow*, 2010, ISBN 978-3-933761-96-5

193 Weber, Karolin (Hrsg.): *12. Treffen junger WissenschaftlerInnen an Wasserbauinstituten*, 2010, ISBN 978-3-933761-97-2

194 Bliefernicht, Jan-Geert: *Probability Forecasts of Daily Areal Precipitation for Small River Basins,* 2011, ISBN 978-3-933761-98-9

195 Hrsg.: Koschitzky, Hans-Peter; Braun, Jürgen: *VEGAS-Kolloquium 2010 In-situ-Sanierung - Stand und Entwicklung Nano und ISCO -,* Tagungsband zur Veranstaltung am 07. Oktober 2010 an der Universität Stuttgart, Campus Stuttgart-Vaihingen*,* 2010*,* ISBN 978-3-933761-99-6

196 Gafurov, Abror: *Water Balance Modeling Using Remote Sensing Information - Focus on Central Asia,* 2010, ISBN 978-3-942036-00-9

197 Mackenberg, Sylvia: *Die Quellstärke in der Sickerwasserprognose: Möglichkeiten und Grenzen von Labor- und Freilanduntersuchungen,* 2010, ISBN 978-3-942036-01-6

198 Singh, Shailesh Kumar: *Robust Parameter Estimation in Gauged and Ungauged Basins,* 2010, ISBN 978-3-942036-02-3

199 Doğan, Mehmet Onur: *Coupling of porous media flow with pipe flow,* 2011, ISBN 978-3-942036-03-0

200 Liu, Min: *Study of Topographic Effects on Hydrological Patterns and the Implication on Hydrological Modeling and Data Interpolation,* 2011, ISBN 978-3-942036-04-7

201 Geleta, Habtamu Itefa: *Watershed Sediment Yield Modeling for Data Scarce Areas,* 2011, ISBN 978-3-942036-05-4

202 Franke, Jörg: *Einfluss der Überwachung auf die Versagenswahrscheinlichkeit von Staustufen,* 2011, ISBN 978-3-942036-06-1

203 Bakimchandra, Oinam: *Integrated Fuzzy-GIS approach for assessing regional soil erosion risks,* 2011, ISBN 978-3-942036-07-8

204 Alam, Muhammad Mahboob: *Statistical Downscaling of Extremes of Precipitation in Mesoscale Catchments from Different RCMs and Their Effects on Local Hydrology,* 2011, ISBN 978-3-942036-08-5

205 Hrsg.: Koschitzky, Hans-Peter; Braun, Jürgen: *VEGAS-Kolloquium 2011 Flache Geothermie - Perspektiven und Risiken,* Tagungsband zur Veranstaltung am 06. Oktober 2011 an der Universität Stuttgart, Campus Stuttgart-Vaihingen, 2011, ISBN 978-3-933761-09-2

206 Haslauer, Claus: *Analysis of Real-World Spatial Dependence of Subsurface Hydraulic Properties Using Copulas with a Focus on Solute Transport Behaviour,* 2011, ISBN 978-3-942036-10-8

207 Dung, Nguyen Viet: *Multi-objective automatic calibration of hydrodynamic models – development of the concept and an application in the Mekong Delta,* 2011, ISBN 978-3-942036-11-5

208 Hung, Nguyen Nghia: *Sediment dynamics in the floodplain of the Mekong Delta, Vietnam,* 2011, ISBN 978-3-942036-12-2

209 Kuhlmann, Anna: *Influence of soil structure and root water uptake on flow in the unsaturated zone,* 2012, ISBN 978-3-942036-13-9

210 Tuhtan, Jeffrey Andrew: *Including the Second Law Inequality in Aquatic Ecodynamics: A Modeling Approach for Alpine Rivers Impacted by Hydropeaking,* 2012, ISBN 978-3-942036-14-6

211 Tolossa, Habtamu: *Sediment Transport Computation Using a Data-Driven Adaptive Neuro-Fuzzy Modelling Approach,* 2012, ISBN 978-3-942036-15-3

212 Tatomir, Alexandru-Bodgan: *From Discrete to Continuum Concepts of Flow in Fractured Porous Media,* 2012, ISBN 978-3-942036-16-0

213 Erbertseder, Karin: *A Multi-Scale Model for Describing Cancer-Therapeutic Transport in the Human Lung,* 2012, ISBN 978-3-942036-17-7

214 Noack, Markus: *Modelling Approach for Interstitial Sediment Dynamics and Reproduction of Gravel Spawning Fish,* 2012, ISBN 978-3-942036-18-4

215 De Boer, Cjestmir Volkert: *Transport of Nano Sized Zero Valent Iron Colloids during Injection into the Subsurface*, 2012, ISBN 978-3-942036-19-1

216 Pfaff, Thomas: *Processing and Analysis of Weather Radar Data for Use in Hydrology*, 2013, ISBN 978-3-942036-20-7

217 Lebrenz, Hans-Henning: *Addressing the Input Uncertainty for Hydrological Modeling by a New Geostatistical Method*, 2013, ISBN 978-3-942036-21-4

218 Darcis, Melanie Yvonne: *Coupling Models of Different Complexity for the Simulation of CO_2 Storage in Deep Saline Aquifers*, 2013, ISBN 978-3-942036-22-1

219 Beck, Ferdinand: *Generation of Spatially Correlated Synthetic Rainfall Time Series in High Temporal Resolution - A Data Driven Approach*, 2013, ISBN 978-3-942036-23-8

220 Guthke, Philipp: *Non-multi-Gaussian spatial structures: Process-driven natural genesis, manifestation, modeling approaches, and influences on dependent processes*, 2013, ISBN 978-3-942036-24-5

221 Walter, Lena: *Uncertainty studies and risk assessment for CO_2 storage in geological formations*, 2013, ISBN 978-3-942036-25-2

222 Wolff, Markus: *Multi-scale modeling of two-phase flow in porous media including capillary pressure effects,* 2013, ISBN 978-3-942036-26-9

223 Mosthaf, Klaus Roland: *Modeling and analysis of coupled porous-medium and free flow with application to evaporation processes,* 2014, ISBN 978-3-942036-27-6

224 Leube, Philipp Christoph: *Methods for Physically-Based Model Reduction in Time: Analysis, Comparison of Methods and Application*, 2013, ISBN 978-3-942036-28-3

225 Rodríguez Fernández, Jhan Ignacio: *High Order Interactions among environmental variables: Diagnostics and initial steps towards modeling*, 2013, ISBN 978-3-942036-29-0

226 Eder, Maria Magdalena: *Climate Sensitivity of a Large Lake*, 2013, ISBN 978-3-942036-30-6

227 Greiner, Philipp: *Alkoholinjektion zur In-situ-Sanierung von CKW Schadensherden in Grundwasserleitern: Charakterisierung der relevanten Prozesse auf unterschiedlichen Skalen*, 2014, ISBN 978-3-942036-31-3

228 Lauser, Andreas: *Theory and Numerical Applications of Compositional Multi-Phase Flow in Porous Media*, 2014, ISBN 978-3-942036-32-0

229 Enzenhöfer, Rainer: *Risk Quantification and Management in Water Production and Supply Systems*, 2014, ISBN 978-3-942036-33-7

230 Faigle, Benjamin: *Adaptive modelling of compositional multi-phase flow with capillary pressure*, 2014, ISBN 978-3-942036-34-4

231 Oladyshkin, Sergey: *Efficient modeling of environmental systems in the face of complexity and uncertainty*, 2014, ISBN 978-3-942036-35-1

232 Sugimoto, Takayuki: *Copula based Stochastic Analysis of Discharge Time Series*, 2014, ISBN 978-3-942036-36-8

233 Koch, Jonas: *Simulation, Identification and Characterization of Contaminant Source Architectures in the Subsurface*, 2014, ISBN 978-3-942036-37-5

234 Zhang, Jin: *Investigations on Urban River Regulation and Ecological Rehabilitation Measures, Case of Shenzhen in China*, 2014, ISBN 978-3-942036-38-2

235 Siebel, Rüdiger: *Experimentelle Untersuchungen zur hydrodynamischen Belastung und Standsicherheit von Deckwerken an überströmbaren Erddämmen,* 2014, ISBN 978-3-942036-39-9

236 Baber, Katherina: *Coupling free flow and flow in porous media in biological and technical applications: From a simple to a complex interface description,* 2014, ISBN 978-3-942036-40-5

237 Nuske, Klaus Philipp: *Beyond Local Equilibrium — Relaxing local equilibrium assumptions in multiphase flow in porous media,* 2014, ISBN 978-3-942036-41-2

238 Geiges, Andreas: *Efficient concepts for optimal experimental design in nonlinear environmental systems*, 2014, ISBN 978-3-942036-42-9

239 Schwenck, Nicolas: *An XFEM-Based Model for Fluid Flow in Fractured Porous Media*, 2014, ISBN 978-3-942036-43-6

240 Chamorro Chávez, Alejandro: *Stochastic and hydrological modelling for climate change prediction in the Lima region, Peru*, 2015, ISBN 978-3-942036-44-3

241 Yulizar: *Investigation of Changes in Hydro-Meteorological Time Series Using a Depth-Based Approach*, 2015, ISBN 978-3-942036-45-0

242 Kretschmer, Nicole: *Impacts of the existing water allocation scheme on the Limarí watershed – Chile, an integrative approach*, 2015, ISBN 978-3-942036-46-7

243 Kramer, Matthias: *Luftbedarf von Freistrahlturbinen im Gegendruckbetrieb*, 2015, ISBN 978-3-942036-47-4

244 Hommel, Johannes: *Modeling biogeochemical and mass transport processes in the subsurface: Investigation of microbially induced calcite precipitation*, 2016, ISBN 978-3-942036-48-1

245 Germer, Kai: *Wasserinfiltration in die ungesättigte Zone eines makroporösen Hanges und deren Einfluss auf die Hangstabilität*, 2016, ISBN 978-3-942036-49-8

246 Hörning, Sebastian: *Process-oriented modeling of spatial random fields using copulas*, 2016, ISBN 978-3-942036-50-4

247 Jambhekar, Vishal: *Numerical modeling and analysis of evaporative salinization in a coupled free-flow porous-media system, 2016, ISBN* 978-3-942036-51-1

248 Huang, Yingchun: *Study on the spatial and temporal transferability of conceptual hydrological models,* 2016, ISBN 978-3-942036-52-8

Die Mitteilungshefte ab der Nr. 134 (Jg. 2005) stehen als pdf-Datei über die Homepage des Instituts: www.iws.uni-stuttgart.de zur Verfügung.